Improving Recovery: A Concentrate Management Strategy for Inland Desalination

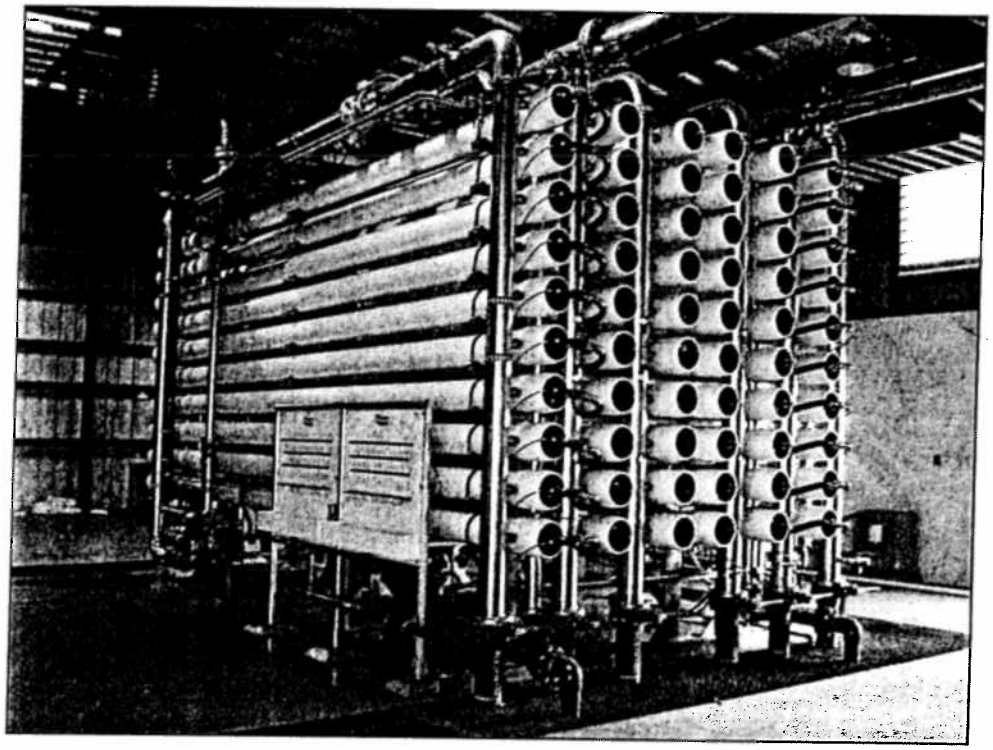

Report

by
Desmond F. Lawler, Ph.D., P.E.
Michael Cobb
Benny Freeman, Ph.D.
Lauren F. Greenlee, Ph.D.
Lynn Katz, Ph.D., P.E.
Kerry Kinney, Ph.D.
W. Shane Walker, Ph.D.

Texas Water Development Board
P.O. Box 13231, Capitol Station
Austin, Texas 78711-3231
August 2010

Improving Recovery: A Concentrate Management Strategy for Inland Desalination

Report

by
Desmond F. Lawler, Ph.D., P.E.
Michael Cobb
Benny Freeman, Ph.D.
Lauren F. Greenlee, Ph.D.
Lynn Katz, Ph.D., P.E.
Kerry Kinney, Ph.D.
W. Shane Walker, Ph.D.

Texas Water Development Board
P.O. Box 13231, Capitol Station
Austin, Texas 78711-3231
August 2010

Texas Water Development Board Report 0704830717

Improving Recovery: A Concentrate Management Strategy for Inland Desalination

by
Desmond F. Lawler, Ph.D., P.E.
Michael Cobb
Benny Freeman, Ph.D.
Lauren F. Greenlee, Ph.D.
Lynn Katz, Ph.D.
Kerry Kinney, Ph.D.
W. Shane Walker, Ph.D.
The University of Texas at Austin

August 2010

Major funding for this project came from the Texas Water Development Board. That funding was supplemented by donations from the environmental engineering firms of Black & Veatch, Inc.; Carollo Engineers; Camp, Dresser and McKee (CDM); HDR, Inc; and Malcolm Pirnie, Inc..

Texas Water Development Board

Published and distributed
by the
Texas Water Development Board
P.O. Box 13231, Capitol Station
Austin, Texas 78711-3231

August 2010
Report
(Printed on recycled paper)

This page is intentionally blank.

Table of Contents

List of Figures

List of Tables

This page is intentionally blank.

1 Executive summary

As fresh water sources are limited, desalination technology is rapidly developing to meet the demand for potable waters by taking advantage of abundant saltwater resources. Reverse osmosis (RO) is a treatment process that utilizes high pressure to force water through membranes while rejecting the dissolved ions. In inland applications, brackish groundwater is predominantly treated using RO, and disposal of the resulting concentrate can be costly. Antiscalants are applied to improve treatment efficiency by preventing scale formation on membrane surfaces and thus allow the process to be operated at a higher recovery to reduce concentrate disposal volume.

This research investigated the feasibility of two treatment processes for recovering water from inland brackish groundwater RO concentrate waste and thereby minimizing the volume of concentrate waste disposal. The first method considered chemical treatments for precipitative removal of sparingly soluble-salts (*e.g.*, calcium carbonate, calcium sulfate, barium sulfate, and strontium sulfate), allowing for further membrane treatment of the supernatant. The second method uses electrodialysis to separate the RO concentrate waste stream into a smaller-volume, more concentrated waste stream and a less concentrated (product) stream with the potential for further membrane treatment. Two closely related water samples were used throughout this research. The first was a synthetic solution manufactured in the laboratory to replicate the ionic constituents and antiscalant of the concentrate from the North Cameron Regional Water Supply Corporation (NCRWSC) brackish groundwater RO desalination plant in south Texas. The second was actual concentrate from the NCRWSC plant.

The antiscalant was shown to be inactivated by oxidation with ozone at the natural pH of the water (pH 7.8). The use of hydrogen peroxide along with the ozone (*i.e.*, peroxone) was expected to improve oxidation of the antiscalant, but the opposite effect was found at this pH. Precipitation experiments were performed with and without prior ozonation at several increasing pH values (to increase the supersaturation of calcium carbonate and dolomite). These experiments showed that, at intermediate values of the saturation ratio, oxidation could increase the amount of precipitation; nevertheless, at these values, the precipitation achieved did not aid recovery sufficiently in a desalination system. At high saturation values (corresponding to pH of approximately 10), substantial precipitation of calcium was achieved, with or without oxidation. The optimal condition, therefore, was to use this high pH without ozonation.

Results in batch and continuous-flow softening experiments were virtually identical with the synthetic and real concentrate. The continuous-flow softening experiments, even though performed at laboratory scale, show that precipitation followed by solid/liquid separation could be quite effective in improving recovery.

Experimentation with batch-recycle electrodialysis demonstrated that ionic components of RO concentrate could be separated to removal ratios of at least 99% with concentrate volumetric recovery ratios at least 75%. The ED diluate could potentially be recycled and blended with the RO feed or treated for removal of uncharged species, which are not separated by ED. The ED concentrate could be treated by the precipitative softening described here, with expected removal ratios greater than those on the RO concentrate. An RO concentrate treatment scheme such as this could result in overall system recovery ratios greater than 95%.

A preliminary cost analysis also indicated that these processes could substantially reduce the cost of concentrate handling by the reduction in concentrate flow rates that would require disposal.

2 Introduction

2.1 Background

In the United States today, reverse osmosis (RO) is the predominant option for desalination treatment. This process involves applying a high pressure to drive water molecules through reverse osmosis membranes while rejecting the salt. The product water is potable, while the remaining water is concentrated with salt and needs to be disposed. In typical coastal RO processes, the source water is the typically seawater, and when properly engineered, the concentrate stream can generally be returned to the sea with minimal impact to the environment.

In an inland environment, the typical source water for desalination is brackish groundwater. This influent water is less concentrated than seawater, but the disposal of concentrate is not as straightforward. Rarely is a large saltwater reservoir such as the ocean available nearby for easy disposal, so an alternate, often more expensive method must be used (*e.g.*, evaporation ponds or deep-well injection). As a typical inland RO plant purifies approximately 80% of the influent water, 20% remains to be disposed (Burbano *et al.* 2007). This disposal is often the single greatest operating cost associated with brackish groundwater desalination (Reedy and Tadanier 2008).

The fraction of pure water produced per volume of raw water treated is referred to as the recovery of the treatment process. Recovery is currently limited by the potential for scale formation as sparingly-soluble salts accumulate in the concentrate stream. Any precipitation during treatment must be avoided as it would impede water flux through the membranes and potentially damage the membranes. Chemicals called antiscalants mitigate this complication by allowing supersaturation conditions to exist to a certain extent without precipitation for a period of time longer than the hydraulic residence time of the RO desalination process. While these chemicals do allow the brackish water reverse osmosis (BWRO) process to be operated at a higher recovery than otherwise would be possible, even further reduction in concentrate volume requiring disposal is economically desirable. Addressing this issue in a more efficient and cost-effective manner was the primary focus of this study.

2.2 Objectives

The overall goal of this study was to improve the recovery of the inland brackish water reverse osmosis (BWRO) desalination treatment process and minimize the volume of concentrate waste disposal. The technical and economic feasibilities of two alternative concentrate treatment methods were considered in lieu of complete disposal. The first objective was to investigate the chemical treatment of concentrate waste – specifically, the effects of antiscalant oxidation (using peroxone) to allow precipitation and the effects of pH adjustment to promote precipitation of carbonate salts. The second objective was to investigate the electrical and hydraulic effects of electrodialysis desalination/concentration of the RO concentrate.

2.3 Approach

Laboratory experimentation was conducted on two similar waters: (1) a sample of the concentrate waste taken from the North Cameron Regional Water Supply Corporation (NCRWSC) brackish groundwater RO plant in Cameron County, Texas, and (2) synthetic water

replicating the ionic and antiscalant concentrations of the NCRWSC concentrate. Additional experimentation was conducted on-site at the NCRWSC plant with live concentrate waste.

The first approach was to investigate chemical methods for inactivating or overcoming the effect of the antiscalant remaining in the solution. The application of an advanced oxidation process was selected as a method to oxidize the antiscalant and thus inactivate its function of preventing precipitation. Specifically, ozone and hydrogen peroxide were utilized in varying proportions to determine an optimal dosage and ratio. The ability to overcome the effects of the antiscalant by pH adjustment was also considered (with and without the effects of antiscalant oxidation). Jar tests at varying degrees of supersaturation followed by filtration as a solid/liquid separation process were conducted with a focus on the removal of calcium carbonate, a predominant RO scalant.

The second approach involved the use of a laboratory-scale batch-recycle electrodialysis (ED) system (which mimics full-scale ED operation) to separate the RO concentrate waste into a smaller-volume, higher-concentrated waste stream and a less concentrated (product) stream with the potential for further membrane treatment. Experimentation with varying stack voltage, cell velocity, and recovery ratio was conducted to examine the effects of these parameters on the efficiency of electrodialysis treatment of inland brackish groundwater RO concentrate waste.

Laboratory experimentation with both of these approaches successfully simulated an increase in inland RO recovery and a reduction of concentrate disposal volume and cost.

3 Summary of literature and technology

3.1 Water sources and treatment

A reliable fresh water supply is one of the most crucial components to the sustenance and growth of any modern society. A survey of population density today shows that, without an ample supply of fresh water, the sustainable population of a given area is dramatically limited. This issue is of particular importance given that, over the past two centuries, we have seen a six-fold increase in world population. As population continues to grow, so does the need for fresh water use in sectors such as agriculture (irrigation), domestic and industrial applications, sanitation, and energy production (Al Radif 1999). The Texas Water Development Board has estimated that the State's population will grow from approximately 25 million in 2010 to more than 46 million in 2060 (TWDB 2010a). Many fresh water sources are becoming insufficient in both quality and quantity to meet this growing need. The future of human society is greatly dependent on the ability to provide fresh water at higher rates than ever before.

Historically, fresh water sources in the U.S. have been in excess of human necessity, especially in non-arid regions. As population increased over time, contamination of these sources was of more concern than insufficient supply. To deal with this issue, traditional water and wastewater treatment plants have been designed and utilized which ensure the protection of human health and limit any negative environmental impacts. The Safe Drinking Water Act was passed in 1974 and gave a clear standard for the overall quality of product water from drinking water treatment plants. Since that time, many revisions and updates have been released to bring us to the water quality standard of today.

In recent decades, many heavily populated or arid regions of the country have encountered another inevitable limitation: quantity of fresh water sources. In many cases, surface water sources as well as fresh groundwater aquifers are proving insufficient to meet today's demand. To cope with this ever-increasing need, the water treatment field is undergoing a shift to the most abundant yet challenging drinking water source on the earth: saltwater. According to the (USGS 2010), 97% of the earth's water is saltwater, and much of the remaining 3% is inaccessible for drinking water (e.g., in glaciers).

Despite the predominance of saltwater in the earth's water composition, it has never been as broadly utilized as fresh water because of the extensive treatment necessary. For such a critical undertaking, the most up-to-date technology and resources must be combined with innovative and groundbreaking research and design.

Brackish groundwater is relatively abundant with estimates of 2.7 billion acre-feet throughout the State of Texas (Kalaswad *et al.* 2004), and is certainly present in the areas of the State that were identified in the 2007 Water Plan as having the greatest water needs (TWDB 2010b). Water needs are defined as "projected water demands in excess of existing supplies that would be physically and legally available during a repeat of the drought of record" (TWDB 2010b).

3.2 Desalination methods and applications

Desalination is the process by which saltwater is converted into potable, fresh water. Currently, four primary methods of desalination can be distinguished as either using thermal energy or membrane technology to accomplish salt and water separation. They include: multi-effect

distillation (MED), multi-stage flash (MSF), reverse osmosis (RO), and electrodialysis (ED) (Van der Bruggen and Vandecasteele 2002). MED dates back to the mid-19th century and utilizes heat to evaporate seawater and then condense water. MSF is a similar method which began in the 1960's and incorporates both heat and pressure chambers in series for increased heat recovery. RO became a competitive method in the 1980's and uses pressure and membranes that are permeable to water molecules but not monovalent ions (*e.g.*, Na^+, Cl^-). ED is a method utilizing cationic and anionic membranes to separate salt ions through the application of a gradient in electric potential. As membrane technology continues to develop, RO and ED are becoming the most competitive desalination methods of drinking water treatment. According to Global Water Intelligence (2010), 57% of the 2010 global desalination capacity was derived from membrane processes, and approximately 97% of the United States desalination capacity came from membrane processes. This distribution of current capacity is clear evidence of the worth of research devoted to the advancement and optimization of this technology.

While many water sources may require some form of desalination treatment for their purification, primary sources of salty water are brackish groundwater and seawater. According to Global Water Intelligence (2010), approximately 69% of the plants used brackish water and river sources, while only 8% of the plants treated seawater. (The remaining 23% was from wastewater and the use of drinking water or fresh water to create high purity water for industrial use.) This breakdown highlights the importance placed on brackish water desalination. As the need for alternative water supplies continue to develop in many areas, inland desalination technology and process optimization will be relied upon more than ever before.

Two major factors currently limit the widespread use of RO as a method for inland freshwater production. The first limitation is the operational energy demand, which can be costly in any application (*i.e.*, coastal or inland). The second is a more specific limitation associated with inland applications, namely the disposal of the concentrate. This disposal can be the single greatest operating cost over the lifetime of a plant, greatly limiting the feasible applications of membrane technology (Reedy and Tadanier 2008). These two limitations need to be further understood and addressed if membrane processes are to be more competitive water treatment options in the future.

As mentioned, in a typical RO process, the driving force to achieve an adequate degree of purity of the product water is energy intensive. RO membranes require energy to generate the required pressure to force the water through a membrane by diffusion, while rejecting the salt content. Recent advancements in membrane technology include increased structural stability, lower pressure demand, and inherent resistance to fouling. Although these advancements have yielded significant reductions in the overall operating cost, the energy demand continues to limit desalination technologies from becoming economically competitive with conventional treatment of freshwater.

The second limitation is the costly disposal of the produced concentrate stream after treatment. The volume requiring disposal is directly influenced by the overall process recovery, that is, the volume fraction of incoming raw water effectively converted into fresh water. Recovery (r) can be calculated as follows:

$$r = \frac{Q_{permeate}}{Q_{\text{inf}\,luent}} \times 100\% \qquad (3\text{-}1)$$

where $Q_{influent}$ is the flow rate of raw water entering the plant and $Q_{permeate}$ is the flow rate of purified water produced from the plant. Typical values for overall process recovery are 30-50% for coastal (seawater) applications (Rautenbach and Linn 1996) and 80% for inland applications (Burbano *et al.* 2007). This recovery is the current feasible efficiency mainly because of the potential for precipitation of the sparingly soluble salts within the membrane system as they accumulate in the concentrate stream. Once this limit is approached, the concentrate water must be disposed of or treated in another way to prevent solids from accumulating on the membranes.

In many coastal applications, ocean disposal of the concentrate stream is acceptable and cost-effective. However, in inland environments, alternate disposal methods (*e.g.*, deep-well injection or evaporation ponds) are required, and they may be both costly and detrimental to the environment. In the case of deep-well injection, the Underground Injection Control program has been initiated to regulate the estimated 300,000 existing injection wells in the U.S. (Mickley 2006). Costs associated with drilling, well construction, pumping, and monitoring can accumulate substantially. Alternatively, evaporation ponds require the use of a large land area which may not be cost effective in many urban regions. Acquiring permits for these disposal options may also be tedious and time consuming. In any case, reducing the total volume requiring disposal may have significant economic advantages.

A proposed environmentally friendly and potentially economical option to decrease the disposal volume involves using this concentrate to produce various high quality salts as commercially marketable products (Ahmed *et al.* 2003). Another potential use is the irrigation of salt-tolerant plants, provided that salt levels in the soil are regulated and groundwater contamination is minimized (Ahmed *et al.* 2001). As researchers continue to explore alternate possibilities, this limitation remains a major obstacle that must be further addressed in order to broaden the scope of potential membrane desalination applications in the future.

3.3 Scale formation

A typical RO treatment scheme for inland desalination includes two or three stages of membranes in series. As raw water passes through the first stage, a portion of the water diffuses through the membrane into a pure water stream (or permeate), leaving an accumulation of salt in the remaining concentrate stream (or brine). This concentrated stream continues to subsequent stages where more water is recovered. Eventually, the concentrate stream is supersaturated to the extent that precipitation is inevitable. At this point, further treatment would result in an accumulation of precipitated salt on the membrane surface that would dramatically increase the pressure required to force more water through the membrane and could permanently damage the membrane. This phenomenon is called scaling.

Scale formation can be understood as a function of several variables related to the conditions of flow and operation in a given plant. The first of these is the development of a concentration polarization (CP) layer. As pure water passes through the membranes, the dissolved ions are rejected at the membrane surface. Rejected ions accumulate near the surface because the diffusion of ions back into the feed solution is slower than the convection of ions toward the membrane. This accumulation causes a gradient in concentration that can lead to significant supersaturation very close to the membrane surface. The result of this supersaturation is the formation of nucleation sites which are crystal structures that give way to the growth and formation of crystalline precipitates. This growth reduces the degree of supersaturation and thus fewer nucleation sites are produced leading to further growth of the existing sites, and ultimately

visible scale formation (Gloede and Melin 2008). Because this growth occurs on the initially formed sites, the crystals composed of ion pairs with the lowest solubility will grow and are of primary concern. As this understanding of scaling has significant implications to the RO treatment process, a detailed study has been conducted on the formation and growth of gypsum crystals in view of the development of RO membrane scale formation models (Uchymiak *et al.* 2008).

In practice, scale must be prevented from accumulating on the membrane surface, as no further treatment would be economically feasible once it occurs. Preventative measures include increased crossflow velocity and antiscalant use. A discussion of antiscalant use can be found later in this chapter.

3.4 Precipitation chemistry

Precipitation equilibrium and kinetics play major roles in desalination by membranes. The extent to which raw water can be treated is directly related to the possibility of membrane scaling. Solubility products must be used to determine the limiting concentrations of sparingly soluble ion pairs which could potentially precipitate as salts. A general precipitation reaction with its corresponding solubility product equation may be denoted in the following way:

$$A_z B_y \leftrightarrow zA^{y+} + yB^{z-} \tag{3-2}$$

$$K_{so} = \frac{\{A^{y+}\}^z \{B^{z-}\}^y}{\{A_z B_y\}} \tag{3-3}$$

where the ions and the precipitate are given in activity (instead of concentration), and K_{so} is the solubility constant of the salt. The activity of the salt, $\{A_z B_y\}$, is 1 (unity) for a pure solid which simplifies Equation 3-3. Once a particular ion pair is in solution at a level above its given solubility product, precipitation can occur and is limited only by kinetics. A description of such kinetics can be found in the discussion of antiscalant use later in this chapter.

3.4.1 Ionic strength and activity coefficients

Ionic strength (I) is a parameter describing the overall abundance of ions in a given solution. Equation 3-4 is used to calculate ionic strength of a given solution, where a given dissolved species (i) has a concentration (c) and a charge (z).

$$I = \frac{1}{2} \sum_{all\ i} c_i z_i^2 \tag{3-4}$$

As I increases, the concentration of a species in a solution becomes an inaccurate measure of its tendency to precipitate with other ions. The "active" concentration, also known as the activity of a species, must then be used. Activity (a) is defined as the product of the concentration of a given species (X) and its corresponding activity coefficient (γ_X), as seen here:

$$a_X = \gamma_X [X] = \{X\} \tag{3-5}$$

Determining the activity coefficient of a species requires the use of the ionic strength as well as an applicable mathematical model developed for this purpose, as described below.

3.4.2 Mathematical models for determining activity coefficients

Models for determining activity coefficients have been developed and are valid within a given range of ionic strength. At relatively low ionic strengths (< 0.1 M), the Debye-Huckel model can be used. At this level, the difference between activity and concentration is still negligible for most applications and thus activity coefficients are approximately 1.0. As ionic strength increases (0.1 M < I < 0.5 M), a more sophisticated model must be employed. One such model is the Davies equation which is applicable up to 0.5 M. In this range, activity and concentration begin to show dramatic differences. The activity coefficient based on this model is typically calculated to be between 0.2 and 0.8. In cases when ionic strength is above the limit for the Davies model (> 0.5 M), another even more sophisticated model, the Pitzer model, may be applied. In this study, all activity concentrations were found using the Davies model since typical ionic strengths of the synthetic and real waters (RO concentrates) ranged from 0.3-0.4 M.

The distinction between concentration and activity has significant implications in understanding precipitation limits in the RO treatment process for typical seawater or brackish groundwater. As the raw water is treated and ions accumulate in the concentrate stream, this distinction between concentration and activity is even more dramatic. The fact that the activity is smaller than the corresponding concentration, allows for a greater degree of solubility without the risk of precipitation and membrane scale formation. Even so, the solubility product of a particular ion pair based on their corresponding activities is still a major limitation to the recovery of the treatment process. In an effort to address this limitation, chemicals called antiscalants have been developed and are discussed below.

3.4.3 Speciation and the carbonate system

Speciation is also a major factor in precipitation chemistry because it is directly related to the concentration (and thus activity) of a given species in solution. Speciation refers to the various forms a given dissolved molecule can take in solution as it combines with other ions (such as H^+), generally as a function of pH. In natural waters, the carbonate system undergoes speciation with important implications related to precipitation. In a system open to the atmosphere, the dissolved carbonate in solution at equilibrium is dependent on the local partial pressure of $CO_2(g)$ according to the following reaction and equilibrium equation:

$$H_2O + CO_2(g) \leftrightarrow H_2CO_3^* \tag{3-6}$$

$$K_H = \frac{\{H_2CO_3^*\}}{pCO_2} \tag{3-7}$$

where $\{H_2CO_3^*\}$ refers to the activity of dissolved carbon dioxide in its fully protonated form and K_H is the equilibrium constant. Most natural waters are open to the atmosphere, causing the carbonate system to be the dominant pH buffer. In solution, $H_2CO_3^*$ will undergo speciation to take one of three forms according to the following chemical reactions:

$$H_2CO_3^* \leftrightarrow H^+ + HCO_3^- \tag{3-8}$$

$$HCO_3^- \leftrightarrow H^+ + CO_3^{2-} \tag{3-9}$$

These reactions are dependent on pH as seen in the following equilibrium equations:

$$K_{a1} = \frac{\{H^+\}\{HCO_3^-\}}{\{H_2CO_3^*\}} \tag{3-10}$$

$$K_{a2} = \frac{\{H^+\}\{CO_3^{2-}\}}{\{HCO_3^-\}} \tag{3-11}$$

where K_{a1} and K_{a2} denote equilibrium constants ($K_{a1} \approx 10^{-6.3}$ and $K_{a2} \approx 10^{-10.3}$). For simplicity in calculating carbonate speciation, the equilibrium constants (Eqs. 3-7, 3-10, and 3-11) may be modified to be based on concentration instead of activity. These modifications are as follows:

$${}^cK_H = \frac{[H_2CO_3^*]}{pCO_2} = \frac{K_H}{\gamma_{H2CO3*}} \tag{3-12}$$

$${}^cK_{a1} = \frac{[H^+][HCO_3^-]}{[H_2CO_3^*]} = \frac{K_{a1}\gamma_{H2CO3*}}{\gamma_{H+}\gamma_{HCO3-}} \tag{3-13}$$

$${}^cK_{a2} = \frac{[H^+][CO_3^{2-}]}{[HCO_3^-]} = \frac{K_{a2}\gamma_{HCO3-}}{\gamma_{H+}\gamma_{CO3^{2-}}} \tag{3-14}$$

Given the total carbonate (or partial pressure of $CO_2(g)$ if at equilibrium with the atmosphere) and the solution pH, it is possible to calculate the concentration of each carbonate species using the following equations:

$$[H_2CO_3^*] = C_{T,CO3}\left[1 + \frac{{}^cK_{a1}}{[H^+]} + \frac{{}^cK_{a1}\,{}^cK_{a2}}{[H^+]^2}\right]^{-1} \tag{3-15}$$

$$\left[HCO_3^-\right] = C_{T,CO3}\left[\frac{\left[H^+\right]}{{}^cK_{a1}} + 1 + \frac{{}^cK_{a2}}{\left[H^+\right]}\right]^{-1} \tag{3-16}$$

$$\left[CO_3^{2-}\right] = C_{T,CO3}\left[\frac{\left[H^+\right]^2}{{}^cK_{a1}\,{}^cK_{a2}} + 1 + \frac{\left[H^+\right]}{{}^cK_{a1}}\right]^{-1} \tag{3-17}$$

where $C_{T,CO3}$ is the total carbonate concentration in the solution, the sum of all the species after speciation, as seen here:

$$C_{T,CO3} = \left[H_2CO_3^*\right] + \left[HCO_3^-\right] + \left[CO_3^{2-}\right] \tag{3-18}$$

Two of the most common precipitates of concern in the desalination of natural waters are calcium carbonate ($CaCO_3$(s)) and gypsum ($CaSO_4$(s)). The chemical reaction and solubility equations for calcium carbonate are as follows:

$$CaCO_3(s) \leftrightarrow Ca^{2+} + CO_3^{2-} \tag{3-19}$$

$$K_{CalciumCarbonate} = \frac{\left\{Ca^{2+}\right\}\left\{CO_3^{2-}\right\}}{\left\{CaCO_3^{2-}(s)\right\}} \tag{3-20}$$

where $K_{CalciumCarbonate}$ is the solubility constant for calcium carbonate. Comparing Equations 3-17 and 3-20 reveals that an increase in pH results in an increase in the concentration (and activity) of CO_3^{2-}, ultimately raising the driving force for calcium carbonate precipitation. Since most natural waters are in the pH range of 6.5 to 9.5 (approaching $K_{a2} \approx 10^{-10.3}$), a slight increase in pH could have major impacts on precipitation.

The saturation ratio (*S*) is a term used to describe the degree of undersaturation or supersaturation of a particular salt. A saturation ratio less than unity indicates undersaturation, and an increase in saturation ratio greater than unity corresponds to a greater driving force of precipitation for the given salt. The saturation ratio for a given salt can be calculated using the ion activity product (*IAP*) and the corresponding solubility constant as follows:

$$S = \left(\frac{IAP}{K_{so}}\right)^{\frac{1}{\eta}} \tag{3-21}$$

where η is the number of ions precipitating in each molecule (*e.g.*, $\eta = 2$ for calcium carbonate). In desalination using membrane treatment processes, the ability to attain a greater saturation ratio without precipitation (scaling) during the residence time of the process would allow for improved overall performance and recovery. Antiscalants are added to the brackish feed to avoid precipitation in the presence of a greater saturation ratio.

3.5 Antiscalant type, function, and application

Antiscalants are synthetic organic polymers developed for pre-treatment application in RO systems based on their ability to alter (slow) the kinetics of precipitation. Phosphonates are the main classification of antiscalants commonly used in drinking water applications. They are characterized by the presence of one or more phosphorus-carbon bonds and may come in different chains to prevent precipitation of specific target compounds (*e.g.*, calcium carbonate, gypsum, *etc.*). At the time of study, the cooperating North Cameron Regional Water Supply Company BWRO plant used a proprietary antiscalant from American Water Chemicals, Inc., and the manufacturer would not reveal the formula. (Based on physical appearance and experimental results, it is assumed to be a blend of phosphonate compounds.) Another type of antiscalant is based on acrylic acid and may be blended with phosphonates. When antiscalants are applied in practice, they function to prolong the kinetics of precipitation to such an extent that any undesirable precipitation is prevented during the typical residence time within a RO treatment process. However, precipitation will still ultimately occur if the water remains supersaturated.

A basic knowledge of precipitation kinetics must be understood before the effect of antiscalants can be fully grasped. For a solution existing at supersaturated conditions to reach a point of visible precipitation, two things must happen. First, a number of nucleation crystals must be formed which give ions in solution many sites on which to precipitate. These sites are called metastable nanoparticles (Gloede and Melin 2008). Second, these nanoparticles must grow in size through the diffusion and attachment of surrounding ions in solution until they become visible, stable crystals. At this point, the turbidity of the solution rises dramatically, indicating that precipitation has occurred. The time associated with reaching this point from an initial condition of supersaturation is referred to as the induction time, which is a function of temperature, the degree of supersaturation, and the presence of complexing ions. Antiscalants are designed to lengthen this induction time by affecting both the formation and growth of the nucleation sites.

By preventing crystal growth, antiscalants force many more metastable nanoparticles to be formed in the surrounding solution than would form in the absence of antiscalant. Because of the larger number of such particles, a decrease in supersaturation occurs, leading to a lower concentration gradient in the solution surrounding these particles. This gradient slows down the rate of diffusion according to Fick's law, as shown here:

$$J = -D\frac{\partial c}{\partial x} \tag{3-22}$$

where D is the diffusivity coefficient and $\frac{\partial c}{\partial x}$ is the concentration gradient. Since the flux (J) of ions from the bulk solution toward the newly-formed particles is reduced as the concentration gradient is decreased, the growth rate of these particles is proportionally reduced. The result is a substantial increase in induction time, allowing for a greater degree of supersaturation without scale formation. This result directly increases the feasible recovery of the RO process, and that is the sole reason for the widespread use of antiscalants in RO treatment. While the choice of antiscalant to be used should be based on practical tests under the prevailing conditions in a given plant, a test method for quantifying an optimal dose has not been developed, especially for newly manufactured polymers (Al-Shammiri *et al.* 2000). Currently, manufacturers supply a recommended dose which may or may not be optimal for a specific application in the field.

As mentioned, antiscalants increase recovery while continuing to prevent membrane scaling. However, after the concentrate stream leaves the membrane system, the once advantageous effect of slow precipitation kinetics can become an obstacle. The volume requiring disposal could be drastically reduced if the concentrate stream could undergo precipitation of sparingly soluble ions followed by some form of further desalination treatment without the risk of scale formation. This treatment scheme is a novel approach that will require a great deal of research and development to see widespread benefits. Recently, a study has been done showing the feasibility for such a treatment scheme to achieve 95-98% recovery through alkaline pH adjustments resulting in precipitation softening followed by secondary RO treatment (Rahardianto *et al.* 2007). Further optimization of such a treatment scheme may require the inactivation of the antiscalants in order to overcome their effect prior to precipitation. This inactivation might be achievable using advanced oxidation processes.

3.6 Oxidation and advanced oxidation processes (AOPs)

A chemical reaction called an oxidation-reduction, or redox, reaction is the combination of two half reactions. A species called an oxidant accepts an electron and is reduced, while another species loses an electron and is oxidized. The oxidized component is thus degraded to another form, altering its potential function in the solution.

Oxidation treatment processes utilize chemical reactions to transform an undesirable substance into a more tolerable product. Drinking water and wastewater applications include disinfection, taste and odor elimination, and the removal of hazardous or toxic compounds. Historically, various processes have been developed and applied, such as chlorination, chloramination, ozonation, potassium permanganate application, and hydrogen peroxide dosing. Individually these processes achieve a limited degree of oxidation. In recent application, however, the combination of various processes has been performed and called advanced oxidation processes (AOPs). AOPs are powerful tools used to accomplish high levels of oxidation by exploiting the high reactivity of hydroxyl radicals (*OH) to drive oxidation and complete mineralization of pollutants (Andreozzi *et al.* 1999). Hydroxyl radicals are highly reactive due to the single electron in the orbital structure. Since these radicals are able to degrade organics to a much higher degree, many compounds that once were unable to be oxidized through the use of individual oxidants are now being successfully degraded using AOPs. When this type of oxidation is applied to antiscalants, it may also be described as radical-based dephosphorylation as it effectively cleaves phosphates from the antiscalant molecules into the bulk solution (Frost *et al.* 1987). Evidence of this cleaving confirms that AOPs are appropriate for the inactivation of phosphonates, the most common type of antiscalant used in RO treatment. Some specific applications of this oxidation have been studied more recently in the water treatment arena.

One such treatment that has been used for the oxidation of antiscalants is known as the electro-Fenton process, an electrochemical oxidation process that produces hydroxyl radicals by way of the reaction between Fe^{2+} and hydrogen peroxide (H_2O_2). This process was shown to successfully destroy the function of antiscalants in RO concentrate (Yang *et al.* 2004). Research remains to be done to develop and optimize the inactivation of antiscalants using various other AOPs, such as peroxone treatment.

3.6.1 Peroxone treatment

Peroxone refers to the combination of ozonation (O_3) and hydrogen peroxide (H_2O_2) dosing as two oxidation processes to produce an abundance of hydroxyl radicals. Ozone is unstable in water and this instability is accelerated by the presence of hydrogen peroxide (von Gunten 2003). Because of this accelerated instability, the hydroxyl radical formation rate increases dramatically, yielding a significant increase in overall oxidation.

In peroxone treatment, a major variable influencing the hydroxyl radical production rate and ultimately the rate of oxidation is called the peroxone ratio, that is the molar ratio of hydrogen peroxide dosed to ozone dosed ($[H_2O_2] / [O_3]$). Varying this ratio alters the reaction chemistry significantly. An optimum ratio for oxidation of trichloroethylene (TCE) and perchloroethylene (PCE) has been determined to range from 0.5 to 0.6 (Karimi *et al.* 1997).

von Gunten (2003) has shown that a prediction of the overall oxidation rate of a given compound (*X*) using ozonation is possible. He found that ozone can either react with the organic directly or produce hydroxyl radicals which react with the organic. In either case, the reaction is second order (first order with respect to the organic and first order with respect to the oxidant) and the total oxidation rate is the sum of those two reactions. The equation for this oxidation rate can be written as:

$$r_X = -k_{O3}[X][O_3] - k_{OH}[X][^*OH] \qquad (3\text{-}23)$$

In this equation k_{O3} and k_{OH} refer to rate constants that must be experimentally determined for the reaction of the target compound with ozone and hydroxyl radicals, respectively. The ozone concentration must be directly measured and the hydroxyl radical concentration may be determined through the use of an ozone-resistant probe chemical (von Gunten 2003).

3.6.2 Disinfection by-products

One of the major items of concern related to oxidation in the water and wastewater treatment field is the production of undesirable disinfection by-products (DBPs). These species are products of the oxidation process that remain in the water after oxidation and pose risks to human health and/or the environment. Of the various oxidation processes, ozonation is one of the most conservative in this regard. Trihalomethanes and other common DBPs from chlorination are not significantly produced. However, in waters under the influence of saltwater intrusion, the formation of the carcinogen bromate (BrO_3^-) and associated brominated DBPs can be of particular concern. These DBPs are the product of the reaction between bromide (Br^-) and ozone (O_3), which forms most readily at high concentrations of both substances and at high pH (Huang *et al.* 2003). Since seawater and brackish groundwater can potentially have elevated levels of bromide, bromate production must be closely monitored in the combination of desalination and ozonation.

3.7 Electrodialysis

3.7.1 Separation overview

Electrodialysis (ED) is a proven technology that, prior to the invention of thin composite RO membranes, was a leading desalination technology. ED is more robust than RO with respect to

biological fouling (because of chlorine-tolerant membranes) and chemical scaling (especially with solutions containing high concentrations of silica) (AWWA 1995). ED is less susceptible to some of the scaling problems that plague RO systems because of the difference in the way that the separation is accomplished. In RO, a mechanical pressure is used to drive water through a membrane that rejects the passage of salt ions. However, in ED, the bulk water (and any other neutrally charged compound) is unaffected as an electric field (voltage drop) drives ions through the membranes. ED utilizes two kinds of ion-exchange membranes, anion-exchange membranes (AEMs) and cation-exchange membranes (CEMs), to create a diluate stream which has had ions removed and a waste concentrate containing ions transferred from the diluate, as shown in Figure 3-1. AEMs allow anions to pass through the membrane but reject cations, and CEMs allow cations to pass but reject anions. The space between two membranes is called a cell, and typical installations have hundreds of cell-pairs (*i.e.*, one diluate cell and one concentrate cell). ED is typically operated to achieve a 50-70% recovery in each stage, but multiple stages can be utilized to achieve very high recovery (AWWA 1995). .

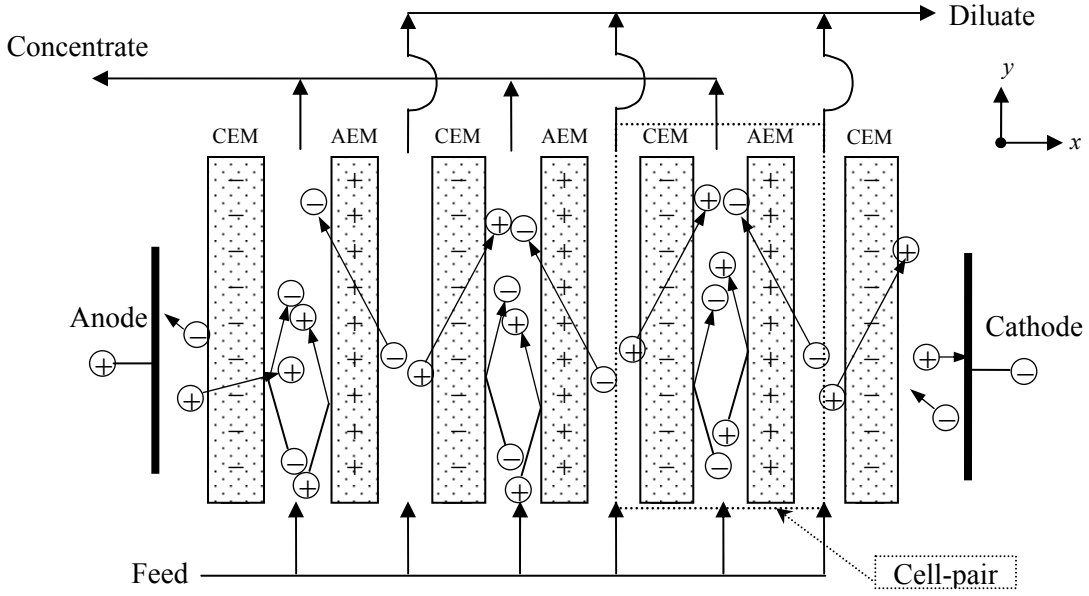

Figure 3-1. Schematic of ionic separation in electrodialysis (adapted from Strathmann 2004).

For brackish groundwater and RO concentrate systems, the transport of a particular ion within the electrodialyzer may be approximated by the Nernst-Planck equation:

$$J_i = -D_i \frac{dc_i}{dx} - \frac{F}{RT} D_i z_i c_i \frac{d\phi}{dx} \tag{3-24}$$

where J is the molar flux of species i, D is the ionic diffusivity, c is the molar concentration , F is the Faraday constant, R is the molar gas constant, T is the solution temperature, z is the sign and magnitude of the charge of the ion, and ϕ is the electric potential (Bard and Faulkner, 2001; Bockris and Reddy, 1998; Newman and Thomas-Alyea, 2004). The first term on the right hand side of the equation describes the flux by Fickian diffusion, and the second term represents flux by electromigration, which is proportional to the voltage drop.

The diffusivity of an ion is sometimes represented as ionic mobility, u_i, or equivalent ionic conductivity, λ_i,, and these parameters are related by the following expression (Bard and Faulkner 2001):

$$\frac{F}{RT} D_i |z_i| = u_i = \frac{\lambda_i}{F} \tag{3-25}$$

The electrical conductivity (κ) of a brackish solution is an aggregate of the ionic composition,

$$\kappa = \sum_{\mathrm{i}} \lambda_{\mathrm{i}} |z_i| c_i \tag{3-26}$$

so it is representative of the bulk salinity of the solution, though the equivalent ionic conductivity of each ion decreases with increasing ionic strength (Eaton *et al.* 2005, §2510 and 2520).

3.7.2 Electrical and hydraulic limitations

As electrical current flows through the electrodialyzer stack, concentration gradients are formed in the stagnant regions adjacent to the membranes (diffusion boundary layers, of thickness δ), as shown in Figure 3-2, because of the restrictive functionality of the ion-exchange membranes. Mixing is typically enhanced in the bulk regions by plastic spacers (not shown) between the membranes. The velocity profile (not shown) is approximated with a no-slip boundary at the membrane surface and significant mixing in the bulk, such that the thickness of the diffusion boundary layer (which is assumed to have negligible mixing) is inversely related to the bulk solution velocity. The concentration profile (in the x-dimension) is idealized as a constant concentration within the well-mixed bulk region and linear concentration gradients in the diffusion boundary layers (Strathmann 2004).

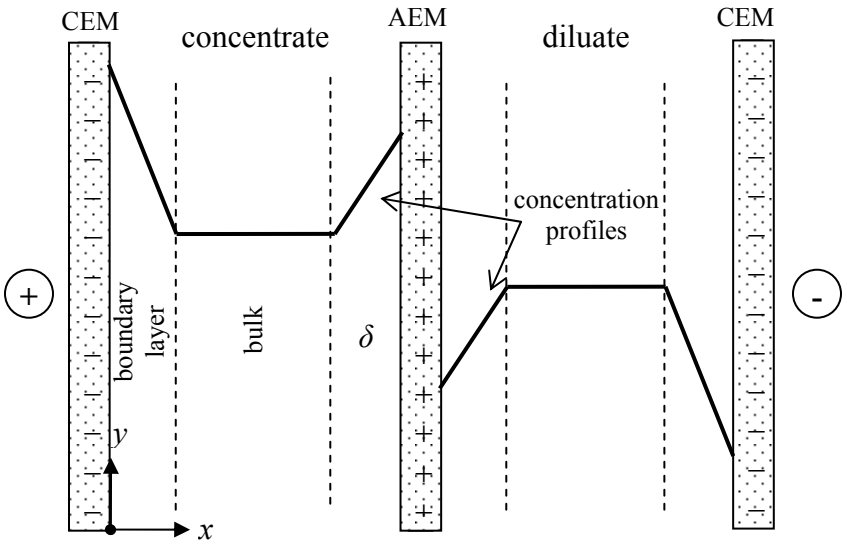

Figure 3-2. Schematic of a single cell-pair: simplified velocity and concentration profiles

The concentration difference from one side of a membrane to the other is known as *concentration polarization* (Strathmann 2004; Tanaka 2007). Since the membranes reject one

type of ion, the concentration gradient within the diffusion boundary layer reaches a magnitude such that the diffusive flux term exactly opposes the electromigration flux of the rejected ion within the diffusion boundary layer. That is, the concentration gradient in the diffusion boundary layer at a given point, *y*, along the flowpath, is proportional to the electrical current density flowing through the electrodialyzer (in the *x*-dimension).

As the current density through the electrodialyzer is increased from zero (by increasing the voltage difference between the electrodes), the concentration gradient in each diffusion boundary layer becomes steeper. If the concentration gradient becomes too steep (or, if the diffusion boundary layer thickness is too large), then the salt concentration in the diluate diffusion boundary layer approaches zero at the membrane surface. The *limiting current density* (i_{lim}) occurs when the ions are "completely" depleted at the membrane surface. This limiting condition makes electrodialysis ill-suited for producing very low conductivity water. (Electrodeionization is a variant of electrodialysis in which the diluate cells are filled with ion-exchange beads and thus allows the production of very low conductivity water.)

In the concentrate diffusion boundary layers, however, the danger of steep concentration gradients (or wide diffusion boundary layers) is the precipitation of scaling salts on the membrane (though it does not pose as significant risks as scaling in an RO unit). Thus, in the context of treating supersaturated RO concentrate wastes, the bulk velocity must be sufficiently high, and the applied voltage must be sufficiently low to avoid scaling the membranes.

3.7.3 Batch-recycle experimentation with electrodialysis

Laboratory-scale ED systems are typically assembled in a batch-recycle to simulate as a function of time what occurs in a full-scale ED system as a function of distance along the flowpath (from inlet to outlet). A finite volume of experimental solution is placed in one reservoir representing the feed to the diluate stream, and another solution is placed in a separate reservoir representing the feed to the concentrate stream, as shown in Figure 3-3. The diluate and concentrate solutions are pumped through the electrodialyzer where a small fraction of ionic content in the diluate cells is separated to the adjacent concentrate cells, and the effluent streams from the electrodialyzer are recycled to their respective reservoirs. A third stream is continuously sweeping away the oxygen and hydrogen gas that is being generated at the anode and cathode, respectively. (The oxidation of chloride to chlorine gas can also occur at the anode, and the quantity of chlorine produced is a function of the anode overpotential and the concentration of chloride in the anolyte solution.)

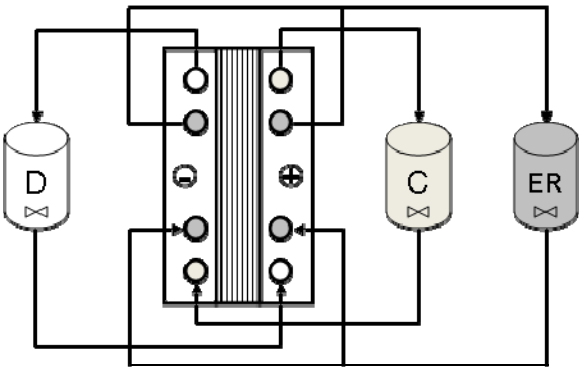

Figure 3-3. Schematic of batch-recycle electrodialysis experimentation

Several experimental investigations of ED treatment of brackish solutions have been performed (Chandramowleeswaran and Palanivelu 2006; Choi *et al.* 2003; Firdaous *et al.* 2007; Koprivnjak *et al.* 2006; Ortiz *et al.* 2008; Xu *et al.* 2008), the research mostly applies to simple salt mixtures with less complexity and lower concentration than RO concentrate wastes. While experimental and full-scale ED treatment of brackish waters have proven technically and economically feasible (AWWA 1995; Reahl 2005; Strathmann 2004; Tanaka 2007; Wiesner *et al.* 2009; Xu *et al.* 2008), further experimentation and demonstration is necessary to identify the useful and challenging conditions of ED treatment of RO concentrate waste.

3.8 Synopsis

The improvement of recovery of the inland RO desalination process is a promising opportunity in the water treatment field. Precipitation softening of the concentrate to remove sparingly soluble calcium and magnesium ions has been recognized as a feasible option. The benefits associated with oxidation of the antiscalants have also been studied in an effort to reduce concentrate disposal volume. This study elucidates the value of these technologies in the application of the inland RO treatment process in Texas.

4 Materials and Methodology

Several experimental procedures and analyses were performed to determine an optimal side-stream treatment process for inland desalination concentrate. Materials ranging from American Chemical Society (ACS) -grade chemicals to custom-made reactors were utilized. Experimental data were collected using an array of standard methods of analysis. These materials and methods are described in this chapter.

4.1 Materials

4.1.1 Cameron County, Texas brackish groundwater

The water source for the majority of the experiments conducted in this research was a synthetic blend produced in the laboratory approximating a typical Texas brackish groundwater from North Cameron, Texas. Detailed data showing the various components and concentrations found in this groundwater were obtained from Ana-Lab Corporation (Kilgore, TX). These data, as well as the concentrations in RO concentrate from a plant operating at 75% recovery ratio and an assumed 100% removal ratio (*i.e.*, four times the concentration of the raw water for all constituents), are shown in Table 4-1.

Table 4-1. North Cameron, Texas raw and concentrated water recipes.

Constituent	C_{raw} [mM]	$C_{conc(4x)}$ [mM]	$C_{conc(4x)}$ [mg/L]
SiO_2	0.3	0.8	48.1
$B(OH)_3$	1.0	4.0	247
Na^+	40.5	170.6	3920
Ca^{2+}	3.8	15.3	612
Mg^{2+}	3.3	13.4	326
K^+	0.4	1.6	62.5
Sr^{2+}	0.1	0.3	26.3
Cl^-	31.3	125.2	4440
SO_4^{2-}	10.4	41.3	3960
Br^-	0.1	0.2	15.8
HCO_3^-	5.5	22.2	1350

This synthetic recipe was chosen as the primary experimental water source because it could be reproduced consistently in the laboratory while allowing the results to be applicable for any typical Texas groundwater. The only modification to the reported data was a 5% increase in the sodium concentration to account for electroneutrality. The initial pH of the synthetic concentrate water was measured to be approximately 7.8.

Production of the synthetic water was accomplished for each experiment using distilled, de-ionized water and ACS-grade salt additions measured on a Mettler-Toledo AT261 DeltaRange balance. Typically, separate solutions containing the sparingly soluble anions (mainly as sodium salts) and cations (mainly as chloride salts) were made and combined at the time of experimentation to produce the full synthetic water. Table 4-2 gives the specific recipe used for

each solution, indicating which salts were added to the cation and anion solutions. The concentrations given describe the solution after combination to produce the full synthetic water.

Table 4-2. North Cameron, Texas synthetic concentrate recipe.

	Salt	Concentration (g/L)
Cation Solution	$CaCl_2*2H_2O$	2.24
	$MgCl_2*6H_2O$	2.72
	$SrCl_2*6H_2O$	0.09
	H_2SiO_3	0.06
	KCl	0.10
	KBr	0.03
Anion Solution	NaCl	3.85
	Na_2SO_4	5.86
	$B(OH)_3$	0.24
	$NaHCO_3$	1.86

Experimental analysis was conducted promptly after these solutions were combined to prevent precipitation of the supersaturated ion pairs. Various experiments were also conducted using natural groundwater obtained directly from North Cameron, Texas. The distinction between the synthetic and real waters is indicated when appropriate in later chapters.

4.1.2 Antiscalant

A stock solution of antiscalant was obtained from the North Cameron Regional Water Supply Corporation RO plant. It was reported that a dose of 2.9 µL of stock antiscalant solution was applied per liter of influent groundwater to be desalinated. As no information was given describing the concentration, chemical type or composition of the antiscalant, a characterization of its composition was required. The total dissolved solids concentration of the stock solution (185 g/L), organic carbon fraction (0.23 g/g carbon to antiscalant), and phosphorus fraction (0.33 g/g phosphorous to antiscalant) were all determined using analytical methods discussed later in this chapter. Based on these analyses, the antiscalant was determined to be a phosphonate.

4.1.3 Ozone generation and application apparatus

A 12-volt Ozone Services (Burton, B.C., Canada) ozone generator (Model: 0L80W1FM100VT) was acquired as the means of producing gaseous ozone. An MKS Mass-Flo Controller powered and regulated by an MKS Type 246 Power Supply was used to control the influent compressed oxygen flow rate. The effluent ozone/oxygen stream was directed by a three-way valve leading either to a 34/28 KIMAX 500 mL gas washing bottle or to a column containing activated carbon for ozone destruction. The complete setup can be seen in Figure 4-1. The type of tubing (1/8" Teflon) and fittings (stainless steel) used throughout the apparatus were chosen specifically because of their ability to transport ozone without the possibility of reacting with the ozone.

Figure 4-1. Ozone generation and application apparatus.

After the ozone passed through the gas washing bottle, a final tube led any remaining ozone into a second catalytic ozone destructor. The ozone destructors ensured the safety of the laboratory by not allowing any ozone to be released into the atmosphere. For added protection, the entire apparatus was always operated under a functioning fume hood.

The ozone generator was calibrated at various operating intensity settings (*i.e.*, the applied electrical power) to accurately translate an influent oxygen flow into an effluent ozone dose. This analysis was performed using the ozone mass flow analysis described in §4.2.4 and can be seen in Figure 4-2.

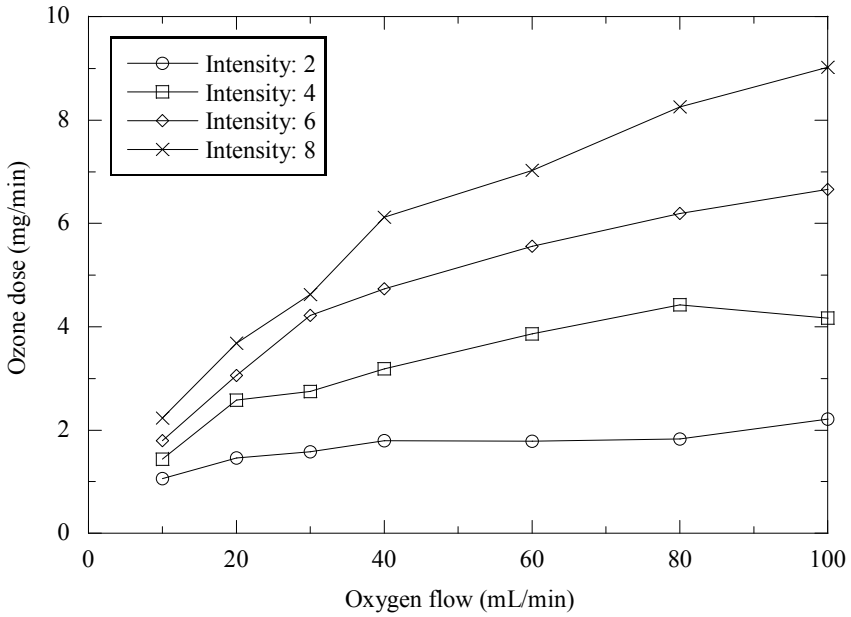

Figure 4-2. Ozone generator calibration curves based on intensity and oxygen flow rate

For experimental consistency and reproducibility, an intensity of 4 and a flow rate of 30 mL per minute were chosen for most experimentation. From the calibration curve above, these conditions translate to an ozone application rate of approximately 3 mg per minute. Since this rate was chosen as the standard operating procedure, the overall ozone dose for a given experiment was able to be varied by adjusting the time of application (*e.g.*, 5 minutes of bubbling leads to a 15 mg ozone dose). Once the desired time of ozone production was achieved, the generator was switched off while bubbling continued for several minutes to ensure that all of the produced ozone passed through the tubes and was applied to the sample.

In experimental application, the produced gaseous stream of ozone passed through a coarse frit at the bottom of a 500 mL gas washing bottle filled (500 mL) with the experimental solution. As these bubbles rose within the solution, the ozone dissolved and reacted within the sample. It was determined that this dissolution of ozone was often incomplete within a single gas washing bottle. For this reason, a second gas washing bottle containing potassium iodide (KI) solution (20 g/L) was placed in series to account for this remaining, gaseous ozone. A schematic of this setup can be seen in Figure 4-3.

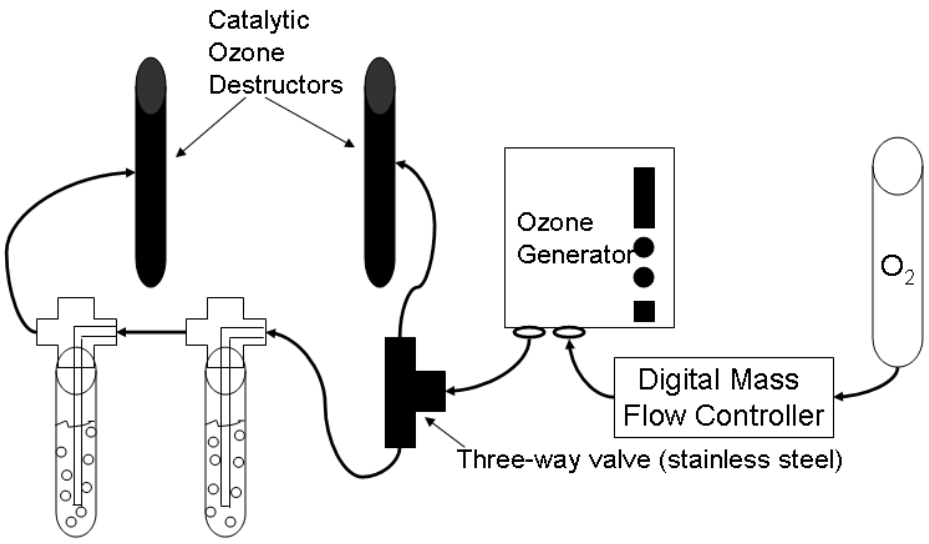

Figure 4-3. Schematic of ozone apparatus with additional gas washing bottle.

The mass of ozone reacted in the second gas washing bottle containing KI solution was determined using the ozone mass flow analysis described in §4.2.4. The amount of ozone that dissolved into the first gas washing bottle containing the sample was calculated as the difference between the mass of ozone produced (based on the ozone generator calibration) and the ozone reacted in the second gas washing bottle containing the KI solution. (A blank experiment was performed to verify that the ozone consumption of the first flask with pure water was negligible.)

4.1.4 Jar test apparatus

An essential part of this research was the effective removal of salt through precipitation using several custom-made jar test reactors and a Phipps and Bird mechanical stirrer (Model: 7790-400). In all, twelve identical jar test reactors were constructed to perform an adequate amount of simultaneous precipitation experiments. The shape and size of the reactors were designed to achieve hydraulic conditions known to accomplish effective mixing (*e.g.*, minimal dead space). The internal range of capacity for each reactor was designed to range from 100 to 200 mL. This volume was small enough to allow for a single oxidized sample of 500 mL from the ozone apparatus described above to be distributed into an array of precipitation experiments at varying conditions. This volume was also large enough to obtain an adequate amount of product water (at least 100 mL) to undergo the necessary analytical methods described later in this chapter. It is also important to note that the reactor tops were designed to fit securely within the reactors and float on the water surface. This design ensured that each sample would be closed to the atmosphere during experimentation, preventing atmospheric equilibration of the carbonate system.

The Phipps and Bird mechanical stirrer was used to simulate a "slow mix" treatment process during the course of most precipitation experiments. The goal was to effectively mix the sample, allowing for maximum chemical precipitation, while not over-mixing, which could cause unnecessary floc breakup due to high shear force. This balance was found at a setting of approximately 40 revolutions per minute. Under these conditions, the velocity gradient within

the jar test reactors was calculated to range from 25 to 18 s^{-1} (Cornwell and Bishop 1983), depending on the experimental volume (100 or 200 mL, respectively).

For each jar test, the necessary reactors were filled with a volume (either 100 or 200 mL) of experimental solution. The solution pH was then raised by adding NaOH (1 N) dropwise into the reactor to reach the desired supersaturation conditions. The reactor covers were immediately inserted to prevent atmospheric equilibration and the samples underwent 1 hour of "slow mix" to allow precipitation to occur. After each jar test experiment, the pH was measured and the solution was filtered through a 0.45 µm filter. The filtrate was stored in plastic bottles for further analyses as appropriate.

4.1.5 Continuous-flow softening experimental apparatus

A simplified design was used to perform all continuous-flow softening experiments in this research. The equipment consisted of a 4-stage, 12 liter, acrylic tank reactor, a Cole-Parmer Masterflex L/S peristaltic pump (Model: 7519-70), and a Phipps and Bird mechanical stirrer (Model: 7790-400). Peristaltic tubing was used to transport and mix the source water with the necessary chemicals to reach the desired experimental conditions. The details of this mixing can be seen in Figure 4-4.

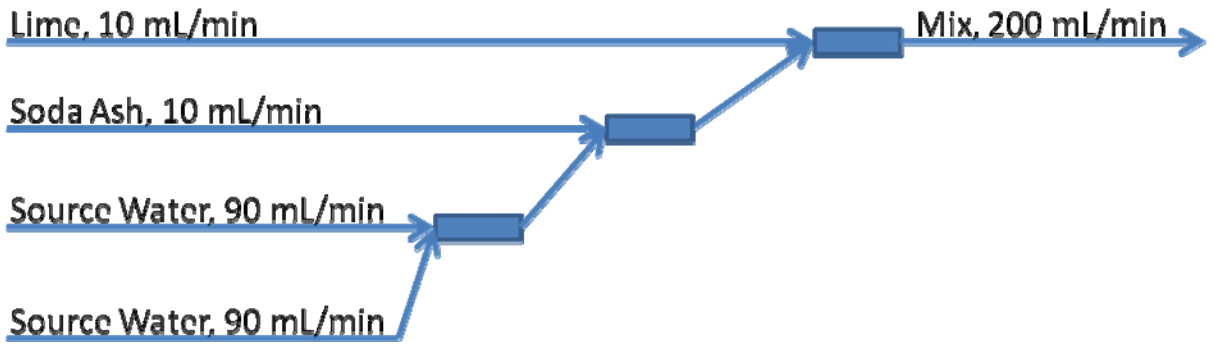

Figure 4-4. Influent and chemical mixing details.

The source water was supplied through two 0.19" inside diameter tubes (Masterflex L/S 25) at a flow rate of 90 mL/min each (180 mL/min total). When using synthetic water, these two tubes would supply the cation and anion solutions separately. The lime and soda ash solutions were supplied through 0.06" inside diameter tubes (Masterflex L/S 14) at a flow rate of 10 mL/min each. The four tubes were pumped simultaneously with a single peristaltic pump drive using four adjustable cartridge pump heads. The relative tube sizes (and corresponding relative flow rates) were chosen to prevent significant (greater than 10%) dilution of the source water. The three junctions shown in Figure 4-5 (each having 2 inputs and 1 output) were connected using an appropriately sized Y-shaped connector to match the inside diameter of the tubing. A tubing size adjustment (from 0.19" to 0.06" inside diameter) was made between the source water junction and the soda ash junction using a straight connector with tapered ends. The effluent mixed solution was supplied to the inlet of the 4-stage tank reactor.

The operation of the 4-stage tank reactor was divided into 2 well-mixed tanks of approximately 3 liters each followed by 2 quiescent tanks of similar size wherein settling and removal of precipitated salts was observed. The Phipps and Bird mechanical stirrer was utilized in only the

first two reactors at a setting of 80 revolutions per minute to produce a well-mixed environment. The velocity gradient was estimated to be 72 sec^{-1} within these reactors (Cornwell and Bishop 1983). The apparatus can be seen in Figure 4-5.

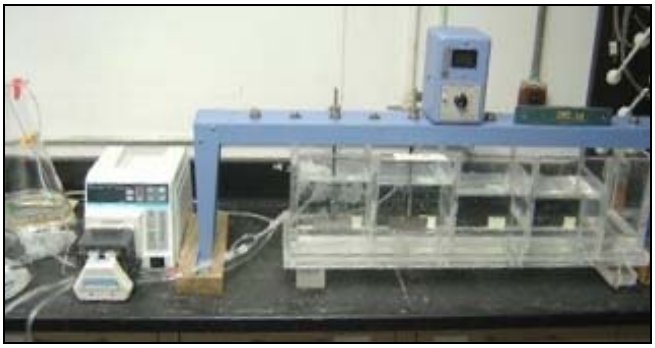

Figure 4-5. Continuous-flow softening apparatus.

As continuous-flow softening operation is a more practical and "real-life" application of the science being developed, many of the operating decisions were made to support both theoretical and practical considerations. One such decision was to set the hydraulic residence time (HRT) within each stage of the treatment process to be comparable to that required in practice. The HRT was set to be 30 minutes in each of the well-mixed and settling portions, leading to a total HRT of 60 minutes. Using this HRT and given the capacity of the apparatus, it was calculated that a constant flow rate of 200 mL/min should be used. This flow rate then dictated the sizing of the pumps, tubing, and storage capacity.

A second decision based on practical considerations was the choice of chemical addition to reach the desired precipitation conditions. In many of the batch experiments conducted in the laboratory, NaOH was used to reach a desired pH during precipitation. This choice of chemical was mainly because NaOH gave excellent control and was completely soluble. However, in practice, NaOH is often replaced with $Ca(OH)_2$ (hydrated lime) and, if necessary to provide sufficient carbonate, Na_2CO_3 (soda ash) due to economic considerations. In accordance with the practical emphasis of this portion of the research, $Ca(OH)_2$ and Na_2CO_3 were effectively used to reach the desired precipitation conditions. These chemicals were mixed with the sample water within the tubes in aqueous/slurry form just before entering the first stage of the tank reactor. A stock concentration of these chemicals was used that would allow for minimal (10%) dilution to the source water. The difficulty in using lime, especially in small scale reactors, is the possibility of incomplete dissolution of the $Ca(OH)_2$ particles resulting in a waste of chemical and less control of the experiments.

4.1.6 Batch-recycle electrodialysis apparatus

A batch-recycle electrodialysis experimental apparatus was assembled similarly to those used by others (Choi *et al.* 2003; Moon *et al.* 2004; Ortiz *et al.* 2005); a schematic is shown in Figure 4-6. Laboratory-scale gear pumps were used to circulate each of the three process streams: diluate (D), concentrate (C), and electrode rinse (E); the flow rate (Q) through each stream was monitored continuously. The flow rates of the concentrate and diluate streams were controlled by electronic liquid flow-controllers. The electrode rinse stream combined the anode and cathode in parallel because, during operation, the reactions at the anode and cathode produce equivalent

amounts of protons and hydroxides, respectively, and the stack loses the equivalent amount of cations to the catholyte that it gains from the anolyte. The reservoirs were one-liter Erlenmeyer flasks that were stirred vigorously by non-heating magnetic stirrers and were approximately ideal continuous-flow, stirred-tank reactors (CFSTRs); they were monitored continuously for pH, conductivity (κ), and temperature (T) with Orion 4-star meters. The mass of the diluate reservoir was monitored continuously to gravimetrically quantify water and electrolyte transfer. Pressure (P) was monitored at the inlet and outlet of the electrodialyzer for each of the process streams to characterize the headloss through each stream and the average trans-membrane pressures. A custom heating- and cooling-bath system controlled the experimental temperature (not shown in Figure 4-6) within one-degree Celsius change; without this feature, the temperature of the process streams would increase during an experiment because of electrical resistance and hydraulic resistance dissipated as heat.

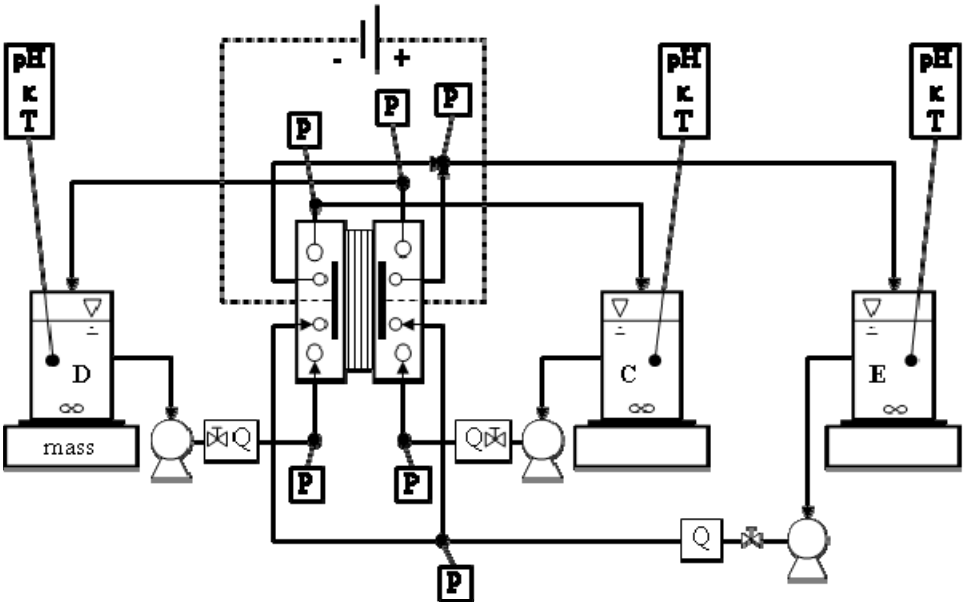

Figure 4-6. Schematic of batch-recycle experimental ED apparatus.

A PCCell ED 64002 electrodialyzer was acquired from PCCell/PCA, GmbH (Germany). The active cross-sectional area subjected to the applied electric field was 64 cm^2. Plastic diagonal screen/mesh spacers of thickness 0.41 mm physically separated the anion- and cation-exchange membranes. The anode was expanded titanium metal with platinum/iridium coating, and the cathode was expanded stainless steel. The end-plates surrounding the electrodes and compressing the stack were machined polypropylene. The electrodialyzer was fitted with eleven CMV and ten AMV membranes, which are low resistance Selemion (Asahi Glass) membranes for general desalination (Strathmann 2004) to form ten cell pairs. This configuration has the advantage of preventing anions (especially chloride) in the concentrate or diluate from entering the electrode rinse, and *vice versa* (thus protecting the anion exchange membranes, which may be damaged by chlorine).

A custom National Instruments LabVIEW supervisory control and data acquisition (SCADA) software program was developed for controlling and monitoring the electrodialysis experimentation; this program allows the user to specify electrical conditions for automated

control and to record hydraulic, electrical, and chemical experimental conditions throughout the experiment with three-second periodicity.

The laboratory scale gear pumps (Greylor Co. Model PQM-1/115 via Cole-Parmer) used to supply the flow rate of each of the three process streams were 115 VAC, 3500 rpm, 1.6 L/min gear pumps. These gear pumps were used instead of peristaltic pumps to minimize pressure oscillation within the electrodialyzer.

Volumetric flow rate through the concentrate and diluate streams was controlled and monitored with two McMillan Co. analog Liquid FLO-CONTROLLERS® (model 401-6-A4), and the electrode rinse stream was operated at maximum capacity through a McMillan Co. FLO-SENSOR® (model 101-6-D-AB) analog flow meter. Each flow controller/meter was calibrated by pumping a 100 mM NaCl solution at an electronically specified flow rate and measuring the mass of its throughput at periodic intervals. The flow controllers and meter were powered by a 12 VDC signal from a BK Precision® 1696A programmable direct current (DC) power supply.

The mass of the diluate reservoir was monitored continuously to the nearest 0.1 g with a Mettler Toledo® XS6001S digital mass balance, which facilitated the quantification of the mass of water and salt transported across the membranes.

Pressure-head of the concentrate and diluate streams was monitored at the electrodialyzer inlets with OMEGA® PX481A-015G5V analog pressure transducers (linear range of 0–15 psi) and at the electrodialyzer outlets with ICSensor® 114-005G analog pressure transducers (linear range of 0-5 psi). Pressure-head of the electrode rinse stream was monitored at the anolyte and catholyte inlets and outlets (which were in hydraulic parallel) with ICSensor® 114-005G analog pressure transducers. All six pressure transducers were periodically calibrated simultaneously with a wall-manometer at multiple water heights. The pressure transducers were also powered by same 12 VDC signal from the BK Precision® 1696A power supply that also powered the flow meters.

The electrical voltage and current applied to the electrodialyzer were controlled and monitored by a BK Precision® 9123A switching mode, direct current (DC), regulated, programmable power supply (1-30 V ± 0.1 mV, 0.1-5 A ± 0.05 mA). The voltage applied to the electrodes remained constant throughout the experiment; the stack voltage was the applied voltage less the total electrode voltage loss (which was relatively stable throughout the experimentation and was quantified experimentally with the electrodialyzer configured without membranes).

The pH of each experimental reservoir was monitored with a Thermo Orion 4-Star pH and conductivity meter fitted with an Orion® 9157 pH probe. Each pH probe was calibrated with pH 4, 7, and 10 buffer solutions. The conductivity of each experimental reservoir was monitored with a Thermo Orion 4-Star pH and conductivity meter fitted with an Orion® 013005 conductivity/temperature cell. Each conductivity cell was calibrated using standard solutions: 0.0067 M KCl (100 mS/cm), 0.01 M KCl (1.413 mS/cm), 0.1 M KCl (12.9 mS/cm), and 1.0 M KCl (111.9 mS/cm). Conductivity cells were periodically cleaned by soaking in 1 M hydrochloric acid and thoroughly rinsing with distilled water.

4.2 Analytical methods

4.2.1 pH

For all experiments, pH measurements were taken before and after various stages of treatment. These measurements were taken with an Orion semi-micro pH probe while the sample was being

stirred with a magnetic stirrer. Calibration of the pH probe was done using VWR pH buffer solutions at pH values of 4, 7, and 10. Reported error associated with these solutions was ±0.01 pH units. The ionic strength of the standards was adjusted using NaCl to approximate the ionic strength of the sample being measured. This ionic strength adjustment was performed to achieve a more accurate pH reading of the sample, as ionic strength directly affects the hydroxyl activity being measured (Wiesner *et al.* 2006). For example, the synthetic Texas water mentioned above had an ionic strength of about 0.3 M. Before measuring the pH of a sample of this water, the pH meter was calibrated using standards containing 16 g/L NaCl which corresponds to an ionic strength of 0.3 M. No corrections were made for the pH of the buffers after ionic strength adjustments because the corrections were minor.

4.2.2 Alkalinity

One of the main ways of quantifying experimental precipitation was the measurement of alkalinity through a titration method. Alkalinity data, along with the pH of the sample, could be used to calculate the concentrations of dissolved carbonate species before and after precipitation. The difference between the total carbonate from these two measurements would be the amount that precipitated. Some volume of the sample, typically 50 or 100 mL, was placed in a beaker and mixed using a magnetic stirrer. Slowly, a strong acid (either HCl or H_2SO_4) of known normality was titrated into the sample while measuring the change in pH with each addition of acid. A plot, as seen in Figure 4-7, was developed for each sample, showing the titration endpoint as the point of steepest slope (generally around pH 4).

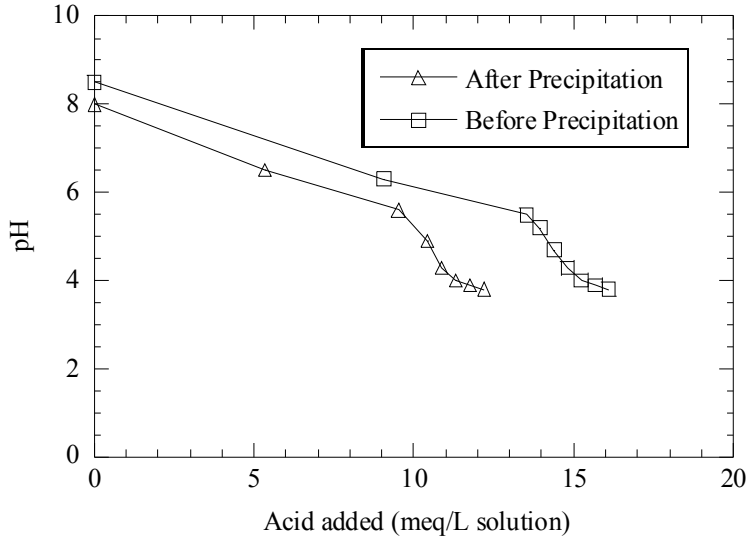

Figure 4-7. Alkalinity titration curves for a sample before and after precipitation

The number of equivalents of acid required to reach the endpoint is the number of equivalents of alkalinity in the initial sample. As shown in Figure 4-7, the alkalinity of a sample was measured both before and after precipitation, and the difference was used to quantify the extent of calcium carbonate precipitation on a carbonate basis.

4.2.3 Flame atomic absorption (FAA)

Another main way to determine the extent of experimental precipitation was the quantification of dissolved ions using a PERKIN-ELMER 1100 B Flame Atomic Absorption Spectrophotometer (FAA). The FAA used a set of PERKIN-ELMER Intensitron Lamps that were element specific. Before each analysis, the lamp was turned on and given a minimum of 30 minutes to warm up before any measurements were taken. The most common analysis was of dissolved calcium using a Ca^{2+} specific lamp, but Mg^{2+} was occasionally measured. For each set of samples analyzed, a standard curve was produced as shown in Figure 4-8.

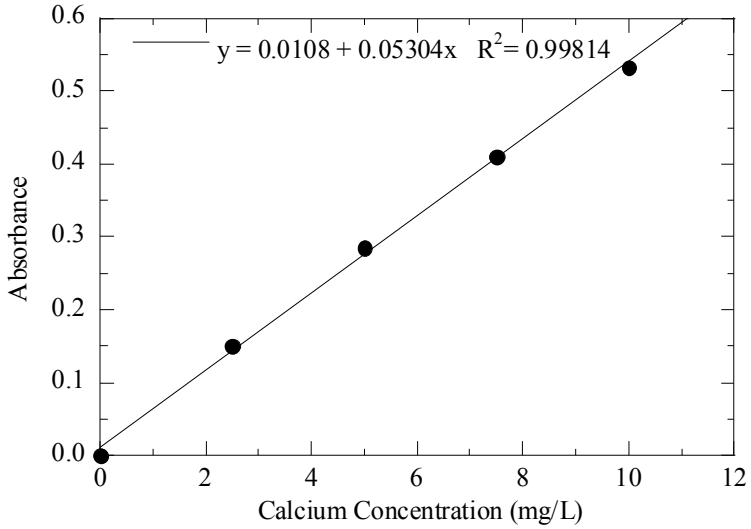

Figure 4-8. Typical calcium standard curve.

To stay within the detectable limits of the instrument, the standard curve ranged from 2.5 to 10 mg/L of dissolved calcium. Samples with high concentrations were diluted to fall within the range of the standard curve. The instrument was set to take five replicate measurements of each sample and the average value was used.

4.2.4 Ozone mass flow

Gaseous ozone was measured on a mass reacted basis using a slight variation of the Ozone Demand/Requirement – Semi-Batch Method from Standard Methods 2350 E (Eaton *et al.* 2005). A 20 g/L potassium iodide (KI) solution was prepared and placed in a 34/28 KIMAX 500 mL gas washing bottle connected to the ozone generator with Teflon tubing. Any ozone entering the solution would react according to the following reactions to produce a yellow solution:

$$3KI + O_3(aq) + H_2O \rightarrow 3KOH + I_3^- + O_2 \quad (4\text{-}1)$$

$$I_3^- \leftrightarrow I^- + I_2 \quad (4\text{-}2)$$

After the ozone completely reacted with the KI, a 10 mL sample was drawn with an automatic pipette and placed in a small beaker (50 mL). A volume of 0.5 mL of 2N H_2SO_4 was added to lower the pH, and the solution was then titrated with 0.01N Sodium Thiosulfate ($Na_2S_2O_3$) until only a slight yellow hue remained. At this point, a few drops of starch indicator were added

causing the solution to turn deep purple. Finally, the solution was titrated further with $Na_2S_2O_3$ until it became clear. The titration reactions are as follows:

$$I_2 + HSO_3^- + H_2O \rightarrow 2I^- + SO_4^{-2}(aq) + 3H^+ \quad (4\text{-}3)$$

$$2S_2O_3^{-2} + I_3^- \rightarrow S_4O_6 + 3I^- \quad (4\text{-}4)$$

$$I_3^- + starch \rightarrow starch/iodine \quad complex \quad (purple) \quad (4\text{-}5)$$

Based on the total volume of 0.01N $Na_2S_2O_3$ added to the original 10 mL of KI sample, the mass and concentration of ozone reacted were determined using the following equations:

$$\text{mg O}_3 \text{ reacted} = (\text{mL Na}_2\text{S}_2\text{O}_3 \text{ Titrant})\left(\frac{0.01 \text{ eq Na}_2\text{S}_2\text{O}_3}{\text{L}}\right)\left(\frac{1\,\text{mol}}{2\,\text{eq}}\right)\left(\frac{1\,\text{mol I}_3^-}{2\,\text{mol Na}_2\text{S}_2\text{O}_3}\right) \times \left(\frac{1\,\text{mol O}_3}{1\,\text{mol I}_3^-}\right)\left(\frac{48\,\text{g}}{1\,\text{mol O}_3}\right)\left(\frac{1\,\text{L}}{1000\,\text{mL}}\right)\left(\frac{1000\,\text{mg}}{1\,\text{g}}\right) \quad (4\text{-}6)$$

$$\frac{\text{mg O}_3}{\text{L}} \text{ reacted} = \text{mg O}_3 \text{ reacted} * \left(\frac{1}{\text{Vol. of Sample (10mL)}}\right)\left(\frac{1000\,\text{mL}}{\text{L}}\right) \quad (4\text{-}7)$$

This concentration could then be used in combination with the time of ozone application and original volume of KI solution to determine an ozone mass flow rate, as follows:

$$\frac{\text{mg O}_3}{\text{L}} * (\text{Total Reactor Volume} = 0.5\text{L}) * \left(\frac{1}{\text{Time}}\right) = \frac{\text{mg O}_3}{\text{min}} \quad (4\text{-}8)$$

The remaining volume of KI solution in the gas washing bottle could be reused for subsequent experiments by accounting for the reduced initial volume (*i.e.*, 490 mL, 480 mL, *etc.*) and subtracting the previously reacted ozone from the subsequent results. This process was used repeatedly to develop the ozone generator calibration curves shown in Figure 4-2 earlier in this chapter.

4.2.5 Phosphorus

One of the results of the oxidation of phosphonate antiscalants is the cleaving of phosphate from the large antiscalant molecules into the solution as dissolved orthophosphate. To quantify the degree of antiscalant oxidation, the concentration of phosphate in solution after a given oxidation experiment was measured using the Ascorbic Acid Method from Standard Methods 4500-P E (Eaton *et al.* 2005). The principle behind this measurement is that "ammonium molybdate and potassium antimonyl tartrate react in acid medium with orthophosphate" (Eaton *et al.* 2005). A byproduct of this reaction will form a blue color when reduced by ascorbic acid. To achieve these conditions, a reagent mixture was made consisting of 50 mL sulfuric acid (5N), 5 mL potassium antimonyl tartrate solution (2.743 g/L), 15 mL ammonium molybdate solution (40g/L) and 30 mL ascorbic acid solution (17.6 g/L). Each sample under analysis was pipetted (50 mL) into an acid washed beaker and combined with the reagent mixture (8 mL). The resulting solution became blue and was analyzed between 10 and 30 minutes after adding the mixture on

an AGILENT 8453 Ultra-violet/Visible Spectrophotometer at 880 nm. A crystal cuvette with a 10 mm light path was rinsed with de-ionized water, then rinsed with the sample, and then filled with the sample for each measurement. Along with each set of samples, a standard curve was produced by adding the reagent mixture to dilutions of a stock phosphate solution. A typical standard curve is shown in Figure 4-9.

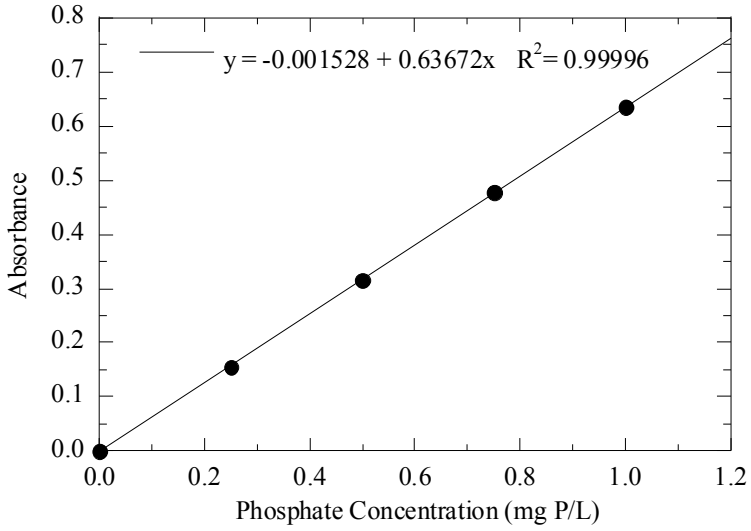

Figure 4-9. Typical phosphorus standard curve.

Using the absorbance results of the spectrophotometer along with the corresponding standard curve, the dissolved orthophosphate in the original sample was determined. This concentration was then compared with the antiscalant concentration and phosphorus fraction to quantify the degree of antiscalant oxidation. A greater fraction of cleaved phosphate indicated a greater degree of antiscalant oxidation and thus inactivation.

4.2.6 Total organic carbon analysis

Another important characteristic of an antiscalant is its organic carbon content. As an antiscalant is oxidized, its organic carbon fraction diminishes. A Teckmarr Dohrmann Apollo 9000 Total and Dissolved Organic Carbon Analyzer was used in determining the carbon fraction of the complete antiscalant as well as the reduction in organic carbon after varying amounts of oxidation. The instrument was given a minimum of 1 hour to warm up to the required internal temperature of 680ºC before analysis. The preparation of 40 mL glass vials used with this instrument included a minimum of 2 hours in a 10% nitric acid bath followed by at least 1 hour in a 550ºC oven. A standard curve with a total organic carbon (TOC) range of 1 to 5 mg/L was produced with each set of samples to be analyzed, as shown in Figure 4-10.

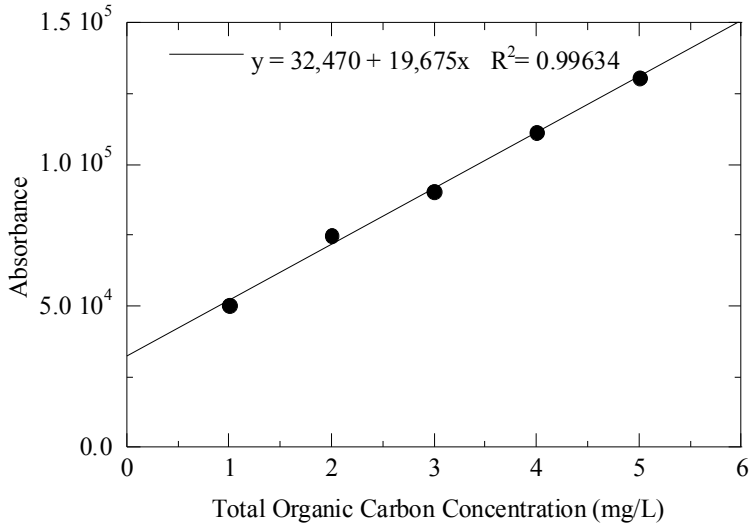

Figure 4-10. Typical TOC standard curve

The standards were made from a stock solution of 2.13 g/L potassium hydrogen pythalate (KHP). Granular KHP was dried in a 103ºC oven for at least 2 hours and cooled in a dessicator before measuring. When not being used, the KHP solution was stored in a brown glass bottle at 4ºC for up to one month to prevent biological growth.

Samples were diluted to fit in the range of the standard curve and analyzed in the 40 mL acid washed, baked vials. Typically either 5 or 7 replicates were measured from the same vial for each sample and an average value was used. Two steps were taken to ensure consistent results and confirm the stability of the instrument. First, vials referred to as "blanks" containing DI water were placed throughout the set of standards and samples. Second, a number of standards were repeated throughout each run and compared to those placed at the beginning. Reported values are those that were determined to be accurate based on these steps.

4.2.7 Ion chromatography (IC)

During batch-recycle electrodialysis experimentation, 50-100 µL samples (depending on concentration) were periodically withdrawn by pipette from the experimental reservoirs and diluted to 10 mL (1/200-1/100 dilutions); 8 mL were retained for ICP analysis, and the remaining 2 mL were used for IC analysis. The retained 2 mL dilution was further diluted by the addition of 2 mL of distilled water, creating final dilutions of 1/400-1/200. Standard concentrations were prepared from mixtures of Certified ACS stocks of NaCl, $NaNO_3$, and Na_2SO_4. Example standard curves for chloride, nitrate, and sulfate are shown in Figure 4-11.

The concentrations of chloride, nitrate, and sulfate ions in experimental samples were determined according to Standard Methods (Eaton *et al.* 2005, §4110) using an ion chromatography (IC) system composed of Metrohm® hardware (838 Advanced Sample Processor, 762 IC Interface, 752 IC Pump Unit, 733 IC Separation Center, 732 IC Detector, and 709 IC Pump) fitted with a 150 mm Metrosep A supp 5 IC column (PN 6.1006.520, SN 7704583). Metrohm software *IC Net® v. 2.3 SR3* was used to perform the IC analyses. Wash and rinse solutions of 0.1 M H_2SO_4 and distilled water were used to regenerate the internal carbonate suppressor. The eluent was composed of 3.2 mM Na_2CO_3 and 1.0 mM $NaHCO_3$ in distilled water.

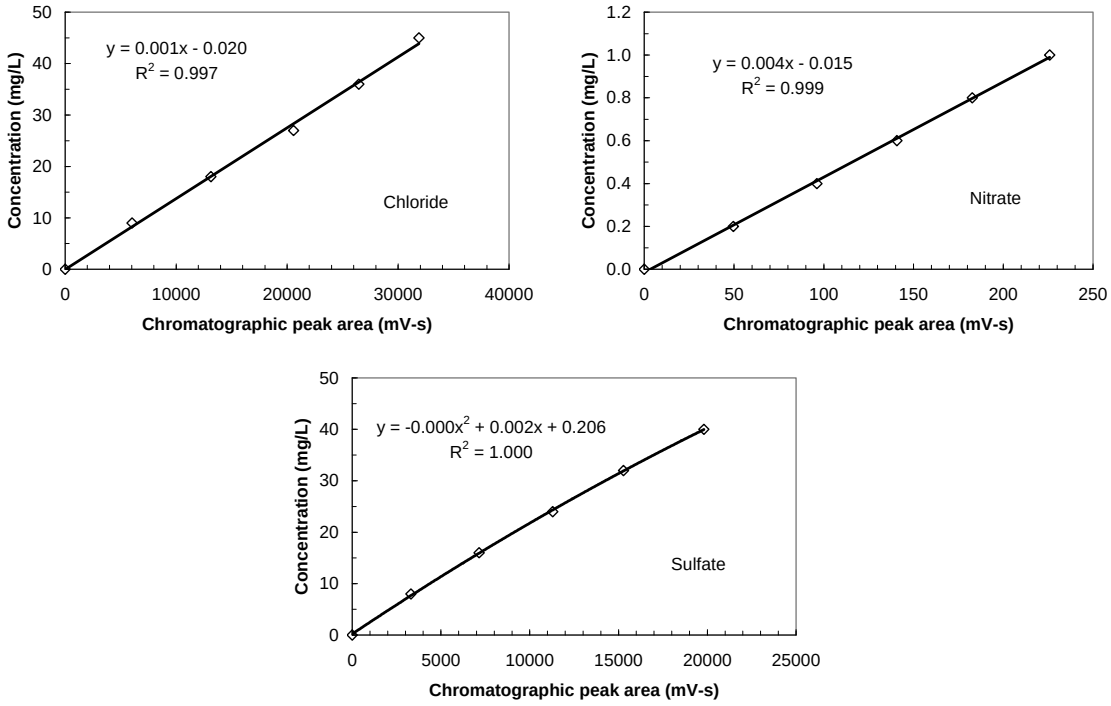

Figure 4-11. Example IC calibration standard curves for chloride, nitrate, and sulfate

4.2.8 Inductively coupled plasma – optical emission spectroscopy (ICP-OES)

The remaining 8 mL dilutions retained from above for ICP analysis were acidified (2% by volume) with the addition of 160 µL of concentrated (70%) nitric acid. The concentrations of cations in solution were determined using a Varian 710-ES ® ICP Optical Emission Spectrometer (OES) with a SPS 3 Autosampler and *ICP Expert II*® software (v. 1.1), according to Standard Methods (Eaton *et al.* 2005, §3125). Argon was used as the nebulizer propellant, and wavelengths analyzed in the OES for each cation are presented in Table 4-3. Example standard curves for calcium, magnesium, and sodium by ICP are shown in Figure 4-12.

Table 4-3. Elements and wavelengths analyzed by ICP-OES

Element	Wavelengths (nm)		
B	249.678	249.773	
Ca	315.887	317.933	
K	766.490	769.897	
Mg	280.270	285.213	
Na	588.995	589.592	
Si	250.690	251.611	288.158
Sr	407.771	421.552	460.733

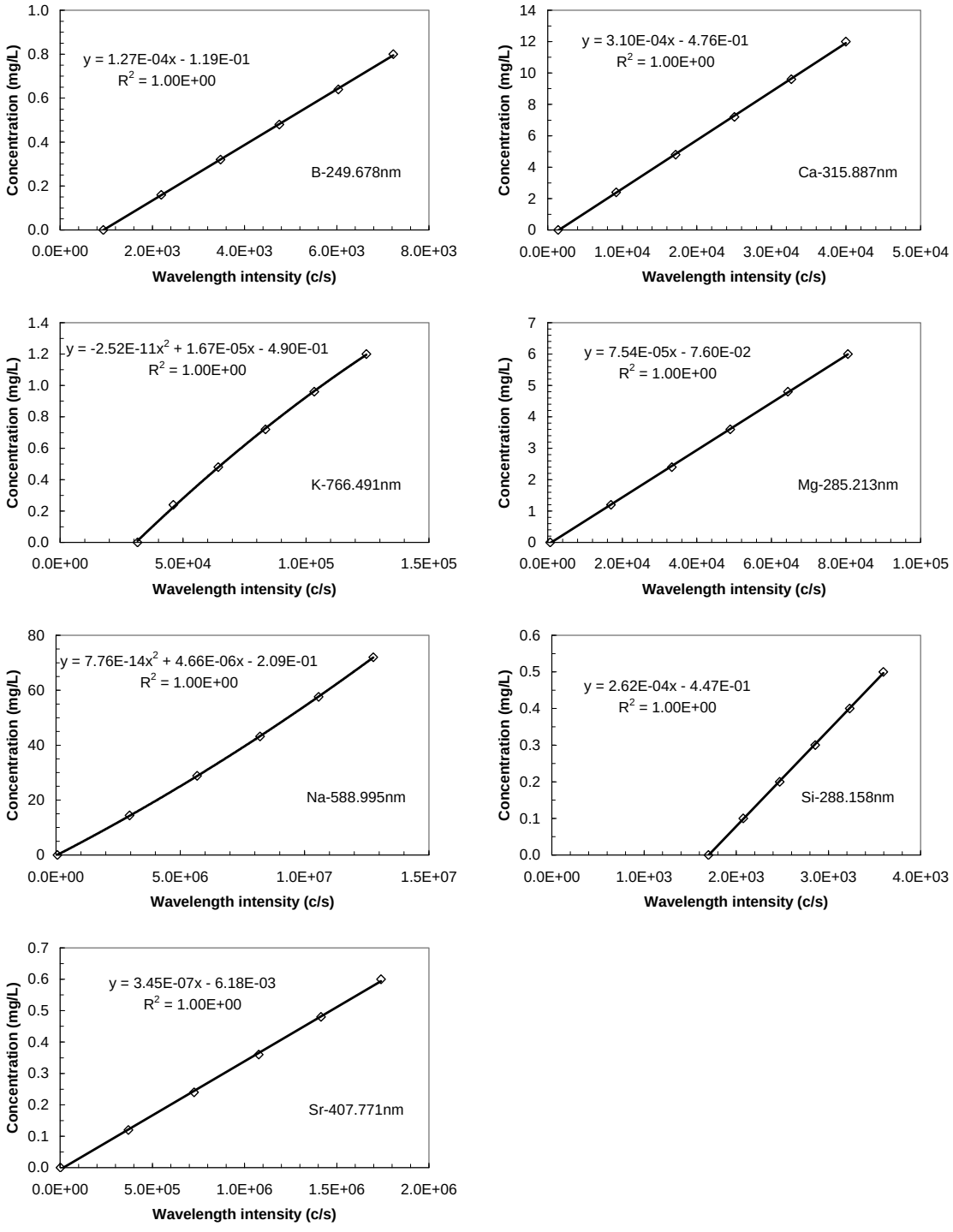

Figure 4-12. Example ICP calibration standard curves for B, Ca, K, Mg, Na, Si, and Sr

5 Results

5.1 Brackish water analysis

The source water used for this study was the concentrate stream from a brackish water RO desalination plant. For much of the initial experimentation, a synthetic approximation of this water was made in the laboratory based on the reported raw water ion concentrations, assuming 75% recovery. The synthetic water was used in an effort to obtain approximate and reproducible results before direct analysis of the natural water. The natural water taken as concentrate from the North Cameron Regional Water Supply Corporation (NCRWSC) RO plant was analyzed in the laboratory, and the calcium and total carbonate concentrations were compared to the synthetic water. For both species, the natural concentrate water was measured to be within 5% of the calculated synthetic water recipe.

Using the software Visual MINTEQ (version 2.61, 2009), an aqueous equilibrium modeling software which accounts for ion-pair (complex) formation, the synthetic and natural waters were determined to be supersaturated with respect to three salts: calcium carbonate, dolomite, and celestite. The degree of supersaturation as indicated by the saturation ratio (*S*) for each salt was calculated using the initial concentrations from Table 4-1, a pH of 7.8, and total carbonate concentration of 22.2 mM. These results are shown in Table 5-1.

Table 5-1 Saturation ratios of select salts for synthetic NCRWSC RO concentrate (pH = 7.8).

Salt	*S*
Calcite ($CaCO_3$)	5.6
Dolomite, ordered ($CaMg(CO_3)_2$)	5.9
Gypsum ($CaSO_4*2H_2O$)	0.9
Magnesite ($MgCO_3$)	1.7
Strontianite ($SrCO_3$)	2.1
Celestite ($SrSO_4$)	1.4

Calcite and dolomite have the greatest driving force to precipitate, while celestite is only slightly supersaturated. Immediate precipitation of all three salts is being prevented (or at least delayed) by the presence of antiscalant. Increasing the recovery of the system would increase the saturation ratios and would risk causing scale formation on the membrane surface.

Precipitation processes focused on the removal of calcium and carbonate would effectively lower the saturation ratio of calcium carbonate and dolomite, the two most supersaturated salts in the NCRWSC RO concentrate, allowing for further treatment without the risk of scale formation. To accomplish this goal, the antiscalant must be either inactivated or overcome to achieve chemical precipitation and solid/liquid separation. With this objective in view, antiscalant oxidation was investigated.

5.2 Recovery improvement by chemical treatment of concentrate waste

5.2.1 Antiscalant inactivation by oxidation or pH adjustment (synthetic water)

The synthetic water used in this research approximated the natural water in both ion concentration and antiscalant type and dose. A stock solution of the proprietary antiscalant was obtained from the North Cameron Regional Water Supply Corporation RO plant. A reported dose of 0.535 mg/L (or, since the antiscalant comes as a liquid, 2.9 μL/L) was applied to the raw water which results in 2.15 mg/L accumulation in the concentrate. For all analyses done on the synthetic water, a dose of 2.15 mg/L was applied (unless otherwise stated).

To determine an optimal ozone application dose for the oxidation of the antiscalant, varying amounts of ozone were applied, and the resulting phosphate released into solution was measured. These oxidation experiments were all conducted at the initial pH of 7.8. Since the chemical formula or structure of the proprietary antiscalant was not revealed by the manufacturer, the maximum release of phosphate was taken to be the maximum measured in solution after significant ozone application (*e.g.*, 45 mg/mg ozone to antiscalant). Because this method was employed, fractional oxidation as measured by phosphate should be understood as the fraction of maximum oxidation feasible with ozone and not necessarily the fraction of full antiscalant mineralization. The results of ozone-dose optimization experiment can be seen in Figure 5-1.

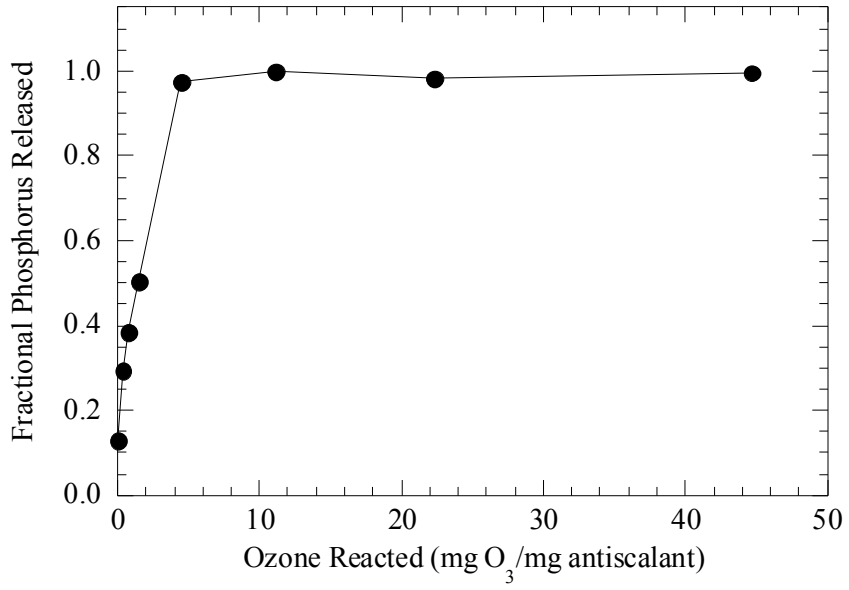

Figure 5-1. Ozone efficiency at antiscalant oxidation (synthetic water).

To achieve nearly complete antiscalant degradation, a dose of approximately 4.5 mg/mg (ozone to antiscalant) was required. Application of approximately 11 mg/mg caused the release of approximately 0.54 mg/L PO_4-P from the sample that contained 2.15 mg/L antiscalant, which is approximately 0.25 mg/mg phosphorous to antiscalant. Further ozonation beyond this point achieved a negligible increase in antiscalant oxidation. Thus, a dose of 11 mg/mg was applied in subsequent experimentation to determine an optimal peroxone ratio. Samples were dosed with varying concentrations of hydrogen peroxide at this constant ozone dose and the same pH of 7.8.

Combining ozone with hydrogen peroxide is known to increase the hydroxyl radical formation rate and thus increase oxidation in many applications. An optimal ratio between zero and one would be expected, but the results in Figure 5-2 do not match that expectation.

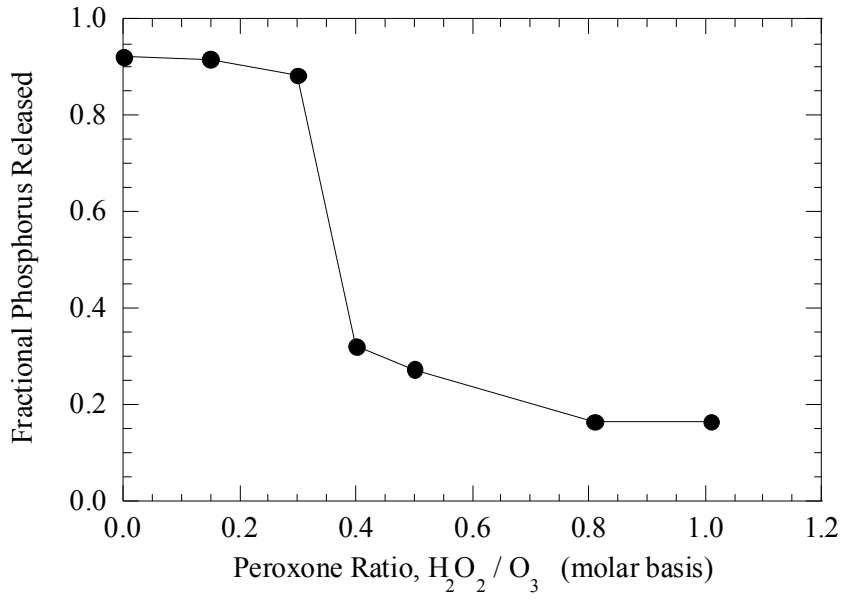

Figure 5-2. Impact of peroxone ratio on antiscalant oxidation efficiency (synthetic water).

Contrary to the expected benefit of peroxide addition, a decrease in oxidation efficiency is observed. For peroxide:ozone ratios equal to or greater than 0.4, a dramatic reduction in oxidation occurred. One possible explanation for this decrease is that the antiscalant itself is an active promoter of hydroxyl radical formation. As the hydrogen peroxide concentration increased, less ozone reacted with the antiscalant itself, thus reducing the efficiency of the overall process. In any case, it is apparent that optimal oxidation of the antiscalant is achieved at 11 mg of ozone per mg of antiscalant with no hydrogen peroxide addition at pH 7.8. Adjusting the pH prior to oxidation may have significant impacts on this optimization but was not investigated in this research.

Having found the optimal conditions for the oxidation of the antiscalant, an appropriate range of application for this process must be determined. Chemical softening processes typically require an increase in pH to precipitate a substantial fraction of calcium and carbonate ions from solution. As the pH increases, a corresponding increase in the saturation ratio of carbonate salts occurs because of the conversion of HCO_3^- to CO_3^{2-}, as shown in Figure 5-3. These saturation ratios increase dramatically between a pH of 7 and 10 because, in this range, the HCO_3^- is converted to CO_3^{2-}, raising the dissolved CO_3^{2-} concentration.

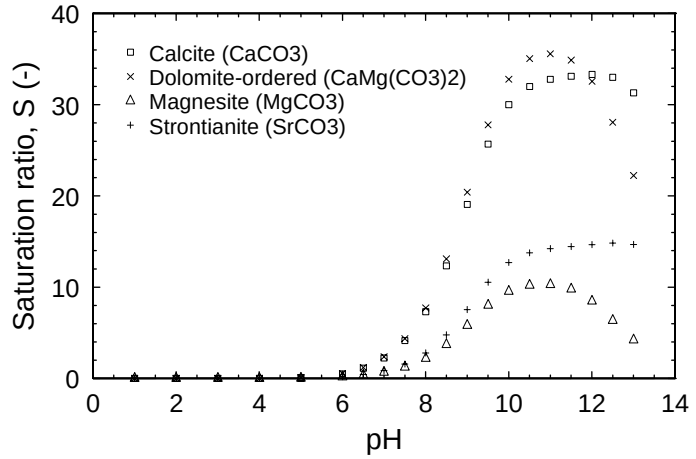

Figure 5-3. Saturation ratio dependency on pH for select carbonate salts in NCRWSC RO concentrate.

At lower saturation ratios, antiscalants are able to prevent precipitation to varying degrees. To demonstrate this function, pairs of samples (one with and one without antiscalant addition) were brought to several selected saturation ratios. These ratios were controlled by the addition of NaOH to reach a predetermined pH value and corresponding saturation ratio. Figure 5-4 shows the resulting fractional calcium removal for these experiments.

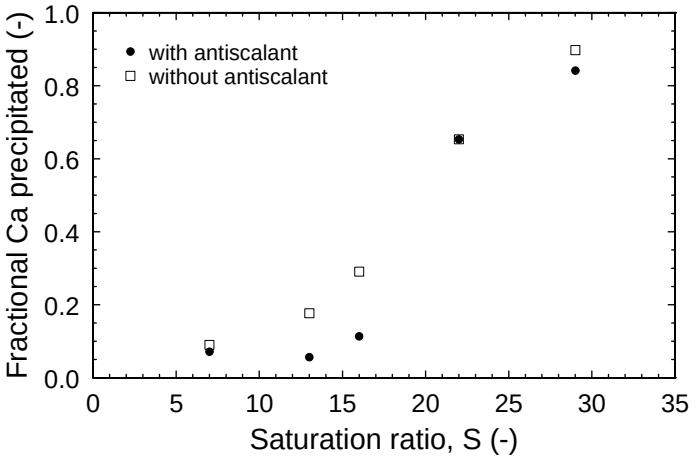

Figure 5-4. Effective antiscalant functional range (synthetic water).

The presence of antiscalant results in a decrease in calcium removal for almost every saturation ratio tested. This difference in removal is the effective function of the antiscalant. At the smallest saturation ratio chosen (7), the driving force to precipitate is very small. With such a small driving force, only a small fraction of calcium was removed regardless of antiscalant addition. Conversely, at the largest saturation ratio chosen (29), the driving force to precipitate is quite large, and a large fractional calcium removal was observed regardless of the presence of antiscalant. Between these two extremes, a range of saturation values (approximately 13 to 18) shows a relatively substantial decrease in calcium removed when antiscalant is present. In this

range, the function of the antiscalant, which was once advantageous in the RO process, must be overcome in the softening process.

Although the optimal conditions for the oxidation of the antiscalant have been shown, the ability of oxidation to inactivate the function of the antiscalant has not been demonstrated directly. To test for antiscalant inactivation, further experimentation was performed at saturation ratios of 16 and 29. For each saturation ratio, three samples were analyzed: one without antiscalant applied, one with 2.15 mg/L antiscalant applied, and one with 2.15 mg/L antiscalant applied and oxidized with 11 mg of ozone per mg of antiscalant (no peroxide). The calcium and carbonate concentrations were measured before and after precipitation to determine the amount of precipitation that occurred. The precipitation results for a saturation ratio of 16 (*i.e.*, pH = 8.7) are shown in Figure 5-5. The scale of the ordinate reflects the fact that the solution had 15.3 mM of calcium (Ca) and 22.2 mM of total carbonate (C_t), so that the maximum possible precipitation would be 15.3 mM.

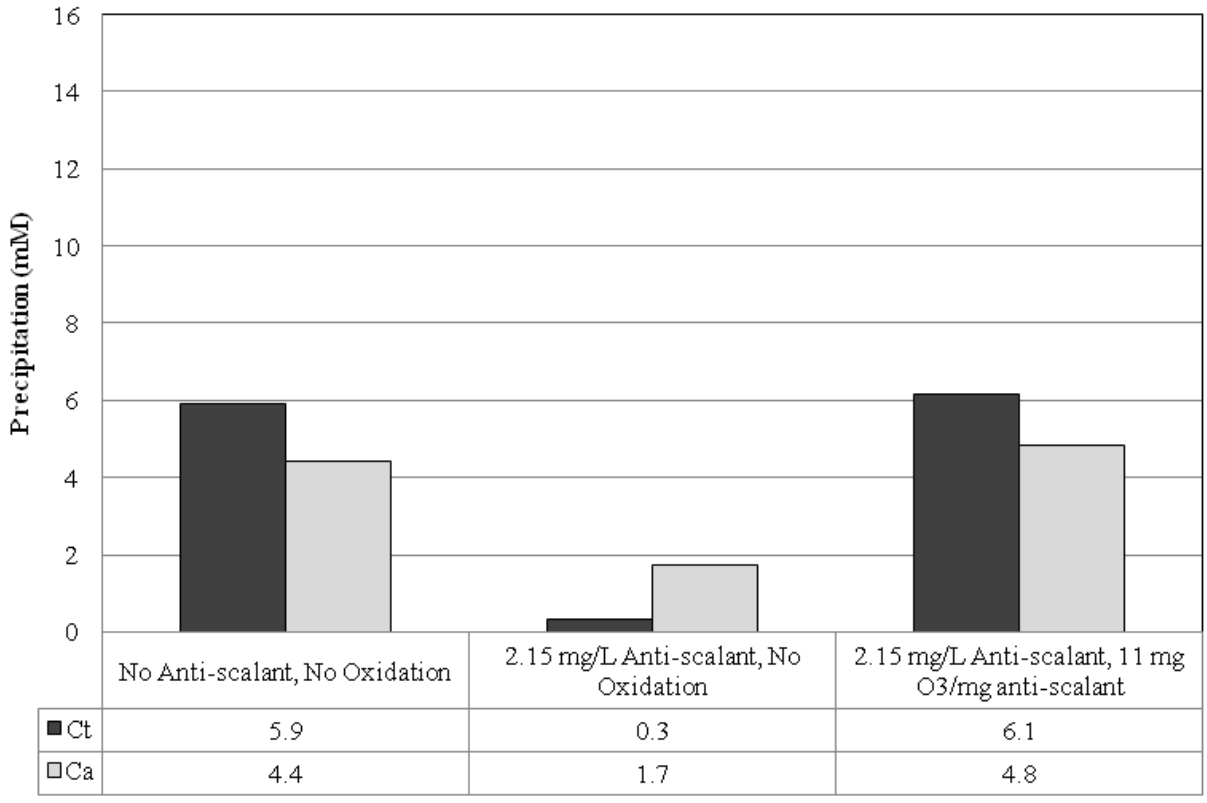

Figure 5-5. Benefit of antiscalant inactivation; *S* = 25, pH = 8.7 (synthetic water).

By comparing the first two samples on Figure 5-5, the function of the antiscalant as shown in Figure 5-4 is confirmed. At the saturation ratio of 16, antiscalant presence causes a dramatic reduction in precipitation. Further comparison of the third (ozonated) sample demonstrates the effective benefit of antiscalant oxidation on precipitation. The precipitation observed is nearly identical to the sample with no antiscalant addition, indicating that antiscalant oxidation (as achieved by optimal ozone application) is successful at completely inactivating the function of the antiscalant. The softening process may be greatly benefited by this inactivation, increasing

both calcium and carbonate removal. However, at such low saturation ratios, the fractional removal of calcium was only one third of the total calcium in solution. To achieve higher fractional removal, the saturation ratio must be increased. Figure 5-6 shows the function of the antiscalant and the benefit of oxidation for an identical experiment conducted at a saturation ratio of 29 (*i.e.*, pH = 9.8).

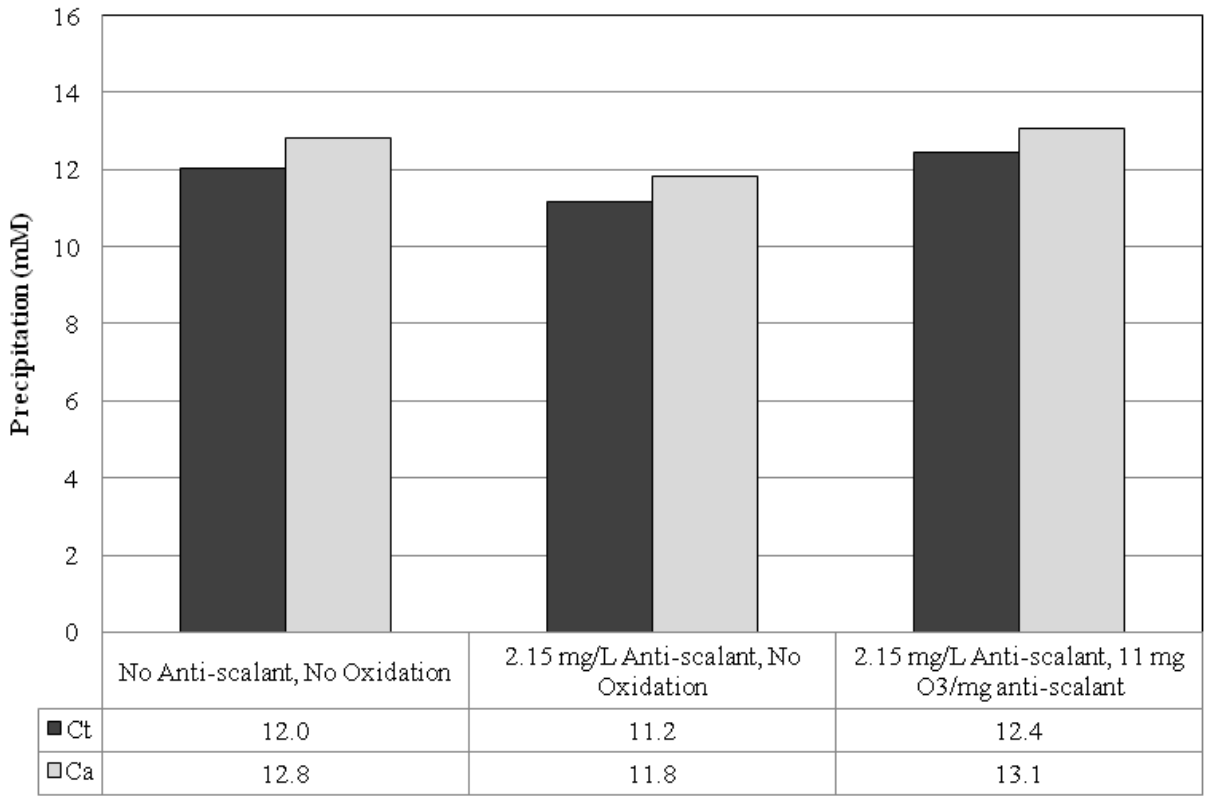

Figure 5-6. Benefit of antiscalant inactivation; *S* = 29, pH = 9.8 (synthetic water).

At this saturation ratio, a comparison of the first two samples shows a minor difference in precipitation caused by the antiscalant. In addition, the benefit of oxidation, indicated by the third sample, is also not dramatic. Actually, both the function of the antiscalant and the benefit of oxidation are observed but they are insignificant relative to the overall fractional removal of calcium (above 80%). When such a high saturation ratio is achieved in the precipitation process, the benefit of antiscalant inactivation is rendered relatively insignificant. Antiscalant oxidation, therefore, is also unimportant under these conditions. To confirm and expand these initial results obtained with the synthetic water, subsequent experimentation was necessary using the natural water taken directly from the RO plant effluent, as described in the following section.

5.2.2 Antiscalant oxidation (natural water)

The optimal ozone application to most effectively degrade the antiscalant was determined with the synthetic water to be 11 mg of ozone per mg of antiscalant. To confirm that this finding is appropriate for field application, natural water was examined. Throughout this report, the term "natural water" refers to the concentrate obtained from the North Cameron plant. The natural

water sample was analyzed to have pH=7.8, [Ca^{2+}] = 15.2 mM, and C_T = 21.2 mM, all virtually identical to the synthetic water produced in the laboratory. The primary difference between the natural water and the synthetic water was the potential presence of relatively low concentrations of several additional inorganics and the presence of natural organic matter (NOM) in the natural water. A sample of natural water was analyzed for NOM by degassing the inorganic carbon and using ICP-OES to measure the remaining organic carbon. Carbon concentration standards were prepared using acetic acid. An internal reference of 1 mg/L scandium was used in all analytical solutions. The results showed that approximately 0.13 mg/L of carbon in the form of NOM was present in the raw water (0.5 mg/L in the concentrate). The effect NOM would have on the oxidation process needs to be identified and understood. Figure 5-7 shows the oxidation efficiency for ozone application alone at pH 7.8.

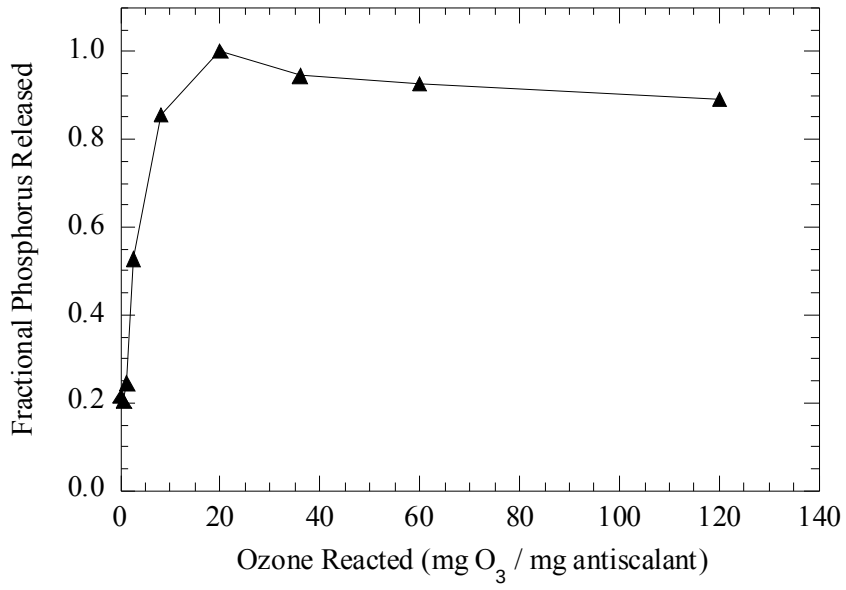

Figure 5-7. Ozone efficiency at antiscalant oxidation (natural water).

An increasing application of ozone alone results in an increasing amount of antiscalant oxidation as indicated by the release of phosphate into solution. This trend is similar to that seen with the synthetic water, with an important difference. The optimum ozone application dose normalized to the concentration of antiscalant increased from 11 mg/mg to 20 mg/mg. Approximately double the ozone dose is required to achieve a similar fractional oxidation. This increase in ozone can potentially be attributed to the presence of NOM because a portion of the ozone would oxidize the NOM instead of the antiscalant, and the rest would oxidize the antiscalant.

Next, the addition of hydrogen peroxide to achieve peroxone treatment was analyzed with the natural water. The results of the synthetic water indicated that peroxide was not beneficial to the process. A reproduction of those results with the natural water would serve as adequate confirmation necessary to recommend no peroxide in the treatment scheme. As seen in Figure 5-8, the experiment was repeated by varying the peroxone ratio at a constant ozone application dose (20 mg O_3 / mg antiscalant) at pH 7.8.

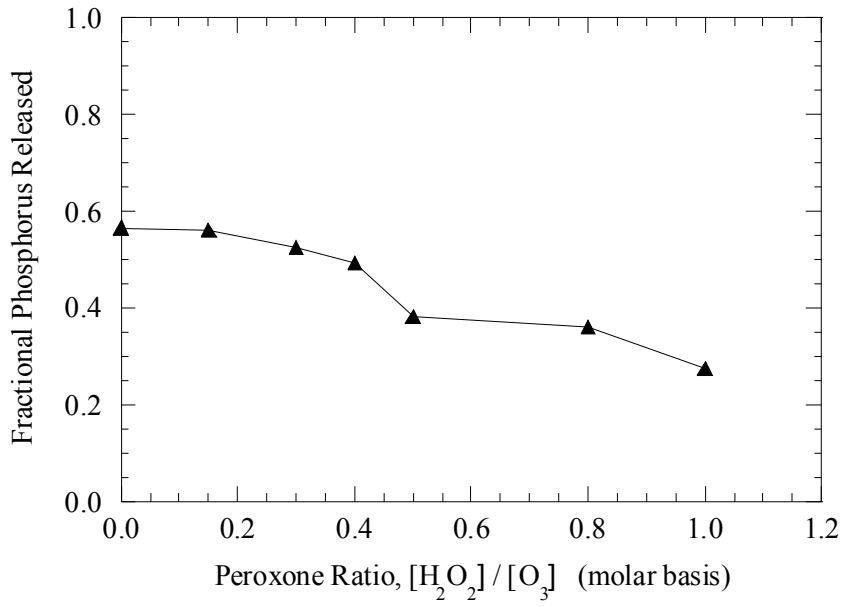

Figure 5-8. Impact of peroxone ratio on antiscalant oxidation efficiency (natural water).

Once again, an increase in peroxone ratio was detrimental to the oxidation of antiscalant. A steady decrease in oxidation is observed, presumably for the same reason mentioned in the discussion of the synthetic water results (*i.e.*, the effect on hydroxyl radical formation rates). A decrease in maximum oxidation efficiency is also observed (potentially due to the presence of NOM) by comparing Figure 5-2 with Figure 5-8 (0.9 versus 0.6 fractional phosphate released in the synthetic and natural waters, respectively). Although these issues are important in understanding the oxidation process, an optimum oxidation scheme based on these results would clearly not include hydrogen peroxide dosing at pH 7.8. With this understanding of the oxidation efficiency, experimentation was performed with natural water to determine and optimize the potential benefits of antiscalant oxidation in practical application.

Antiscalant oxidation was shown on the synthetic water to significantly prevent precipitation under certain conditions. This function must also be reproduced and confirmed on the natural water source. To accomplish this objective, a more thorough study of the function of antiscalant at varying saturation ratios was conducted using effluent from the NCRWSC RO plant. These saturation ratios were controlled by the addition of NaOH to predetermined pH and associated saturation ratio. At each saturation ratio, two samples were tested. Both samples contained a supplied dose of antiscalant (approximately 1.2 mg/L), but only one sample was oxidized at the previously determined optimal ozone dose (20 mg/mg ozone to antiscalant). The benefit (or relative insignificance) of this oxidation at each saturation ratio can be seen in Figure 5-9.

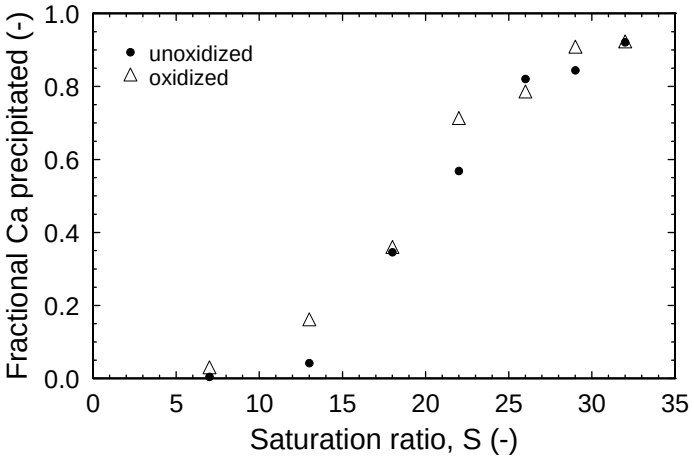

Figure 5-9. Effective benefit of antiscalant oxidation (natural water).

At the lowest saturation ratio, the effect of antiscalant inactivation is not beneficial because the driving force of precipitation is not large enough to force immediate calcium removal even without a functioning antiscalant. At very large saturation ratios (above 26), the driving force of precipitation is quite large and the benefit of antiscalant inactivation is insignificant. While oxidation may cause a noticeable difference in precipitation at these high ratios, this difference is minor relative to the fractional removal of calcium. Within the range of saturation ratios from 13 to 22, however, antiscalant inactivation does result in significant benefit in terms of the overall removal of calcium. At a saturation ratio of 13, for instance, nearly four times the amount of calcium is removed after antiscalant oxidation. Based on these observations, the saturation ratio necessary to achieve the desired calcium removal determines whether antiscalant oxidation is a beneficial treatment step.

To optimize the precipitation process, the optimal removal of calcium (and carbonate) must be achieved which reduces the saturation ratios of calcium carbonate and dolomite in the product water as far as possible before reaching a point of diminishing returns. According to Figure 5-9, a potential range of optimal operation would be from a saturation ratio of 26 to 32. At this range of saturation, the driving force of precipitation is large enough to render the benefits of antiscalant oxidation insignificant. Based on these considerations, an optimal softening process without antiscalant oxidation was chosen for continuous-flow analyses both in the laboratory and on-site at an existing RO plant.

To gain further insight into the precipitation chemistry of this softening process, another set of jar tests were conducted at various saturation ratios. The product water was filtered (0.22 μm) and analyzed for precipitation of total carbonate by alkalinity and precipitation of calcium, magnesium and strontium using a Varian 710-ES ICP Optical Emission Spectrometer. An internal reference of 1 mg/L scandium was used in all analytical solutions. Figure 5-10 presents a comparison of the molar precipitation of these four species for samples without oxidation.

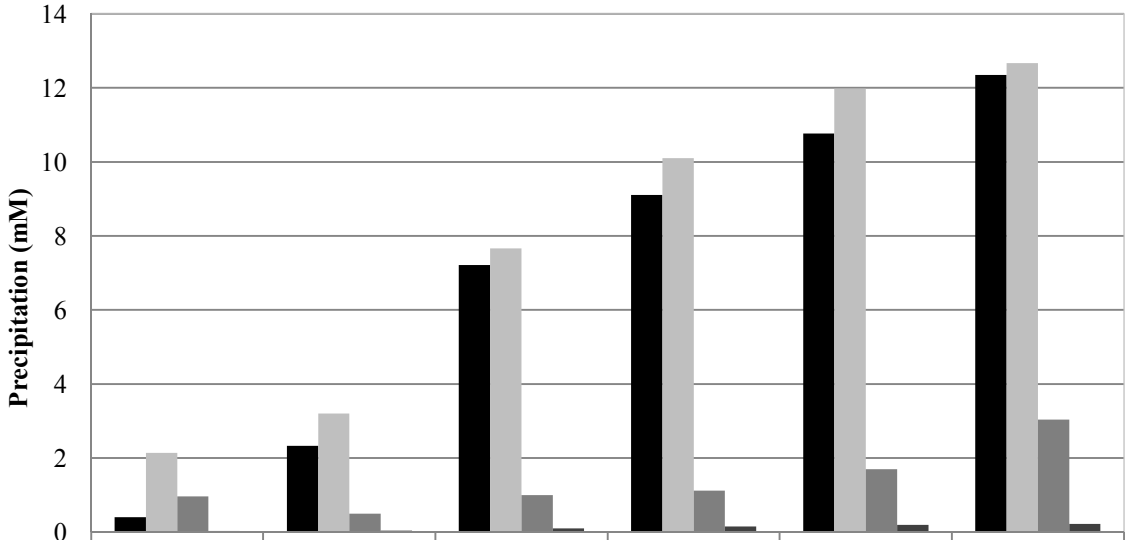

	S = 13, pH = 8.5	S = 18, pH = 9.0	S = 22, pH = 9.3	S = 26, pH = 9.6	S = 29, pH = 9.8	S = 32, pH = 10.5
Ct	0.40	2.33	7.21	9.11	10.77	12.35
Ca	2.14	3.20	7.66	10.10	11.98	12.67
Mg	0.96	0.50	1.00	1.12	1.70	3.04
Sr	0.03	0.04	0.10	0.15	0.19	0.22

Figure 5-10. Comparison of total carbonate, calcium, magnesium and strontium precipitation (natural water).

In all cases shown in Figure 5-10, the molar calcium precipitation was greater than the corresponding molar carbonate precipitation. Precipitation of less carbonate than calcium indicates that dolomite ($CaMg(CO_3)_2(s)$) must not have precipitated because the precipitation of dolomite would remove twice as much carbonate than calcium. On the other hand, the greater precipitation of calcium than carbonate suggests possible precipitation of other calcium salts (*e.g.,* gypsum, $CaSO_4(s)$) in addition to calcium carbonate. Molar sulfate precipitation was not measured to confirm this assumption. This understanding of the precipitation chemistry is verified by the relatively small removal of magnesium shown in Figure 5-10 and by the understanding that, in very saline waters, dolomite is difficult to form because of the "precise Ca-Mg ordering required" (Folk and Land 1975). Magnesium was measured to be 12.5 mM before precipitation, indicating that less than approximately 10% precipitates at nearly all saturation ratios. At a saturation ratio 32, the magnesium removal increased significantly because of the formation of magnesium hydroxide ($Mg(OH)_2(s)$), which forms at higher pH. This sample (S=32, pH=10.5) was observed to have gelatinous flocs distinguishably different than calcium carbonate or dolomite in appearance and ability to settle.

In addition to these observations, the removal of strontium was also quantified in Figure 5-10. An increasing removal of strontium occurred for increasing saturation ratios, and the maximum removal was about two-thirds (0.22 mM of 0.31 mM). Although this molar removal is quite small relative to the removal of other species, strontium has the potential for increasing

nucleation site and scale formation so its removal is of potential importance in relation to further membrane treatment.

5.2.3 Continuous-flow softening (thermodynamic modeling)

The continuous-flow softening portion of this study was designed to demonstrate the feasibility of the practical application of the treatment scheme being developed. To meet this objective, initial experimentation conditions were chosen that would achieve maximum calcium and carbonate removal from the synthetic water. Successful operation at this level would indicate that lesser removal is also attainable (as shown in subsequent experimentation). A saturation ratio of 36 was initially tested with the goal of demonstrating over 90% removal of both calcium and carbonate.

To achieve such a high fractional removal of both calcium and carbonate, the molar concentrations of each ion must be approximately the same (assuming removal of calcium carbonate, $CaCO_3(s)$. Appropriate proportions of lime ($Ca(OH)_2$) and soda ash (Na_2CO_3) were determined and dosed to reach this equality and the desired saturation ratio. These two chemicals were chosen based on economical considerations for practical application. The initial water being treated contained approximately 15 mM calcium and 22 mM total carbonate (C_t). Addition of 11 mM lime and 5 mM soda ash was chosen to achieve a saturation ratio of 36 (and a pH of 9.6) with an approximate equality of total calcium and carbonate concentrations (26 mM and 27 mM, respectively).

Under the conditions described above, MINEQL+ (version 4.5, 2001) was utilized to examine the theoretical removal of calcium carbonate. The concentration of all species (after the addition of lime and soda ash) were input into the program, and Figure 5-11 was generated describing the fraction of calcium present in various forms over a range of pH (corresponding to a range of saturation ratios).

At the initial pH of 7.8, the solution is primarily supersaturated with respect to calcite and dolomite, but precipitation is being prevented by the presence of antiscalant. As pH (and saturation ratio) increases, the fractional calcium distribution becomes dominated by calcite formation, which would overcome the antiscalant. This finding agrees with the understanding that saturation ratio is the driving force of calcium and carbonate removal through the precipitation of calcium carbonate. For a pH of 10.2 (S=41), virtually complete calcium precipitation is predicted (mainly as calcite), giving theoretical confirmation for the objective to demonstrate maximum calcium and carbonate removal with practical and economical chemical addition.

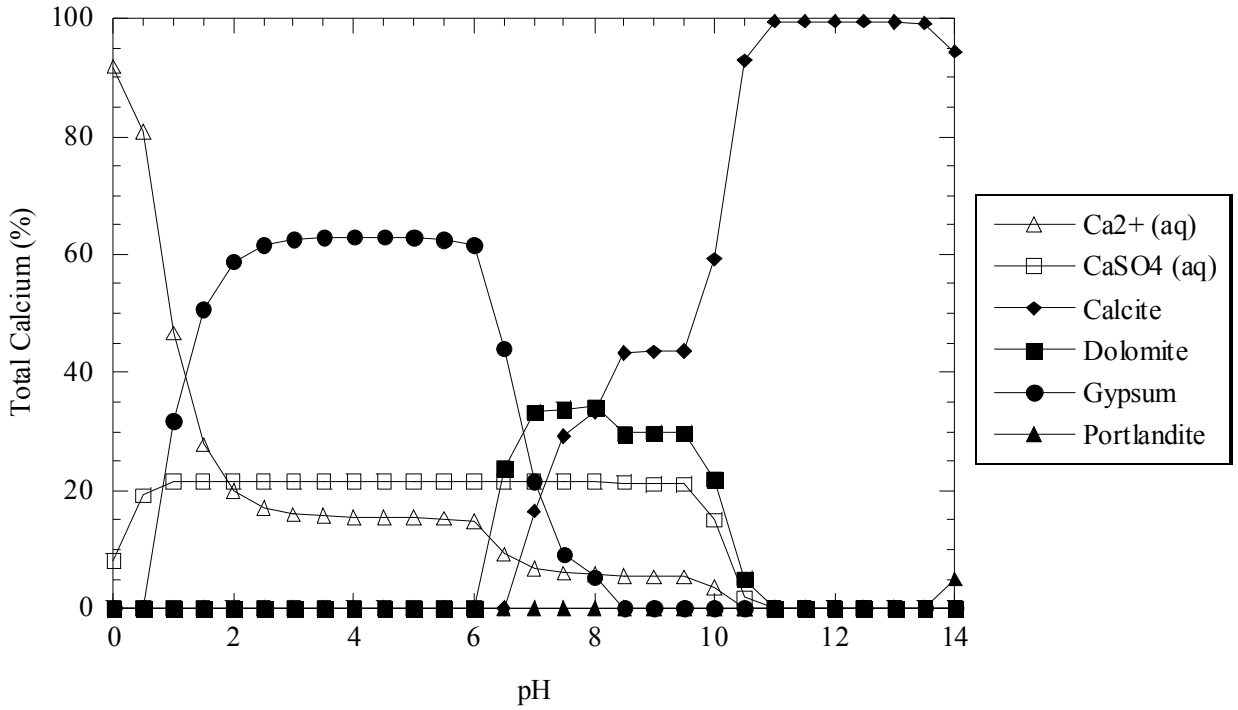

Figure 5-11. Calcium precipitation potential (11 mM lime, 5 mM soda ash added to concentrate).

Once this removal is achieved, the remaining ions in solution are expected to be at such a reduced concentration that additional precipitation can be prevented with a reduction in pH and a fresh dose of antiscalant. Further membrane treatment and recovery should then be feasible without the risk of scale formation. A second analysis with MINEQL+ software was performed to confirm this feasibility. Assuming a 90% removal of calcium and an identical molar concentration of total carbonate (C_t) removal, the product water was analyzed for potential precipitation of the remaining calcium ions (as calcite or dolomite). Figure 5-12 is the resulting calcium distribution.

Assuming that the pH of the product water is reduced to below a pH of 7 after the softening process, the calcium distribution theoretically confirms that no further calcite or dolomite would precipitate. Antiscalant could then be re-dosed and subsequent membrane treatment would be feasible with reduced risk of scale formation. With these confirmations, the synthetic water continuous-flow softening experimental results can now be considered.

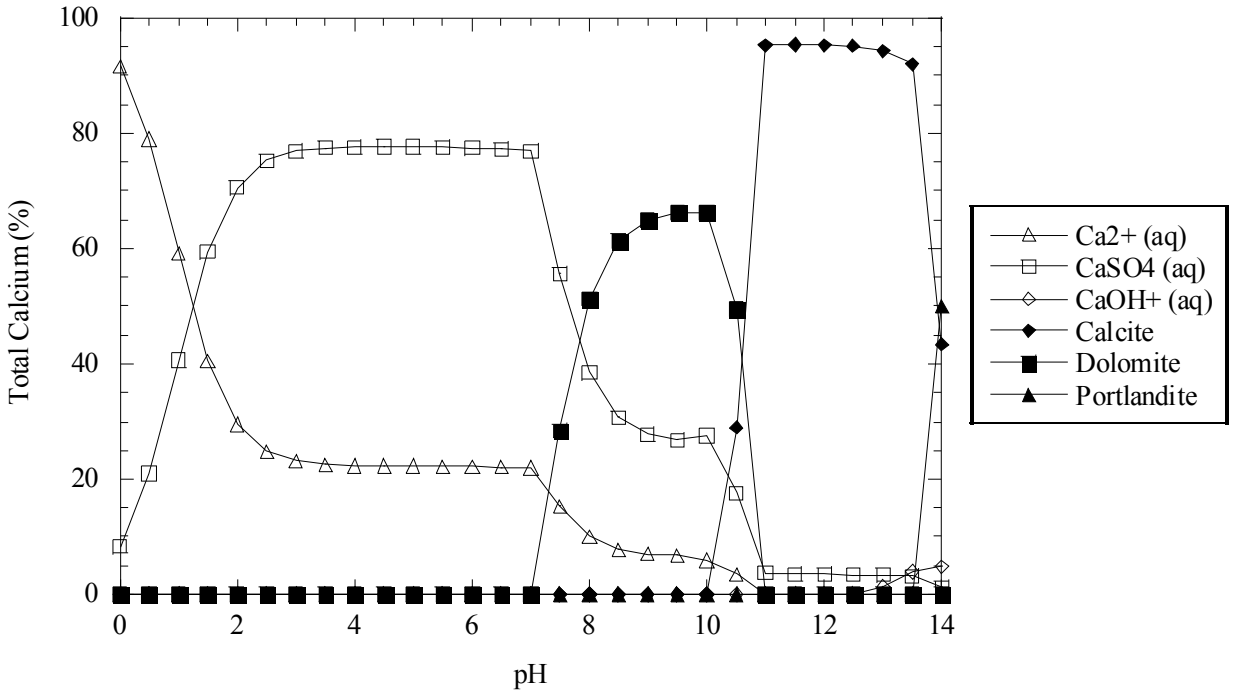

Figure 5-12. Calcium precipitation potential (after 90% calcium removal as calcium carbonate).

5.2.4 Continuous-flow softening (synthetic)

The three objectives of the synthetic water continuous-flow softening experimentation were to demonstrate sufficient calcium and carbonate removal, to demonstrate the ability to obtain mass balance closure accounting for all the solids entering and leaving the system, and to determine the ease of settling and removing solids from solution (*i.e.*, solid/liquid separation). These three objectives are addressed in this section.

Figure 5-13 illustrates the effluent quality of samples taken every 30 minutes over the 3.5 hour experimental run. The saturation ratio prior to precipitation was 36, obtained by the addition of 11 mM lime and 5 mM soda ash. Calcium and carbonate concentrations were measured before and after precipitation and the differences (representing the amount of precipitation) are plotted as a percentage of their initial value.

The results indicate that slight variations in the fractional removal occurred in the first three samples. Based on this observation, steady state conditions were not achieved until 120 minutes after the initiation of the experiment. Once steady state was achieved, the fractional removals of both calcium and carbonate were above 90%. The first primary experimental objective was successfully achieved.

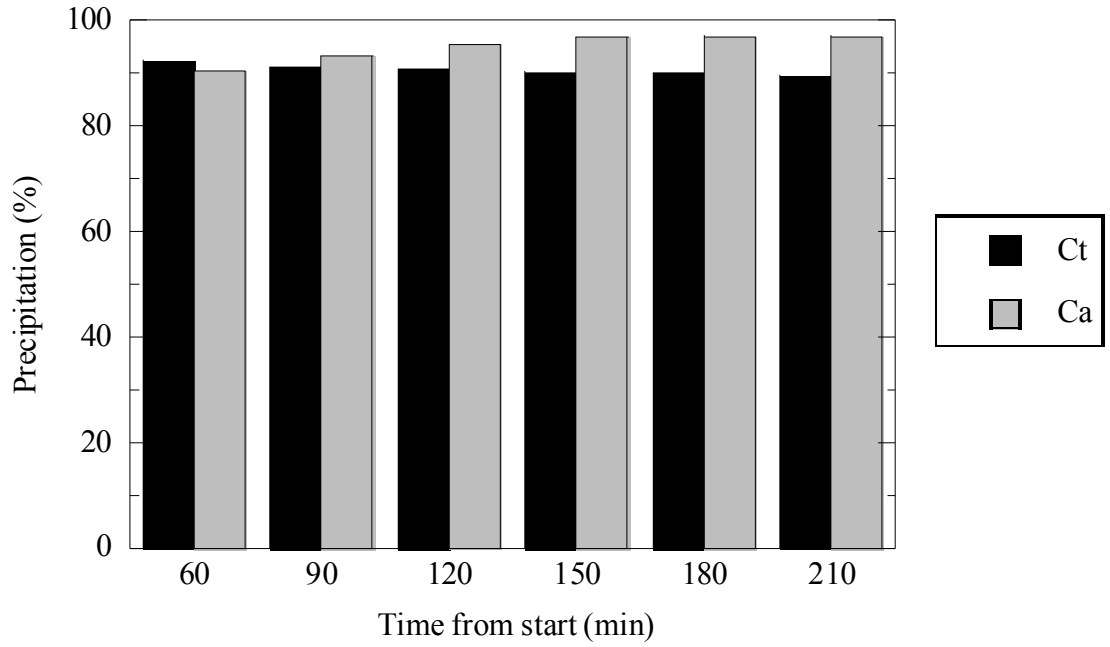

Figure 5-13. Calcium and carbonate removal efficiency (synthetic water).

With respect to a mass balance closure of the solids, influent solids were mainly composed of total dissolved solids (TDS) in the synthetic water (approximately 15 g/L), including the contribution of lime and soda ash addition. Effluent solids included the remaining TDS, the total suspended solids (TSS) in the effluent, and the mass of precipitate that settled and accumulated in the reactor. Figure 5-14 gives a breakdown of total effluent solids, including solids removed (TSS and accumulation in reactor), solids remaining in solution (TDS), and solids unaccounted for.

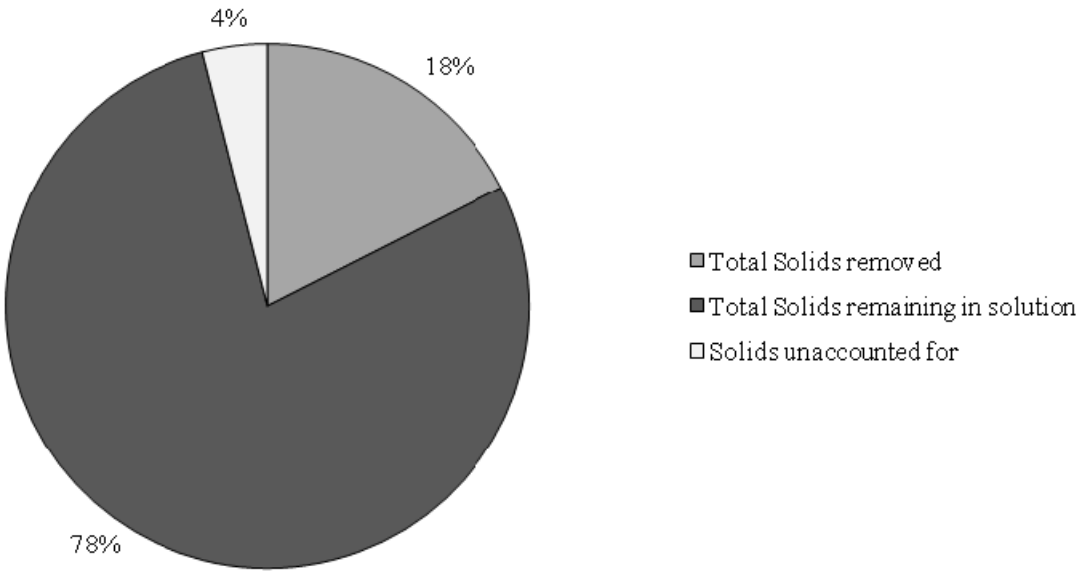

Figure 5-14. Effluent solids mass balance in the continuous flow precipitation experiments (synthetic water).

The primary importance of Figure 5-14 is to show that nearly all (96%) of the influent solids are accounted for as either solids removed (TSS or accumulation in reactor) or solids remaining in solution (TDS). Another important detail to observe is that 78% of the dissolved solids remain in solution after the softening process. Since the experimental objective is to remove the most sparingly soluble ions (*i.e.*, Ca^{2+} and CO_3^{2-}), the remaining majority of the solids are not targeted for removal. This result is acceptable because an additional RO step could remove the remaining dissolved solids with little risk of scale formation on the membrane surface.

Finally, the ease of solid/liquid separation was determined from this experiment. As described in Chapter 4, the continuous-flow softening apparatus was composed of four identical reactors in series. The first two were operated as slow mix reactors and the second two as settling tanks. Accumulation of precipitated solids was measured in both sections of the apparatus and the effluent samples were measured for TSS. These data were used to create a breakdown of total solids removed.

The total solids removed were all accounted for in the three categories. Nearly all (99%) of the solids that precipitated were removed by means of settling within the continuous-flow softening apparatus, with almost identical amounts in the slow mix reactors and in the settling tanks. The remaining 1% was measured as TSS in the effluent samples, demonstrating the ease of solid/liquid separation through settling. It should be noted that the design of this reactor was not optimized for this process; rather, an existing laboratory reactor was used. A reactor (either laboratory or full-scale) designed for this process would prevent settling in the slow mix reactors and have a larger overflow rate (flow rate per unit surface area) in the settling portion of the reactor than in the slow mix portion. Nevertheless, the use of the existing reactor demonstrated the success of this softening and settling process on a continuous basis. A more thorough analysis of the settling characteristics of the sludge is presented in the following section. Having demonstrated the application of this treatment process with synthetic water, natural water analyses must also be performed both in the laboratory and on-site to confirm these findings.

5.2.5 Continuous-flow softening (natural water)

To confirm the feasible application of continuous-flow operation of the softening process, a continuous flow system to allow precipitation of calcium carbonate followed by sedimentation was developed. For these experiments, natural concentrate samples were taken directly from the North Cameron RO plant and stored (at 4º C) for up to 15 days before being used in the laboratory. As noted earlier, initial conditions of the water were measured as follows: pH=7.8, $[Ca^{2+}]$ = 15.2 mM, and C_T = 21.2 mM. The experimental molarities of calcium and carbonate were again chosen to be equivalent for maximum fractional removal of both species. To reach these conditions, lime and soda ash were added at 9 mM and 3 mM, respectively, which yielded a pre-precipitation pH of approximately 10.1 and a final pH (after precipitation) of approximately 9.7. Effluent samples were taken every 30 minutes to determine a steady state fractional removal of calcium and carbonate. These results are shown in Figure 5-15.

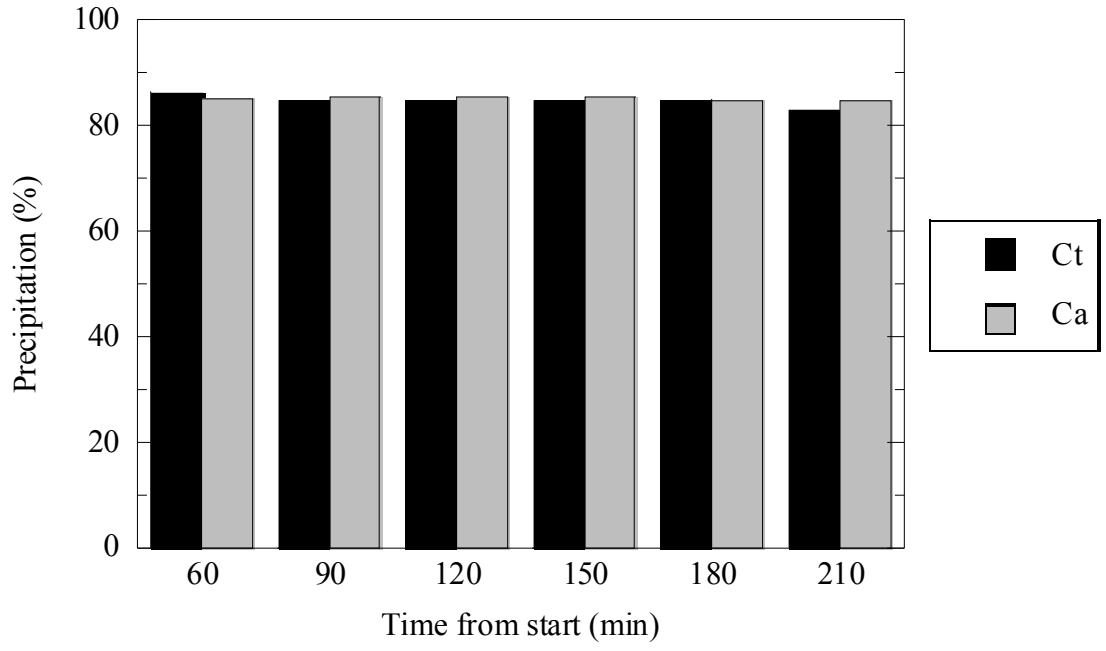

Figure 5-15. Calcium and carbonate removal efficiency (natural water).

Similar to the synthetic water results (Figure 5-13), steady state was achieved by 120 minutes from the start of the experimental run. After this point, a consistent fractional removal of approximately 84% was observed for both calcium and carbonate. The equivalent molar precipitation of Ca^{2+} and CO_3^{2-} indicates that calcium carbonate ($CaCO_3(s)$) is again the primary precipitate. The feasibility of an optimal application of the softening process on natural water has now been confirmed. At this point, a further analysis of calcium carbonate sludge characteristics must be discussed to demonstrate the ability to dewater the accumulated solids that result from this process.

The solids that accumulated from the natural water continuous-flow softening experiment were collected and used to perform a batch thickening analysis. Through the development of a solids flux curve, the ability to dewater this specific type of sludge can be estimated. A series of suspended solids concentrations were produced and allowed to thicken (Type 3 zone settling).

For each concentration, a constant velocity of the solid/liquid interface was measured and used to produce Figure 5-16. Because of the limited availability of solids, these experiments were performed in a 1-L graduated cylinder; it is well-known that larger vessels should be used for precise results, but the results obtained were sufficient to show that these solids settle very rapidly and thicken to a high solids concentration.

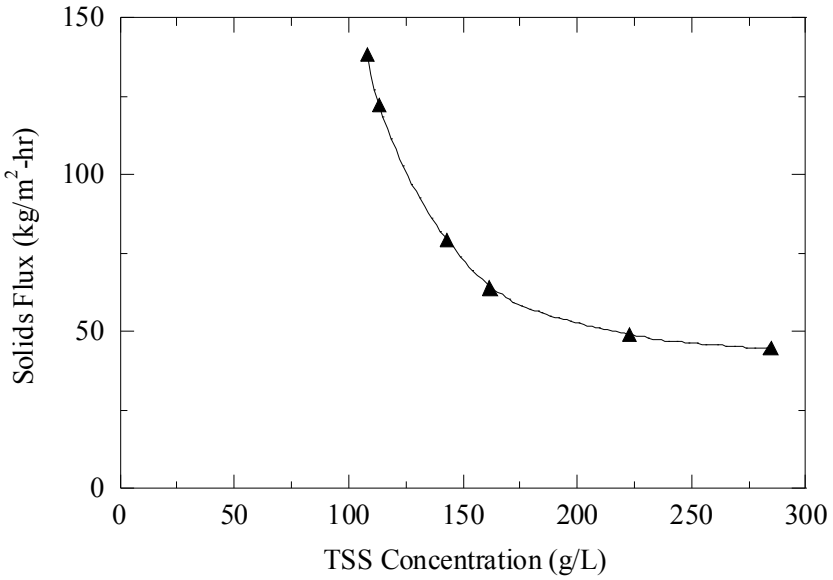

Figure 5-16. Solids Flux characteristics of calcium carbonate sludge

The limiting flux can be obtained from Figure 5-16 for a range of underflow concentrations in the thickening process. This information can be useful in determining the required cross-sectional area of the thickener once a desired underflow concentration has been chosen. The cost of increasing this area (and obtaining a higher underflow solids concentration) must be balanced with the cost of subsequent sludge handling/disposal processes. For further information, the ability to de-water calcium carbonate sludge has been thoroughly studied and a review of that literature may be necessary to determine an optimal sludge treatment scheme for any specific application.

5.2.6 Continuous-flow softening (on-site)

Initial continuous-flow experimentation was performed on the synthetic water to show evidence that maximum removal (over 90%) of calcium carbonate is feasible through the use of chemical softening. A saturation ratio of 100 was necessary to reach this goal. To demonstrate a more optimal removal of calcium carbonate (over 80%) using natural concentrate produced from a typical Texas brackish water RO plant (the North Cameron plant), a saturation ratio of 35 was used. Finally, experimentation was performed on-site at the North Cameron RO plant with a direct feed from the concentrate being produced. This experiment was performed to demonstrate the feasibility of applying this treatment process directly to the field. The following chemical conditions were chosen to reproduce the previous natural water experimentation: lime addition of 9 mM and soda ash addition of 3 mM (to produce a calcium carbonate saturation ratio of 35 at a pH of 9.7), as illustrated in Figure 4-4. Effluent samples were taken every 30 minutes and analyzed for fractional calcium and carbonate removal. The results are shown in Figure 5-17.

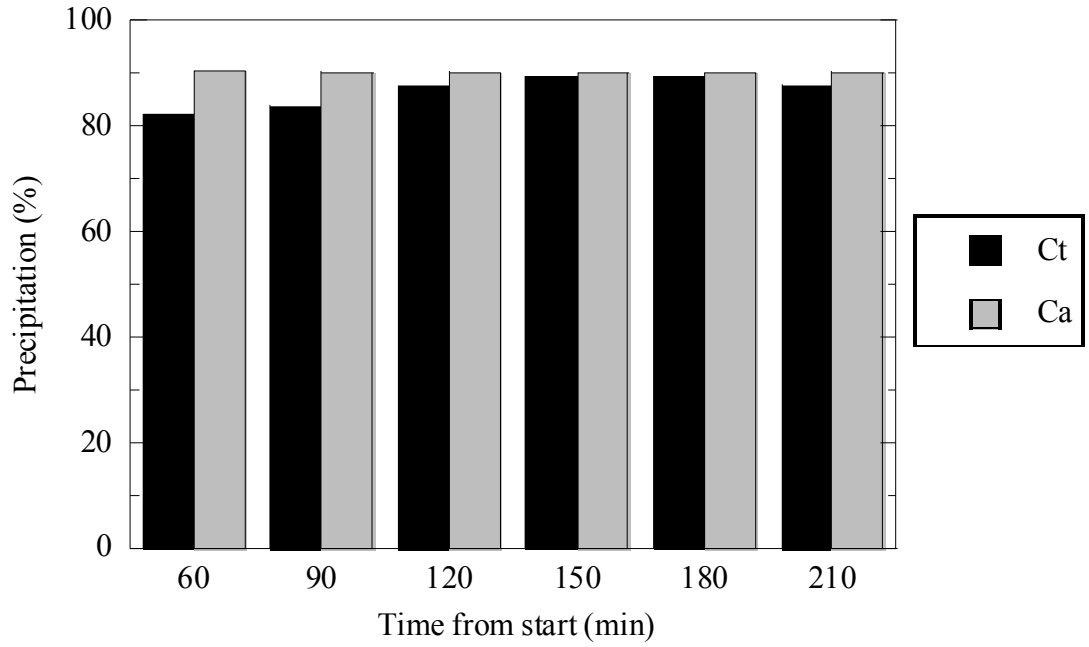

Figure 5-17. Calcium and carbonate removal efficiency (on-site).

As seen in previous results, steady state was achieved within 120 minutes of the initiation of the experiment. After this point, a consistent removal of nearly 90% of both calcium and carbonate was observed. The effluent from this process could be filtered, reduced in pH, and subjected to further membrane desalination treatment with little risk of scale formation. A comparison of Figure 5-15 and Figure 5-17 reveals an increase in calcium and carbonate removal of about 5% for the on-site experiment. These results prove the feasibility of direct application and confirm the reproducibility between the laboratory and on-site experimentation, achieving the primary experimental objectives. The treatment process has been successfully demonstrated on-site within the optimal range of conditions, strongly confirming the potential for wide-spread application.

5.3 Recovery improvement by concentrate treatment with electrodialysis

Batch-recycle electrodialysis (ED) experimentation with the apparatus described in Chapter 4 was conducted on the synthetic North Cameron Regional Water Supply Corporation (NCRWSC) RO concentrate, as well as on-site at the NCRWSC plant. A summary of the principal observations from experimental variations of electrical, hydraulic, and recovery parameters are presented here.

5.3.1 Electrical effects (synthetic)

The stack voltage drop is one of the main performance controls in electrodialysis treatment. Increasing the stack voltage increases the "force" applied to separate the ions (similar to the applied pressure in an RO unit), and as one might expect, an increase in voltage results in an increase in the rate of separation, as shown in Figure 5-18. Voltage applications ranged from moderate (0.7 V/cell-pair) to very high (1.6 V/cell-pair), but the superficial velocity through the stack was constant at approximately 4.8 cm/s for each experiment. Each experiment was started

with equal volumes of the synthetic concentrate and diluate streams with synthetic RO concentrate, which simulated a nominal concentrate recovery of 50%, assuming that the ED product could be utilized entirely (*e.g.*, by recycling to the RO feed). A concentration of 8.75 mg/L of Dequest DQ2006 antiscalant was present in the synthetic RO concentrate used in the electrodialysis experimentation. Over the course of each experiment, the conductivity (shown in part (a) of Figure 5-18 and representing the salinity of the solution) of the diluate was decreased to less than one percent of its original value, which corresponded to conductivity removal ratios (R_κ) greater than 99% (shown in part (b) of Figure 5-18). The conductivity removal ratio was calculated according to Equation 5-1:

$$R_\kappa(t) = 1 - \frac{\kappa_D(t)}{\kappa_D(0)} \tag{5-1}$$

where $\kappa_D(0)$ is the initial conductivity of the diluate solution and $\kappa_D(t)$ is the conductivity of the diluate at time t. The rate of separation was approximately constant for removal ratios less than 40% and was approximately proportional to the applied voltage.

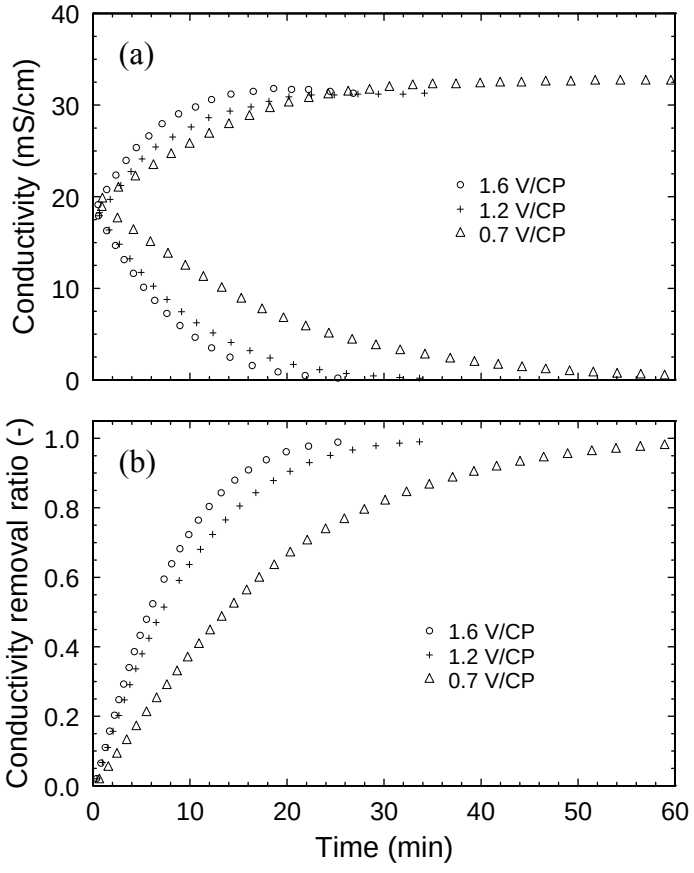

Figure 5-18. Increase in salinity separation efficiency with increase in ED stack voltage.

The concentrate and diluate reservoirs were sampled at conductivity removal ratios of 0, 20, 40, 60, 80, and 99% and subsequently analyzed by ion chromatography (IC) for anion concentrations and inductively coupled plasma optical emission spectroscopy (ICP-OES) for metal and metalloid concentrations. The concentration of most of the ions was separated nearly

proportionally as conductivity, and the rate of separation of the ions was only slightly influenced by the dramatic variation in stack voltage, as shown in Figure 5-19. Analysis of total carbonate separation by alkalinity titrations (not shown) revealed that total carbonate also was separated approximately proportional to conductivity.

The separation of sulfate is a notable exception from the trends of the other ions. Analysis of the composition of the predominant species in the NCRWSC RO concentrate by the water quality modeling software Visual MINTEQ (ver. 2.61, 2009) revealed that approximately 17% of the total sulfate was immobilized in the form of neutral ion-pairs (*i.e.*, $CaSO_4$ and $MgSO_4$), and an additional 15% of the total sulfate was restricted in the form of $NaSO_4^-$. This complexation, coupled with the fact that the diffusivity of sulfate is approximately half that of chloride, explains why the separation of sulfate is significantly slower than the other ions.

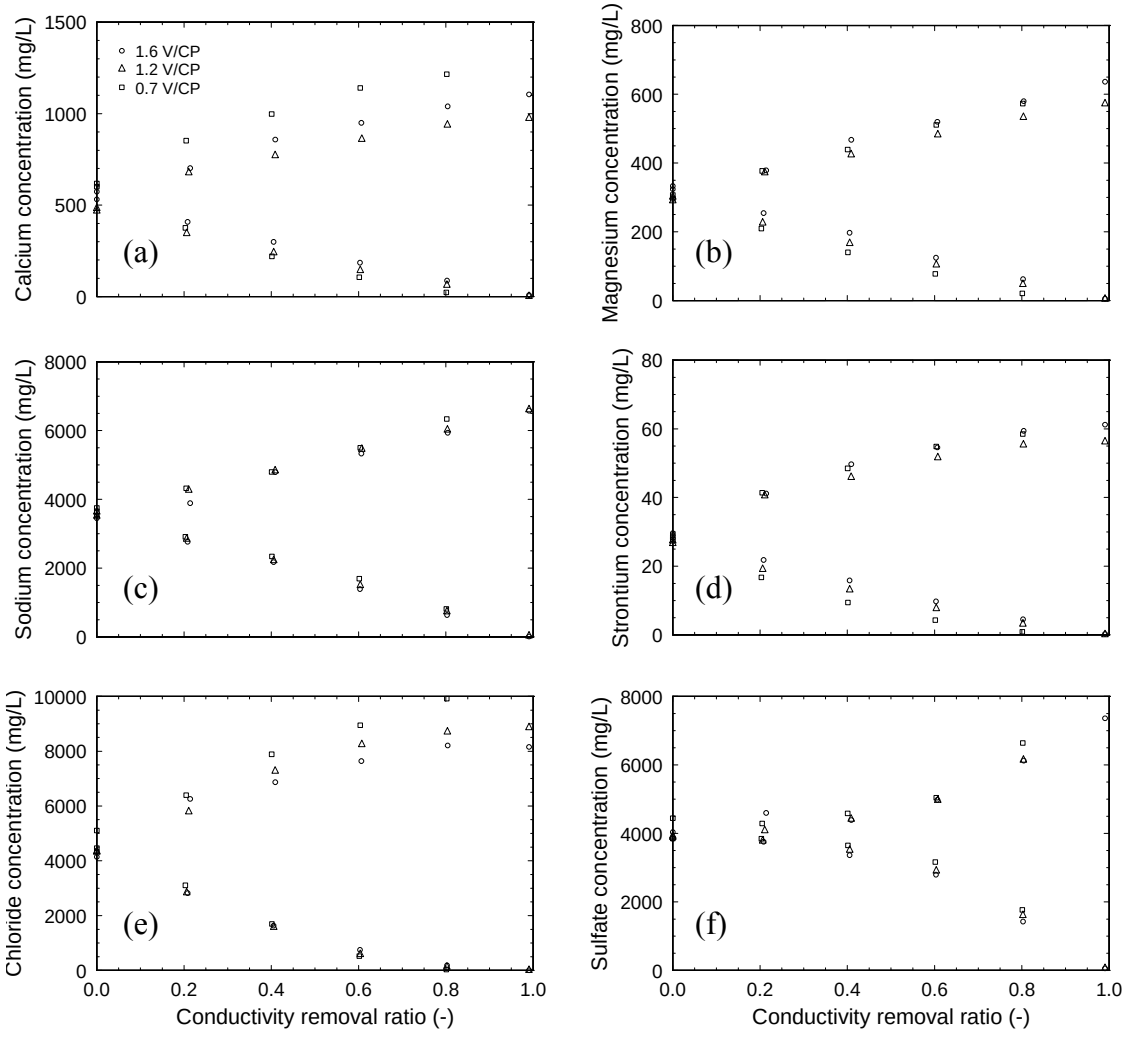

Figure 5-19. Marginal impact of ED stack voltage on separation of select ions.

However, boron and silicon concentrations (not shown) were not separated by ED because the fraction of their acid/base dissociations are essentially entirely in the neutral acid species (*i.e.*, $B(OH)_3$ and H_2SiO_3). Similarly, the pH of the concentrate and diluate streams was

approximately constant near 7.8 up to removal ratios greater than 90% and practically independent of the variation in stack voltage.

The electrical current density through the ED stack (*i.e.*, the flux of ions within the stack) was relatively stable up to removal ratios of approximately 40%, and the current density was approximately proportional to the stack voltage, as shown in Figure 5-20. At higher removal ratios, the electrical resistance of the diluate and the liquid-junction potentials across the membranes reduce the current density. At higher voltage applications, greater electrical losses are expected in the form of liquid-junction and diffusion potentials in the ion-exchange membranes and diffusion boundary layers, respectively (Newman and Thomas-Alyea 2004; Strathmann 2004).

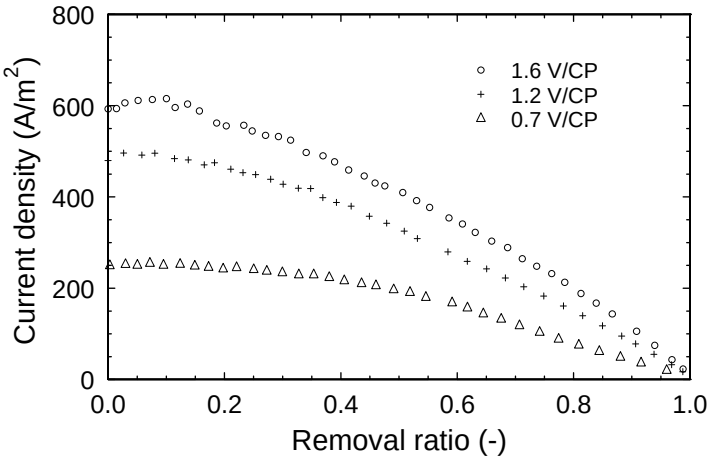

Figure 5-20. Increase in electrical current density with increase in ED stack voltage.

The electrical charge efficiency of the system was analyzed by comparing the mathematical integration of the electrical current as a function of time (*i.e.*, the total amount of electrical charge invested in the separation process) to the charge-equivalent concentration of ions separated. The analysis revealed that the charge-efficiency of this system was consistently greater than 90% (not shown), and not influenced by variation in stack voltage.

The total specific energy of the treatment process was analyzed by normalizing the mathematical integration of the power investment (*i.e.*, the summation of electrical and hydraulic power invested in migrating ions and pumping solution through the stack, respectively) by the diluate volume. The total specific energy was approximately proportional to the ED stack voltage, as shown in Figure 5-21. The total energy invested by hydraulic power was approximately six percent of the total energy for the 0.7 V/cell-pair application and approximately one percent of the total energy for the 1.6 V/cell-pair application at 99% removal ratio. Even at high voltage applications, the total specific energy required for very high removal ratios is still less than alternative thermal separation processes (*e.g.*, 15-30 kWh/m^3).

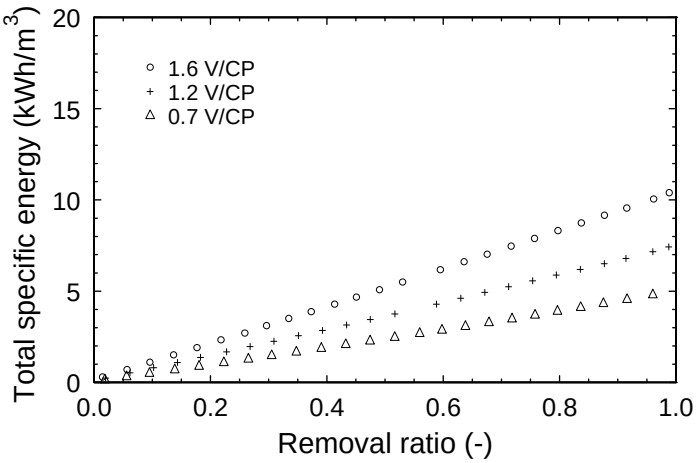

Figure 5-21. Batch-recycle specific energy consumption proportional to ED stack voltage.

5.3.2 Hydraulic effects (synthetic)

One of the principal process limitations in electrodialysis operation is concentration polarization that occurs as a result of diffusion boundary layers adjacent to the membranes. The thickness of these boundary layers (and thus, the significance of their influence in the performance of ED) is minimized with increasing stack velocity, as shown in Figure 5-22. An increase in the velocity results in a decrease in the diffusion boundary layer thickness and an increase in the rate of mass transfer. However, there is a tradeoff in the design and operation of ED with respect to stack velocity – a faster velocity requires a longer flowpath to maintain the mean hydraulic residence time necessary to accomplish a certain removal ratio. For example, quadrupling the velocity (from 1.2 to 4.8 cm/s) only increased the separation rate by approximately 50% for removal ratios up to 80%; thus, the system operating at 4.8 cm/s would require twice the total flowpath length as the system operating at 1.2 cm/s to achieve 80% removal.

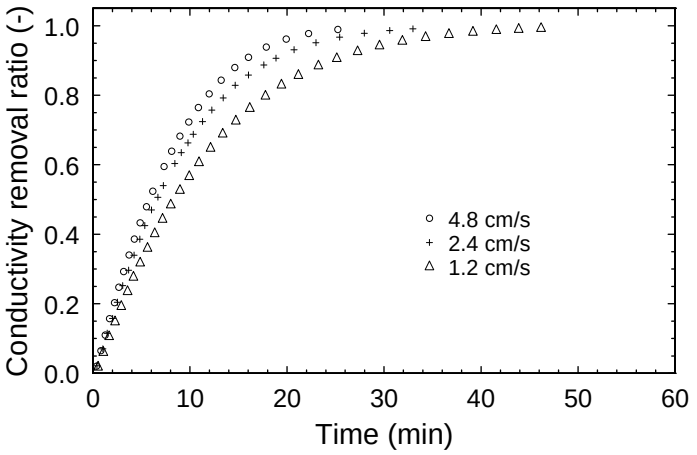

Figure 5-22. Diminishing returns of salinity separation efficiency with increasing ED stack superficial velocity.

The moderate influence of velocity on the performance of ED is further illustrated by the comparison of ionic concentration and bulk conductivity removal ratios, as shown in Figure 5-23. While some variation in the separation selectivity was observable (especially with sulfate), the extent to which selectivity was influenced was marginal compared to the degree of variation in the velocity (*i.e.*, four-fold, from least to greatest).

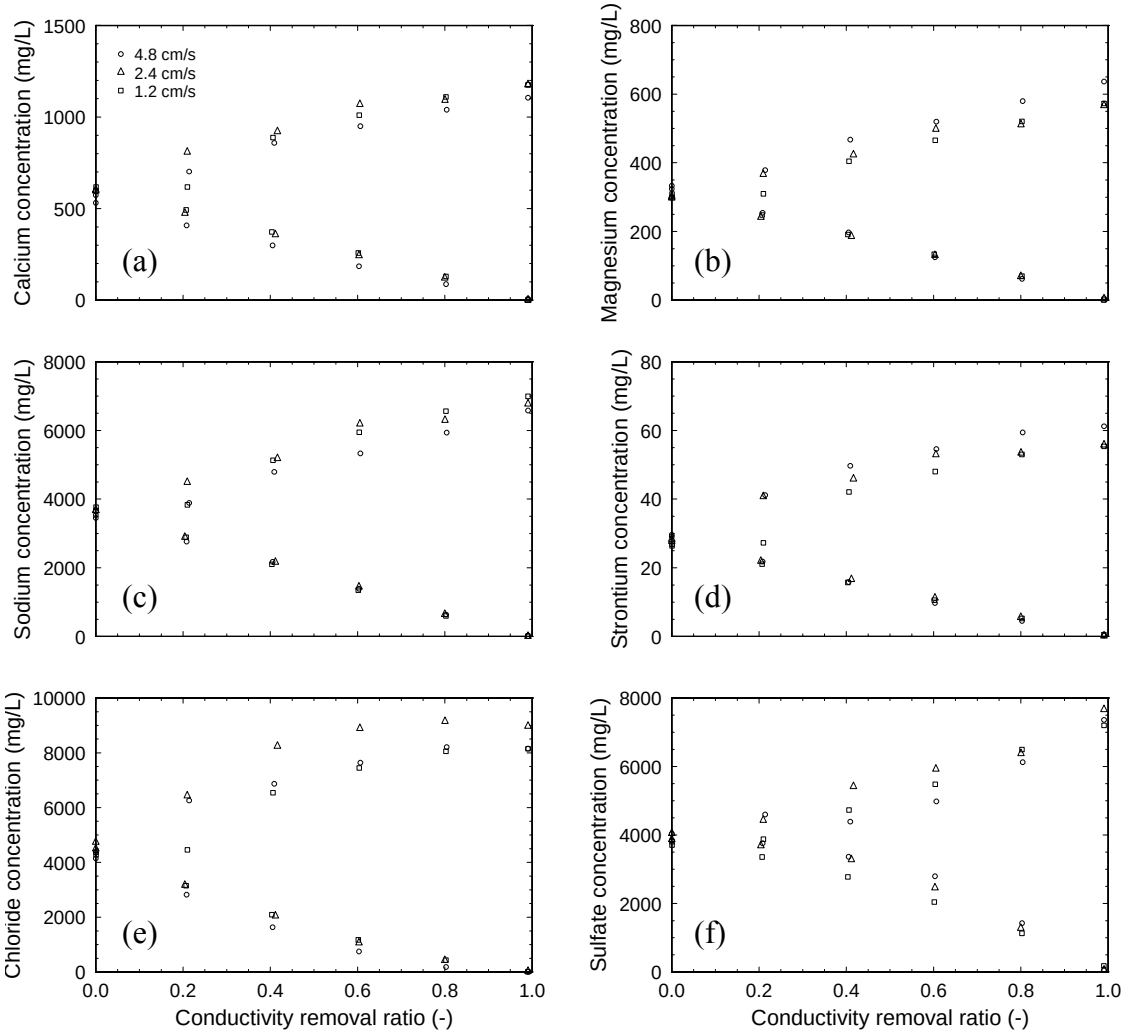

Figure 5-23. Marginal impact of ED stack superficial velocity on separation of select ions.

Increasing the ED stack velocity did result in an increase in electrical current density (as shown in Figure 5-24) by decreasing the thickness (and therefore electrical resistance) of the diffusion boundary layers in the diluate cells. In the electrodialytic treatment of waters with lower conductivity, the electrical resistance of the diluate diffusion boundary layers can contribute a large fraction of the total electrical resistance of the cell-pair, but in the treatment of waters with higher conductivity, the electrical resistance of the membranes make up a larger fraction of the total electrical resistance so that the system is less sensitive to the stack velocity.

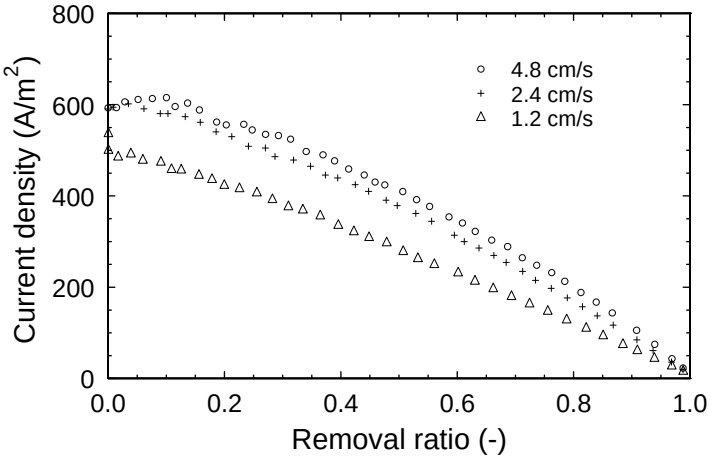

Figure 5-24. Diminishing returns of electrical current density with increasing of ED stack superficial velocity.

Furthermore, since the hydraulic power invested in pumping the solutions through the electrodialyzer is small compared to the electrical power invested to separate ions, the total specific energy was practically insensitive to the variation of stack velocity, as shown in Figure 5-25.

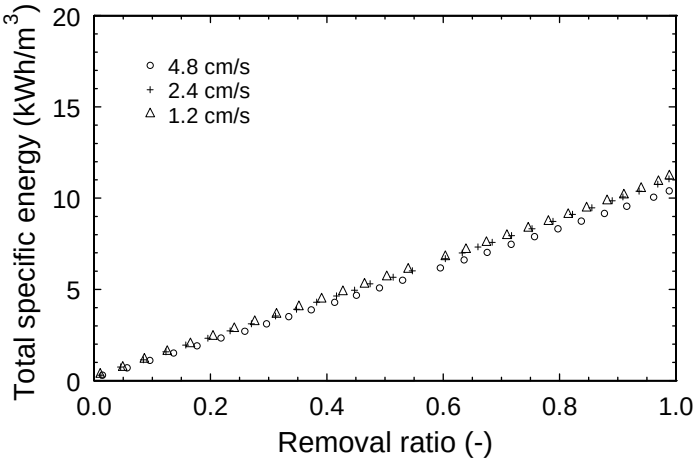

Figure 5-25. Independence of batch-recycle specific energy consumption with respect to of ED stack superficial velocity.

5.3.3 Process effects (on-site)

Several experiments were performed on-site at the North Cameron Regional Water Supply Corporation (NCRWSC) facility with samples of RO concentrate waste collected during production to demonstrate the feasibility of treatment by electrodialysis on real waters. Two experiments were performed with equal volumes of real RO concentrate as the initial concentrate and diluate solutions (simulating nominal single-stage ED recovery of 50%) for a moderate and high voltage application. The ED concentrate from these two experiments was retained and used as the initial concentrate and diluate solutions in a subsequent experiment to demonstrate high

system recovery operation. The effectiveness of ED in the ionic separation of real RO concentrate is shown in Figure 5-26. The concentration of the NCRWSC RO concentrate (*ca.* 15 g/L) is approximately four times the concentration of the feed, and in the first stage of ED treatment (ED-1), the final concentration of the ED concentrate (*ca.* 28 g/L) was almost double the concentration of the RO concentrate. In the second stage of the ED treatment (ED-2), the concentration of the ED concentrate reached approximately 45 g/L before the experiment was terminated (at 80% conductivity removal ratio) because water transport by electroosmosis overflowed the batch-recycle concentrate reservoir.

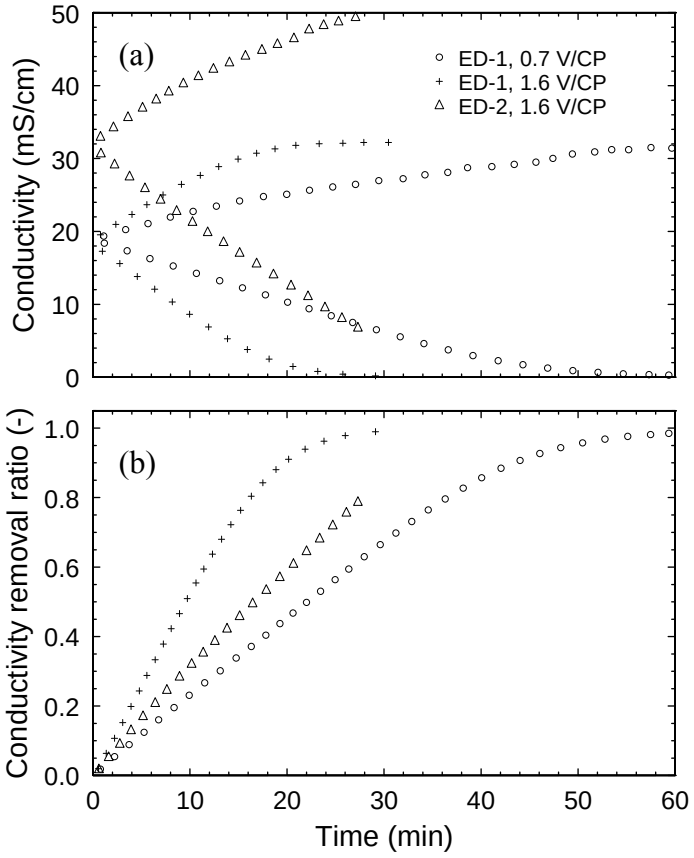

Figure 5-26. Effectiveness of ED treatment of real RO concentrate.

Precipitation was not observed in any of the experiments on synthetic or real concentrates, even with the batch-recycle treatment times, which are much longer than the mean hydraulic residence times of typical full-scale ED systems. Thus, the phosphonate antiscalants used in this research were effective at preventing precipitation of carbonate and sulfate salts with saturation ratios shown in Table 5-1. (Saturation ratios for ED-2 were computed by accounting for electroosmosis and the minor variations in ionic removal based on Figure 5-19.) Comparison of the saturation ratio of calcite of these ED concentrates to Figure 5-9 suggests that concentration by ED could be used to achieve even higher saturation ratios before precipitation would occur during the brief hydraulic residence time of a full-scale system.

Table 5-1. Saturation ratios (*S*) of select salts for concentrates from RO and sequential ED stages (pH = 7.8 for all).

Salt	RO r = 75% R = 100%	ED-1 r = 50% R_κ = 99%	ED-2 r = 50% R_κ = 80%
Calcite ($CaCO_3$)	5.6	9.1	12.9
Dolomite, ordered ($CaMg(CO_3)_2$)	5.9	9.5	13.5
Gypsum ($CaSO_4*2H_2O$)	0.9	1.1	1.3
Magnesite ($MgCO_3$)	1.7	2.7	3.8
Strontianite ($SrCO_3$)	2.1	3.5	4.9
Celestite ($SrSO_4$)	1.4	2.0	2.7

Analysis of the total specific energy investment in the two stages of ED treatment of RO concentrate (Figure 5-27) reinforces the observations noted previously that the specific energy consumption is proportional to the applied voltage and the concentration of salt separated. At very high ionic concentrations, the energy required to desalinate the solution by electrodialysis (which depends on the applied voltage) could be greater than that of thermal processes used in brine concentration (*e.g.*, 20-40 kWh/m^3). For example, based on this research, complete separation of a 60 g/L sodium chloride solution is estimated to require 25-30 kWh/m^3 at a voltage application of 1.0 Volt/cell-pair.

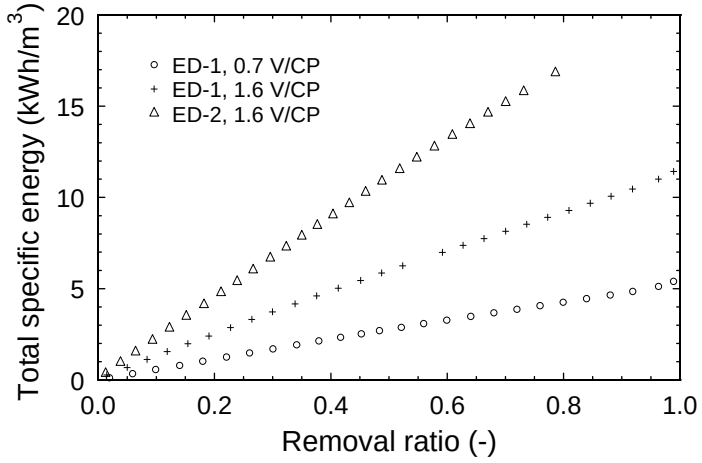

Figure 5-27. Proportionality of batch-recycle specific energy with stack voltage and ionic separation.

5.4 Economic feasibility

In an effort to quantify the economic benefit potentially associated with the application of this process, a basic cost-benefit analysis was performed. As mentioned, the goal of the chemical softening process and the electrodialysis process is to improve the recovery of valuable water and reduce the volume of inland RO concentrate requiring costly disposal. The summation of the reduction of disposal cost and the value of recovered water must be greater than the increased operating and capital cost associated with this additional treatment.

5.4.1 Chemical softening

First, the increased capital and operating costs associated with an additional treatment process must be considered. For the chemical softening process, the capital cost (including mixing tanks, settling tanks, pumps, chemical feeds, and thickening reactors was estimated according to Howe and Clark (2002), and applying a 20 year amortization with an 6% interest rate, monthly capital cost payments would total approximately 0.72% of the total capital cost.

The operating costs primarily include the chemical (lime and soda ash) addition required to reach the optimal saturation ratio for precipitation. The sludge disposal costs (not included in this cost analysis) may also be significant, since sludge cannot be deep-well injected like soluble waste. Lime and soda ash were estimated to be $78 and $100 per kilogram, respectively (Danesh *et al.* 2008; Graff 2003). (In chemical softening, energy costs are generally small compared to chemical costs and thus were not included in this chemical softening cost analysis.) Based on the experimentation in this research, a summary of the estimated capital and chemical costs associated with softening the NCWR RO concentrate for improved recovery is shown in Table 5-2. A system feed flow rate of 2 MGD, RO recovery of 75%, and softening recovery of 90% were assumed for these calculations.

Table 5-2. Cost analysis for chemical softening of NCRWSC RO concentrate

Saturation Ratio of $CaCO_3$	[Ca] precipitated	Estimated Concentrate Recovery	Overall Recovery	Disposal Required	Amortized Capital Cost	Chemical Cost	Total Softening Cost
(--)	(%)	(%)	(%)	(MGD)	($/day)	($/day)	($/day)
7	-	-	75	0.50	-	-	0
13	4	4	76	0.48	161	8	169
18	35	31	83	0.34	161	23	184
22	57	51	88	0.24	161	48	209
26	82	74	93	0.13	161	71	232
29	84	75	94	0.12	161	121	282
32	92	83	96	0.09	161	221	382

Second, the benefits (cost reductions) associated with the process itself were considered. For a given inland RO desalination plant, a certain flow rate of concentrate requires disposal. The operating capacity and process recovery (typically near 75%) of the plant determine the concentrate flow rate. Without any concentrate treatment, this entire concentrate flow rate (25%) would require disposal. With the implementation of a chemical softening and/or electrodialysis treatment of the RO concentrate, the treated concentrate could be recovered to product water by subsequent RO treatment. (In this analysis, the production of the BWRO system was assumed to be constant, such that the additional recovery increased the overall plant capacity.) For example, if calcium carbonate is the essential limitation of RO recovery, then removal of 80% of calcium and carbonate in the concentrate would allow for an approximate recovery of 80% of the treated concentrate. In such case, the concentrate requiring disposal would be reduced from 25% to 5% of the feed, effectively increasing the overall process recovery from 75% to 95%. The cost of this disposal (per volume treated) could then be estimated at various operating conditions by calculating the potential recovery associated with a range of fractional calcium carbonate

removals. An increase in calcium carbonate removal corresponds to an increase in overall recovery and a decrease in disposal volume. Since the cost of disposal per million gallons may vary significantly from plant to plant, this analysis is only a proof-of-concept.

The marginal cost of disposal of brackish water RO concentrate was modeled with two regressions from Mickley (2006, p. 182, 239-40): deep well injection at 500 ft and Zero Liquid Discharge (ZLD) with two percent rejection and $0.12/kWh. The marginal cost of disposal by evaporation pond was calculated assuming 8 ft/yr of net evaporation, $60,000/acre for pond construction, and a 20 year amortization with a 6% interest rate (TWDB 2007). (For small brackish systems, concentrate disposal by surface water discharge can be much less costly that the alternatives just listed. This analysis assumes that the total solids load of the concentrate waste would not be feasibly disposed by surface water discharge.) Subtracting the cost of the softening system from the estimates of disposal cost savings gives an expected net benefit; the estimated net benefits of implementing the chemical softening system in a BWRO system with one of the three disposal methods is shown in Figure 5-28.

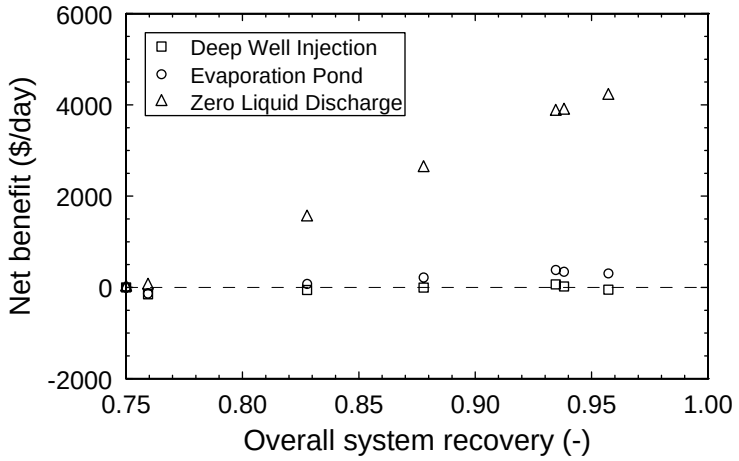

Figure 5-28. Estimated net benefits of chemical softening of NCRWSC RO concentrate for three disposal options.

Based on the assumptions made in this analysis, the implementation of a chemical softening system for concentrate treatment would approximately break even in the deep-well injection scenario, but it would be economically advantageous for improving recovery in systems disposing of concentrate by evaporation pond and zero liquid discharge. Annual cost savings of nearly $1,000,000 are estimated for improving recovery from 75% to 88% with in the zero liquid discharge scenario. However, the marginal cost of shallow deep well injection (inexpensive relative to other disposal methods) is competitive with the estimated cost of chemical softening, and therefore should be reviewed carefully with site-specific details when considering the economic viability of implementing chemical softening for improving recovery.

5.4.2 Electrodialysis

Similarly, a cost-benefit analysis was performed for RO concentrate treatment by ED, and capital and operating expenses for an ED system were estimated based on Badruzzaman (2009) and also accounting for the proportionality of energy investment with salinity removal. A system feed flow rate of 2 MGD was assumed, and each ED stage was assumed to achieve a modest removal

ratio and recovery ratio of 75% and 65%, respectively (though ED systems can be designed with even higher removal ratios and single-stage recoveries).

Table 5-3. Cost analysis for ED treatment of NCRWSC RO concentrate

System Configuration	Overall System Recovery (%)	Disposal (MGD)	Capital Cost ($/day)	Non-electrical O&M ($/day)	Electrical Cost ($/day)	Total ($/day)
w/o ED	75%	0.500	0	0	0	0
ED-1	87%	0.256	475	358	436	1269
ED-1&2	93%	0.131	752	487	660	1898

If the cost of disposal is less expensive than RO and ED costs (such as certain shallow deep well injection systems), then it would not be advantageous to add ED treatment to improve the overall system recovery. However, as with the chemical softening benefit analysis, the ED treatment was estimated to be economically viable for systems with disposal by zero liquid discharge. Even with the implementation of a single-stage of ED, savings of approximately $500,000 per year were estimated in comparison to zero liquid discharge.

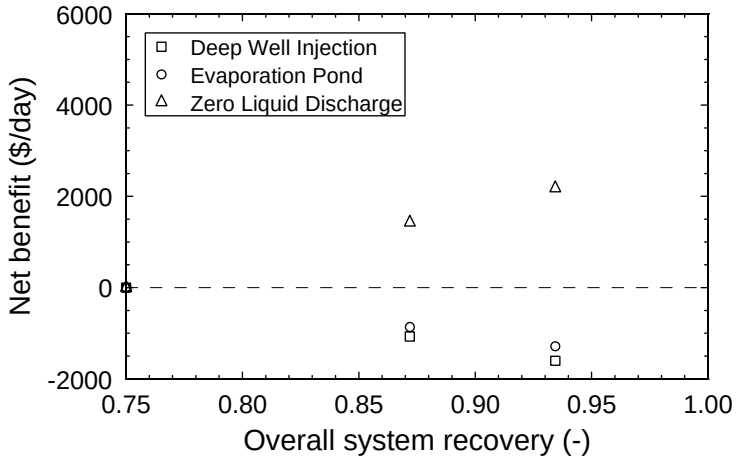

Figure 5-29. Estimated net benefits of ED treatment of NCRWSC RO concentrate for three disposal options.

6 Conclusions

Currently, the cost of concentrate disposal is generally quite high and can render potential desalination projects economically infeasible. In this study, improving the recovery of the inland brackish water reverse osmosis (BWRO) desalination process was attempted through development of an alternative treatment process on the concentrate. All of the experimentation in this research was performed using a concentrate from the North Cameron Regional Water Supply Corporation BWRO plant in South Texas; most of the preliminary work was performed using a synthetic equivalent of this concentrate from a recipe of salts that were added to distilled water. All of the major results were then confirmed using real concentrate from that plant. A characterization of the chemical properties of the concentrate was performed, focusing on the precipitative inhibition of antiscalant presence and promotion of precipitation by oxidation of the antiscalant and adjustment of pH. This characterization was performed through a combination of two types of batch experimentation: peroxone (O_3/H_2O_2) oxidation and chemical precipitation. Optimal results from these batch experiments were the basis for the development of a continuous-flow concentrate chemical softening process for the removal of calcium carbonate, one of the primary RO scaling salts in the NCRWSC plant. Also, RO concentrate treated with a batch-recycle electrodialysis system to investigate the performance effects of stack voltage and velocity, as well as multiple stage recovery. In addition to the demonstration of technical feasibilities of these processes, the economic feasibilities were briefly demonstrated with a simplified cost-benefit analysis.

6.1 Antiscalant behavior

Characterization of the concentrate was performed to determine the effect of antiscalant presence, antiscalant oxidation, and pH adjustments on resulting precipitation. Antiscalant presence was found to prevent calcium carbonate precipitation significantly at a range of saturation ratios from 13 to 22. Above 22, a relatively insignificant fraction of calcium carbonate is prevented from precipitating by antiscalant function. Oxidation of the antiscalant was shown to inactivate the function of the antiscalant for all saturation ratios. An optimal oxidation application was determined to be 20 mg O_3 per mg antiscalant with no hydrogen peroxide at a pH of 7.8. The benefit of this oxidation is complete inactivation for all saturation ratios tested (13to 32). However, antiscalant inactivation is not worthwhile at saturation ratios of 50 or above because the function of the antiscalant is relatively insignificant at that degree of supersaturation. The adjustment of pH was the means of altering the saturation ratio because the dissolved HCO_3^- was converted to CO_3^{2-}. At a pH of approximately 9.2 (S=26) and above, pH adjustment alone is sufficient to achieve optimal calcium carbonate removal. In this range, a high fractional removal of calcium carbonate (above 80%) was observed independent of antiscalant presence or oxidation.

6.2 Chemical softening

A concentrate chemical softening process was developed based on this characterization. Lime ($Ca(OH)_2$) and soda ash (Na_2CO_3) were used to increase the saturation ratio to the desired level while simultaneously equalizing the molarities of calcium and total carbonate. This equalization allowed for a high fractional removal of both species. By dosing a direct feed of the concentrate with 9 mM of lime and 3 mM of soda ash, a total of 24.2 mM of both calcium and total

carbonate was achieved at a saturation ratio of 32 (pH = 10.2). Approximately 90% of both calcium and carbonate was removed, primarily as calcium carbonate.

After pH reduction, the softened concentrate could be re-dosed with antiscalant and subsequently treated with another RO unit with little the risk of calcium carbonate scale formation on the membrane surface. This further treatment would reduce the volume requiring costly disposal and potentially result in significant economic benefit. For the typical Texas brackish water analyzed, a removal of 90% of the calcium carbonate from the concentrate would allow for approximately 80% recovery of the concentrate stream before supersaturation conditions were unable to prevent scale formation. This treatment scheme would increase the overall process recovery from 75% to over 90%, dramatically reducing the volume requiring disposal from 25% to less than 10%.

6.3 Electrodialysis concentration

The RO concentrate was treated by electrodialysis to produce a desalinated product and further concentrated waste. A batch-recycle system with a ten cell-pair electrodialyzer was used to achieve removal ratios greater than 99%. Variation in ED stack voltage demonstrated the proportionality of the rate of separation and the specific energy consumption with stack voltage. Furthermore, the specific energy consumption was approximately proportional to the ionic content separated. Most ions were separated at approximately the same rate as conductivity, though the separation of sulfate was inhibited slightly by complexation with calcium, magnesium, and sodium ions. (Neutral species such as boric and silicic acid were not separated.) Variation in stack velocity demonstrated that the separation rate can be increased by increasing the solution velocity, but the separation rate does not increase proportionally to velocity. Since the energy to pump the solution through the system was a small fraction of the total specific energy consumption, the total specific energy consumption was practically insensitive to variations in stack velocity. Successive concentrate concentration by electrodialysis (beginning with real RO concentrate on-site at the NCRWSC plant) demonstrated that at a large fraction of the RO concentrate waste could be recovered with low ionic concentrations (though it might be necessary to remove neutral species from the ED product prior to use or recycling to the RO feed). It was also observed that transport of water by electroosmosis was not significant in the separation of BWRO concentrate; however, in the treatment of extremely saline waters by electrodialysis, the use of membranes with a lower water content could mitigate the loss of water by electroosmosis.

With respect to the symbiotic integration of electrodialysis in combination with forced precipitation, observations made from this research suggest that the optimal arrangement would be to concentrate the RO concentrate by ED prior to forced precipitation by chemical softening or thermal brine concentration. The ED treatment process appears to be suitable as an intermediate treatment process between RO and precipitation because of its comparable cost to RO and its ability to recover a large fraction of the RO concentrate to a potentially recyclable product of low ionic content and simultaneously produce a more concentrated concentrate with even greater saturation ratios.

6.4 Economic feasibility

With the simplified analysis presented in Chapter 5, the high cost of concentrate disposal provides an opportunity to reduce the overall cost of inland brackish groundwater desalination by minimizing the volume of concentrate disposed through improved recovery.

7 Acknowledgements

The authors gratefully acknowledge the primary financial support from the Texas Water Development Board for this project. Additional financial support was obtained from several environmental engineering consulting firms: Black & Veatch, Carollo, CDM, HDR, and Malcolm Pirnie.

Several people were instrumental in our work with the North Cameron Regional Water Supply Corporation Plant. Bill Norris of NRS Engineers was responsible for making the initial contact and obtaining permission for us to be involved with their plant. Additional help from NRS Engineers was provided by Jesus Leal, Jake White, and Paula Galvan. The North Cameron plant is jointly owned by two water supply companies, and the assistance of managers Chuck Browning of the North Alamo Water Supply Corp. and Brian McManus of the East Rio Hondo Water Supply Corp. is gratefully acknowledged. Jessie Roblis and Stephen Sanchez are involved with the operation of the plant, and their assistance throughout our visits to the plant enabled us to accomplish our goals there; their welcoming attitude and willingness to answer all types of questions is certainly appreciated.

The authors are also very grateful for the review of the draft version of this report provided by TWDB staff. Their comments were detailed and insightful and helped improve the value and readability of this report.

8 References

Ahmed, M., A. Arakel, et al. (2003). "Feasibility of salt production from inland RO desalination plant reject brine: A case study." *Desalination* 158(1-3): 109-117.

Ahmed, M., W. H. Shayya, et al. (2001). "Brine disposal from reverse osmosis desalination plants in Oman and the United Arab Emirates." *Desalination* 133(2): 135-147.

Al-Shammiri, M., M. Safar, et al. (2000). "Evaluation of two different antiscalants in real operation at the Doha research plant." *Desalination* 128(1): 1-16.

Al Radif, A. (1999). "Integrated water resources management (IWRM): an approach to face the challenges of the next century and to avert future crises." *Desalination* 124(1-3): 145-153.

Andreozzi, R., V. Caprio, et al. (1999). "Advanced oxidation processes (AOP) for water purification and recovery." *Catalysis Today* 53(1): 51-59.

AWWA, Ed. (1995). M38 - Electrodialysis and Electrodialysis Reversal. Manual of Water Supply Practices. Denver, CO, American Water Works Association.

Badruzzaman, M., J. F. DeCarolis, et al. (2009). Performance and cost effectiveness of reverse osmosis and electrodialysis reversal for desalination of brackish groundwater containing high silica. AWWA and AMTA Membrane Technology Conference, Memphis, TN, American Water Works Association and American Membrane Technology Association.

Bard, A. J. and L. R. Faulkner (2001). Electrochemical methods: Fundamentals and Applications. New York, Wiley.

Burbano, A. A., S. S. Adham, et al. (2007). "The state of full-scale RO/NF desalination - Results from a worldwide survey." *Journal AWWA* 99(4): 116-127.

Chandramowleeswaran, M. and K. Palanivelu (2006). "Treatability studies on textile effluent for total dissolved solids reduction using electrodialysis." *Desalination* 201(1-3): 164-174.

Choi, E.-Y., J.-H. Choi, et al. (2003). "An electrodialysis model for determination of the optimal current density." *Desalination* 153(1-3): 399-404.

Cornwell, D. A. and M. M. Bishop (1983). "Determining velocity gradients in laboratory and full-scale systems." *American Water Works Association Journal* 75(9): 470-474.

Danesh, P., S. M. Hong, et al. (2008). "Phosphorus and Heavy Metal Extraction from Wastewater Treatment Plant Sludges Using Microwaves for Generation of Exceptional Quality Biosolids." *Water Environment Research* 80: 784-795.

Eaton, A. D., L. S. Clesceri, et al., Eds. (2005). Standard Methods for the Examination of Water & Wastewater. Washington, DC, American Public Health Association, American Water Works Association, and Water Environment Federation.

Firdaous, L., J. P. Maleriat, et al. (2007). "Transfer of monovalent and divalent cations in salt solutions by electrodialysis." *Separation Science and Technology* 42(5): 931-948.

Folk, R. L. and L. S. Land (1975). "Mg/Ca ratio and salinity: Two controls over crystallization of dolomite." *AAPG bulletin* 59: 60–68.

Frost, J. W., S. Loo, et al. (1987). "Radical-based dephosphorylation and organophosphonate biodegradation." *Journal of the American Chemical Society* 109(7): Pages: 2166-2171.

Global Water Intelligence. (2010). "DesalData." Retrieved Aug 31, 2010, from http://desaldata.com/projects/analysis.

Gloede, M. and T. Melin (2008). "Physical aspects of membrane scaling." *Desalination* 224(1-3): 71-75.

Graff, G. (2003). "Cost-squeezed industry likely to seek higher tags." *Purchasing* 132(19): 32C31-32C32.
Howe, K. J. and M. M. Clark (2002). Coagulation Pretreatment for Membrane Filtration. Denver, CO, AWWA Research Foundation.
Huang, W., Y. Tsai, et al. (2003). "Evaluation of disinfection by-products formation during ozonation of bromide-containing groundwater." *Journal of Environmental Science and Health. Part A, Toxic/Hazardous Substances & Environmental Engineering* 38(12): 2919-2931.
Kalaswad, S., B. Christian, et al. (2004). Brackish Groundwater in Texas. Volume II of The Future of Desalination in Texas: Technical Papers, Case Studies, and Desalination Technology Resources. J. A. Arroyo. Austin, TX, Texas Water Development Board.
Karimi, A. A., J. A. Redman, et al. (1997). "Evaluating an AOP for TCE and PCE removal." *Journal AWWA* 89(8): pp. 41-53.
Koprivnjak, J. F., E. M. Perdue, et al. (2006). "Coupling reverse osmosis with electrodialysis to isolate natural organic matter from fresh waters." *Water Research* 40(18): 3385-3392.
Mickley, M. (2006). Membrane Concentrate Disposal: Practices and Regulation (Second Edition). Desalination and Water Purification Research and Development Program, U.S. Department of the Interior, Bureau of Reclamation.
Moon, P., G. Sandí, et al. (2004). "Computational modeling of ionic transport in continuous and batch electrodialysis." *Separation Science & Technology* 39(11): 2531-2555.
Newman, J. S. and K. E. Thomas-Alyea (2004). Electrochemical systems. Hoboken, N.J., J. Wiley.
Ortiz, J. M., E. Expósito, et al. (2008). "Desalination of underground brackish waters using an electrodialysis system powered directly by photovoltaic energy." *Solar Energy Materials and Solar Cells* 92(12): 1677-1688.
Ortiz, J. M., J. A. Sotoca, et al. (2005). "Brackish water desalination by electrodialysis: batch recirculation operation modeling." *Journal of Membrane Science* 252(1-2): 65-75.
Rahardianto, A., J. Gao, et al. (2007). "High recovery membrane desalting of low-salinity brackish water: Integration of accelerated precipitation softening with membrane RO." *Journal of Membrane Science* 289(1-2): 123-137.
Rautenbach, R. and T. Linn (1996). "High-pressure reverse osmosis and nanofiltration, a "zero discharge" process combination for the treatment of waste water with severe fouling/scaling potential." *Desalination* 105(1-2): 63-70.
Reahl, E. (2005). "Half a Century of Desalination with Electrodialysis." from http://www.gewater.com/pdf/Technical%20Papers_Cust/Americas/English/TP1038EN.pdf.
Reedy, K. A. and C. J. Tadanier (2008). Controlling Groundwater Desalination Costs: Facility and Process Planning (Poster). AWWA Annual Conference and Exposition (ACE). Atlanta, GA, AWWA.
Strathmann, H. (2004). Ion-exchange membrane separation processes. Boston, Elsevier.
Tanaka, Y. (2007). Ion exchange membranes: fundamentals and applications. Boston, Elsevier.
TWDB (2007). Self-Sealing Evaporation Ponds for Desalination Facilities in Texas. Austin, TX, Bureau of Economic Geology at The University of Texas at Austin,.
TWDB. (2010a). "2011 Regional Water Plan: Regional and State Total Population Projections 2010-2060." Retrieved June 14, 2010, from

http://www.twdb.state.tx.us/wrpi/data/proj/popwaterdemand/2011Projections/Population/1StatePopulation.pdf.
TWDB. (2010b). "Chapter 9 - Water Supply Needs." 2007 State Water Plan Retrieved June 14, 2010, from http://www.twdb.state.tx.us/publications/reports/State_Water_Plan/2007/2007StateWaterPlan/CHAPTER%209_112806.indd.pdf.
Uchymiak, M., E. Lyster, et al. (2008). "Kinetics of gypsum crystal growth on a reverse osmosis membrane." *Journal of Membrane Science* 314(1-2): 163-172.
USGS. (2010). "Where is Earth's water located? USGS Water Science for Schools." from http://ga.water.usgs.gov/edu/earthwherewater.html.
Van der Bruggen, B. and C. Vandecasteele (2002). "Distillation vs. membrane filtration: overview of process evolutions in seawater desalination." *Desalination* 143(3): 207-218.
von Gunten, U. (2003). "Ozonation of drinking water: Part I. Oxidation kinetics and product formation." *Water Research* 37(7): 1443-1467.
Wiesner, A., A. Zacheis, et al. (2009). Pilot testing of zero liquid discharge technologies using brackish groundwater for inland desert communities. American Membrane Technology Association Annual Conference & Exposition, Austin, TX, AMTA.
Wiesner, A. D., L. E. Katz, et al. (2006). "The impact of ionic strength and background electrolyte on pH measurements in metal ion adsorption experiments." *Journal of Colloid and Interface Science* 301(1): 329-332.
Xu, P., J. Drewes, et al. (2008). Assessment of a Hybrid Approach for Desalination Concentrate Minimization. AWWA Annual Conference and Exposition (ACE), Atlanta, GA, American Water Works Association.
Yang, Q., Z. Ma, et al. (2004). "Destruction of Anti-Scalants in RO Concentrates by Electrochemical Oxidation." *Journal of Chemical Industry and Engineering (China)* 55(2): 339-340.

Appendix - TWDB Comments on the Draft Report and Responses to Comments

The following plain text is a record of comments on the draft version of this report, and the *italics text is a record of responses to those comments*.

DRAFT REPORT
IMPROVING RECOVERY: A CONCENTRATE MANAGEMENT STRATEGY FOR INLAND DESALINATION
TWDB Contract #0704830717

Dealing with concentrate and its disposal is an important factor for inland desalination. An important and helpful feature of this report is that it describes work in areas that were not successful as, for example, the work on peroxone.

The reviewers of the report provided the following comments:

General Comments

1. The following words have been used in two different forms in the report:
   - Seawater (page 2, first paragraph, line 5) and sea water (Page 2, second paragraph, line 2). Please use the word 'seawater' consistently in the report.
   - Saltwater (page 2, second paragraph, line 3) and salt water (Page 4, 3rd paragraph, lines 5 and 6). Please use one or the other word consistently in the report.

   Text was corrected.

2. The name 'North Cameron Regional Water' should be replaced with the full name of the agency, which is North Cameron Regional Water Supply Corporation (NCRWSC).

   Text was corrected.

Specific Comments

Page iii

Names and titles of TWDB's Board members are printed incorrectly. Please visit http://www.twdb.state.tx.us/about/board_members/Board_Members.asp to obtain current names and titles of TWDB's Board members.

Text was corrected.

Section 2 (Pages 2 and 3)

1. Introduction section of the report focused primarily on calcium carbonate scaling, although calcium sulfate scaling is also possible at high recoveries. Please address the issue in the introduction section of the report.

   Text was corrected.

2. Background (Section 2.1): Please spell out the word 'BWRO' in the first instance.

   Text was corrected.

Section 3.2 (Pages 4 to 6)

1. Page 5, first paragraph: Please clearly mention that MED utilizes heat to evaporate seawater and then condense water.

   Text was corrected.

2. Page 5, second paragraph: Please consider using more recent data on desalination capacity published by the Global Water Intelligence. Additionally, in the discussion on desalination processes and source waters in the U.S., please refer to the primary reference (Global Water Intelligence, the 2006 Desalination Plant Survey) rather than to a secondary reference (Zander et al.)

   Text was corrected.

3. Page 6, first paragraph: Please consider using the term "sparingly soluble salts" rather than "sparingly soluble ions".

   Text was corrected.

Section 3.3 (Page 7, second paragraph, lines 2 and 3)

Please add the word 'increased' after the word 'include' and the word 'velocity' after the word 'crossflow'.

Text was corrected.

Section 3.4 (Pages 7 to 11)

1. Page 7, first paragraph under equation 3-3: Please use the words "which simplifies" rather than the words "and thus may be omitted from".

   Text was corrected.

2. Equation 3-2: Please define the term K_{so}.

   Text was corrected.

Section 3.5 (Pages 11 to 13)

1. Please identify the antiscalant that is being used in the NCRWSC plant.

   Text was edited to identify the source of the antiscalant and to explain that the chemical formula of the antiscalant was not known

2. Please identify the factors (pH, temperature, contaminants in a solution) that may affect induction time for a solution.

   Text was corrected.

Section 3.6.1 (Page 14, first paragraph)

Please spell out the words 'TCE' and 'PCE'.

Text was corrected.

Section 3.7.2 (Pages 16 to 17)

The last sentence of the first paragraph in Page 17 may not be accurate because electrodeionization, a version of electrodialysis in which the diluate compartments are filled with ion-exchange beads, is widely used for production of high purity (18 megohm) water.

Text was edited to include this idea about electrodeionization.

Section 3.7.3 (Page 17)

First paragraph: Please include in the discussion that if substantial amount of chloride is fed to the anode, chlorine is produced in preference to oxygen or mixed with it, because of high oxygen overpotential on most anodes.

Text was edited to incorporate this idea.

Section 3.8 (Page 18, first paragraph, lines 1 and 2)

In the first line, please use the word 'a' in between the words 'is' and 'promising'. In the second line, please delete the word 'is' after the word 'field'.

Text was corrected.

Section 4 (Page 19, first paragraph, line 19)

Please spell out the word 'ACS'.

Text was corrected.

Table 4-1 (Page 19)

Since the constituents of the waters are ionic, it would be appropriate to write the charges on the ions, such as Na^{+}, Ca^{++}, etc.

Text was corrected.

Section 4.1.3 (Pages 20 to 22)

1. Page 21, second paragraph: Please clarify if the term 'intensity' is the function of power applied to the unit.

   Text was corrected.

2. Page 22, third paragraph, line 2: Please clearly indicate in the text that the ozone flow analysis is described in Section 4.2.4 of the report.

   Text was corrected.

3. Figure 4-3 and subsequent text: Please discuss if a null test (i.e., a test leaving out the first gas washing bottle) was run to demonstrate that the amount of ozone reacted in the second washing bottle equaled the amount of ozone generated.

   Text was corrected.

Section 4.1.6 (Page 26, first paragraph)

Please add in the discussion that the conventional reason for using cation transfer membranes on both ends of the stack is because the charged groups in the anion transfer membranes are sensitive to chlorine which may be generated at the anode if the electrode rinse solution contains chloride ions.

Text was corrected.

Section 5.1 (Page 35)

Please discuss whether physical inspection was used to determine calcite in the solution.

The text has not been changed here. The concentrate was essentially particle free until precipitation was initiated in our experiments. Therefore, it was not necessary to look for calcite crystals in the water.

Section 5.2 (Pages 36 to 52)

Please consider evaluating the process of recycle within the high recovery section to increase the recovery without affecting operation of the basic plant.

Indeed, the analysis and experimentation in Section 5.2 (and throughout this report) was performed with the hypothesis that either chemical softening or electrodialysis treatment could be added to an existing BWRO facility to recover water from the concentrate that would otherwise be wasted.

Section 5.2.1 (Page 36)

1. Since it appears that a part of the composition of the scale inhibitor was determined, please clarify if the result was verified and confirmed by the manufacturer. If not, it would be more appropriate to label the ordinate scale of Figure 5-1 and other similar figures as milligrams of phosphorus released.

The composition of the scale inhibitor was not revealed by the manufacturer. The text is clear what our definition of the maximum is, and we believe it is better to show the results in the normalized way that we have done. In other experiments with a known composition of another (but closely related) anti-scalant, the oxidation procedure described released all of the phosphate. Therefore, we have not made the suggested change.

2. Figure 5-5 (Page 39): Please define the term 'Ct'.

Text was corrected.

Section 5.2.3 (Page 46, first paragraph, line 5)
Please define the term 'C_T'

Text was corrected. This term was supposed to be the same as Ct (as shown in figures) or C_t (as shown in the text). (The figure software does not allow subscripts.)

Section 5.2.6 (Page 52, first paragraph)
In the Text, please indicate that the "treatment" sequence that results in this finding was illustrated in Figure 4.4.

Text was corrected.

Section 5.3.1 (Pages 52 to 55)
Please define the term 'conductivity removal ratio'.

Text was corrected.

Section 5.3.2 (Pages 56 to 58)
Discussion on the effect of solution velocity on the performance of ED equipment is confusing because within limits, increasing the velocity increases the rate of mass transfer by decreasing the thickness of the boundary layer. Other factors being equal, as the velocity increases, the mass of salt removed increases, but not quite in proportion to the increase of velocity. The volume of solution treated increases in proportion to the velocity, so the difference in concentration in the diluate channel decreases slightly as the velocity increases. Please address the issue in the report.

Text was expanded to incorporate these ideas of the reviewer.

Section 5.3.3 (Page 60, first paragraph)
Please include an estimate (%) of how much greater energy is required to desalinate a solution of high ionic concentration by electrodialysis than by thermal processes typically used in brine solution.

This suggestion was accepted with an addition to the text.

Section 5.4 (Pages 60 to 63)

1. First paragraph of Section 5.4 in page 60: Please include in the discussion that in some cases the potential benefit of increased recovery is a combination of the increased efficiency in the use of the source water (less waste) as well as reduced volumes requiring disposal.

   This suggestion was accepted with an addition to the text.

2. Section 5.4.1 (Page 61, first paragraph): To estimate monthly capital cost payment, please consider using 20 year amortization with 6% interest rate to comply with TWDB's regional planning estimates.

   This new analysis was performed and the text and table revised.

3. Table 5-2 (Page 61): Please add the cost of disposing of the sludge in the Table. Additionally, please re-label the column 'Capital Cost' as 'Amortized Capital Cost'.

   The cost of chemical softening sludge was not included in this analysis, and has been noted in the text. The column title was corrected.

4. Last paragraph of Page 61: The cost used for construction of evaporation ponds, $6,000 per acre, appears to be very low. The report "Self-Sealing Evaporation Ponds for Desalination Facilities in Texas" prepared for TWDB by the Bureau of Economic Geology in 2007 suggests a cost of $50,000 to $70,000 per acre for a five-acre evaporative pond. This cost would be for a minimally equipped pond. Ponds for use with hazardous materials with double liners and leakdetect systems are much more expensive. Please consider revising the estimate.

   In the draft version of this report, the cost of $6000/acre was only the price of purchasing the land, and the cost estimation procedure in Mickley (2006) involves several parameters to estimate the total cost as a function of the purchase price of the land, as well as the costs of dike, liner, fence, and road. Depending on the estimation parameters, the total cost of an evaporation pond rangesfrom $20,000 to $80,000 per acre. However, in deference to the reviewers, the cost estimates for disposal by evaporation pond presented in the final version of this report were calculated based on a total price of $50,000/acre and a 20 year, 6% amortization.

5. First paragraph of Page 62: If the need is 1.5 MGD of pre-blending permeate, at 95% recovery, NCRWSC would require 1.58 MGD of source water or 0.42 mgd less than at 75% recovery. Please clarify if the benefit is accounted for in the analysis. Additionally, for completeness, the narrative should acknowledge the commonly used disposal by surface discharge (understanding that surface discharge would be a much unlikely option for high TDS concentrate streams).

   (See comment and response above regarding Section 5.2.) The analysis was performed assuming that the increase in recovery would increase the overall production of the plant (i.e., that the original BWRO facility would not be affected by the additional treatment

system), so the benefit of decreasing permeate was not considered. The infeasibility of surface discharge was noted in the text.

Section 6.3 (Page 65)

If electro-osmosis is a problem, it can be reduced somewhat by use of tighter, *i.e.*, lower water content, membranes. Please address this issue in the report.

Text was corrected to include this idea.